PLASMA FACING COMPONENT DESIGN CONCEPTS IN HEAT REMOVAL AND STRESS

A Thesis
Presented to
The Academic Faculty

by

Diane Christine Norris

In Partial Fulfillment
of the Requirements for the Degree
Master of Science in Nuclear Engineering

Georgia Institute of Technology
December 1997

PLASMA FACING COMPONENT DESIGN
CONCEPTS IN HEAT REMOVAL AND STRESS

Approved:

W.M. Stacey, Chairman

Seyed M. Ghiaasiaan

James G. Hartley

Date Approved: 11-24-97

DEDICATION

In memory of Annie.

ACKNOWLEDGEMENT

I would like to thank God for inspiring me. I would also like to thank the following persons: my dad Ted Douthitt, family, and my grandfather. I would like to thank Dr. Michael Yaksh and Bill Lee from NAC International. Finally, I thank Dr. Wepfer and the Woodruff School of Mechanical Engineering for their financial support.

TABLE OF CONTENTS

LIST OF TABLES

LIST OF ILLUSTRATIONS

SUMMARY

In a tokamak fusion reactor, high energy particles and radiation from the plasma bombard the surrounding plasma facing components (PFCs). Removal of the heat incident upon the surrounding PFCs from the plasma is a major design problem, and, for next generation tokamaks, a limiting design constraint will determine the size of the plasma chamber.

The purpose of this study was to calculate the heat flux limit for various possible PFC structural material and coolant combinations, based upon the PFC design configuration of the International Thermonuclear Experimental Reactor (ITER). Heat removal, heat conduction, and stress calculations were performed for a single PFC geometry, similar to that, which is being developed for ITER. The ITER design is based upon a SS316 structure and H_2O coolant.

The following material and coolant combinations were considered: SS316/H_2O (5 and 14 MPa), HT-9/H_2O (14 MPa), V-4Cr-4Ti/H_2O (14 MPa), HT-9/He (15 MPa), and V-4Cr-4Ti/He (15 MPa). The constraints which limit the heat flux are maximum allowable temperature, maximum allowable stress (ASME code), and certain practical engineering constraints. The maximum allowable surface heat fluxes were calculated to be 2.0, 1.23, ~0.45, 0.36, <0.5,

and <0.5 MW/m^2 for V-4Cr-4Ti/H_2O (14 MPa), HT-9/H_2O (14 MPa), SS316/H_2O (5 MPa), SS316/H_2O (14 MPa), V-4Cr-4Ti/He (15 MPa), and HT-9/He (15 MPa), respectively. The helium designs were limited to low surface heat fluxes in this geometry because of excessive pumping power.

NOMENCLATURE

A	Poloidal-radial surface area of the first wall unit cell (m^2)	
A_{fw}	Cross-sectional area of the first wall (m^2)	
C_p	Specific heat of coolant (kJ/kgK)	
D	Coolant tube diameter	(m)
$\hat{f}$	Peaking factor	(dimensionless)
$\hat{f}_{ITER}$	ITER peaking factor	(dimensionless)
h	Ratio of volumetric heat source from all particles to volumetric heat source due to 14 MeV neutrons	
h	Film coefficient	(W/m^2K)
$\dot{m}$	Mass flow rate	(kg/s)
P	Coolant pressure	(MPa)
P_{fus}	Fusion power	(MW)
P_R	Pumping power fraction	(%)

q''_{peak}	Peak surface heat flux	(MW/m^2)
q''_{avg}	Average surface heat flux	(MW/m^2)
q'''	Volumetric heat source	(MW/m^3)
q'''_{Be}	Volumetric nuclear heating in beryllium sacrificial layer	(MW/m^3)
q'''_{cool}	Volumetric nuclear heating in the coolant	(MW/m^3)
q'''_{struc}	Volumetric nuclear heating in the structural material	(MW/m^3)
r	Coolant tube radius	(m)
S_m	Design Stress Intensity	(MPa)
t	Coolant tube thickness	(m)
t_{Be}	Beryllium sacrificial layer thickness	(m)
t_{fw}	Thickness of first wall	(m)
t_{min}	Minimum coolant tube thickness when $\sigma=S_m$	(m)
t_{sb}	Strongback thickness	(m)
T_{boil}	Water boiling temperature at saturation pressure	(^0C)
T_c^{exit}	Exit coolant temperature	(^0C)
T_c^{inlet}	Inlet coolant temperature	(^0C)
T_{struc}^{max}	Maximum allowable coolant material temperature	(^0C)
T_w^{exit}	Coolant tube wall temperature at the exit	(^0C)

V	Volume of first wall unit cell	(m^3)
W	Poloidal first wall thickness	(m)
Γ_n	14 MeV neutron flux	(MW/m^2)
μ	Material dependent attenuation coefficient	(m^{-1})
ρ	Radial direction	
σ	Stress from coolant pressure	(MPa)
σ_p	Primary stress intensity	(MPa)
σ_p^{calc}	Calculated primary stress due to fluid pressure	(MPa)
σ_p^{theor}	Predicted stress when $t=t_{min}$	(MPa)
σ_{th}	Thermal stress intensity	(MPa)
σ_u	Ultimate Tensile Stress	(MPa)
σ_y	Yield Stress	(MPa)
Θ	Poloidal direction	
ϖ	Fraction of plasma exhaust energy particles to divertor	(dimensionless)
$1-\varpi$	Fraction of plasma exhaust energy particles to first wall	(dimensionless)

CHAPTER I

INTRODUCTION

1.1 Overview

In a tokamak fusion reactor, high energy particle fluxes and radiation from the plasma bombard the surrounding plasma facing components (PFCs). The radiation and energetic charged particles will constitute an intense surface heat source (on the order of 1 MW/m^2 in future reactors), and the 14 MeV fusion neutrons constitute a volumetric heat source, which attenuates roughly exponentially with an e-folding distance of about 10 cm. Figure 1.1 indicates the configuration of a fusion reactor. A cross sectional view is presented in Figure 1.2.

Removal of the heat incident upon the surrounding PFCs from the plasma is a limiting design constraint that determines the size of the tokamak plasma chamber. The maximum allowable heat flux on the PFCs, for a given PFC geometry, depends on the thermo-mechanical properties of the PFC structural material and on the coolant. Several structural materials and coolants are either available or being developed for PFC application. The purpose of this study was to compare various candidate PFC structural material-coolant

combinations, with respect to maximum surface heat flux capability.

In order to focus the study, the parameters of the International Thermonuclear Experimental Reactor (ITER), are used. The larger the heat flux limit, the smaller the device. For a given power level, the size of the reactor is determined by the heat flux limit on the first wall. The design power level of 1500 MW and the properties of the austenitic stainless steel PFC structure determined the size of ITER.

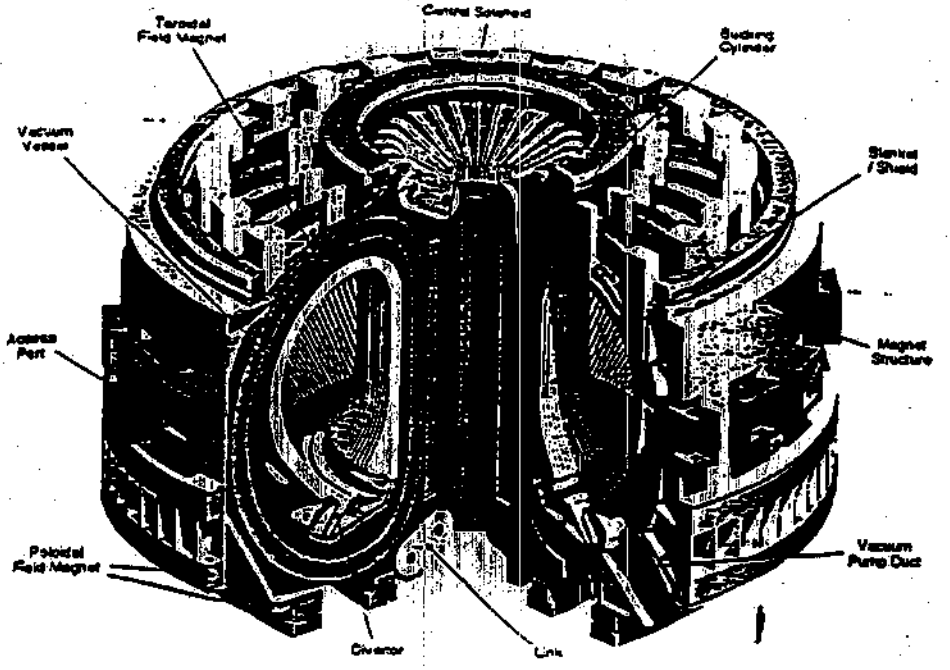

Figure 1.1
Isometric View of ITER

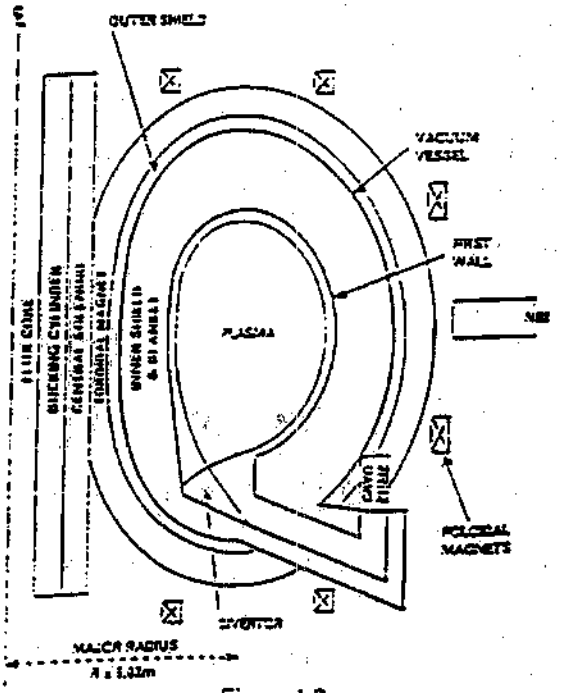

Figure 1.2
Cross-Sectional View of a Tokamak Reactor

In this study, the heat flux limit is determined for the ITER PFC geometric configuration of a tokamak reactor, for several material and coolant combinations. There are two plasma facing components (PFCs) in fusion reactors: first wall and divertor. The first wall was the focus of this study. The first wall design geometry consisted of a bank of coolant tubes attached to a back plate and coated on the plasma facing side with a beryllium sacrificial layer which would be eroded away during operations, as depicted in Figure 1.3. A single coolant tube was used as the geometric model for the heat removal and heat conduction calculations. Based upon ITER research, three different structural materials were considered: type 316 austenitic stainless steel (SS316), vanadium alloy V-4Cr-4Ti, and ferritic-martensitic steel HT-9. Two coolants considered for ITER, H_2O (5 and 14 MPa), and helium (15 MPa), were used to cool the first wall.

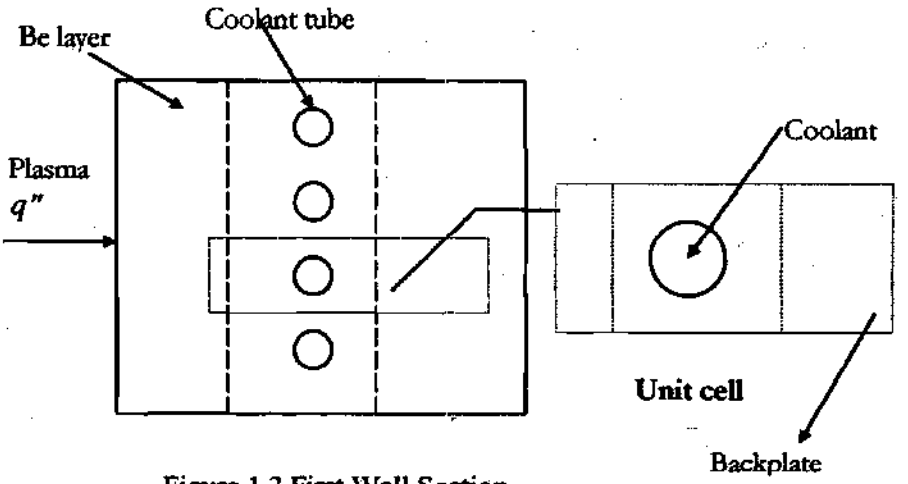

Figure 1.3 First Wall Section

The ITER first wall design geometry was developed for a SS316 and H_2O combination. An optimal first wall design is one with a material/coolant/geometric combination, which would maximize the heat flux limit. The optimum first wall design would be different for other coolant and structural material combinations; however, a common first wall design was used for all of the materials and coolants to obtain a straightforward comparison of the relative heat removal capabilities of the different combinations of structure and coolant.

Constraints on the maximum allowable heat flux consisted of two categories: physical limits based upon material properties, and engineering

design/practicality limits. Physical limits include maximum allowable structural material temperature, maximum allowable beryllium temperature, and the maximum allowable stress criterion as specified by the ASME code. Engineering design/practicality limits include maximum coolant temperatures (water), and maximum allowable pumping power (helium). Considering material compatibility, the following combinations were considered: SS316/H_2O, HT-9/H_2O, HT-9/He, and V-4Cr-4Ti/He, and V-4Cr-4Ti/ H_2O. Coolant pressures of 5 and 14 MPa for H_2O and 15 MPa for He were considered. Vanadium and helium are generally considered incompatible because of the impurities in the helium, so it would only work with an insulation on the vanadium, or with extremely pure helium. For each of these structural-coolant combinations, the maximum allowable surface heat flux from the plasma (heat flux limit) was determined.

CHAPTER II

PLASMA FACING COMPONENT LIMITS

2.1 Overview

Physical and engineering limits are the basis for determining the heat flux limit for a material/coolant combination. We define two categories of limits: physical limits imposed by material properties, and engineering design/practicality limits. Engineering design/practicality limits include maximum coolant temperatures (water), and maximum allowable pumping power (helium). Physical limits imposed by material properties consist of maximum allowable structural material temperature, maximum allowable beryllium temperature, and the maximum allowable stress criterion as specified by the ASME code. Heat removal limits include maximum coolant temperatures (water), and pumping power fraction (helium).

2.2 Engineering Design/Practicality limits

2.2.1 Water

When using water as a coolant, single phase flow is maintained by requiring the coolant temperature at the exit, T_c^{exit}, to remain less than 90% of the boiling temperature at a specific pressure, T_{boil}, which corresponds to ~235 ^{0}C at 5 MPa, and 300^{0}C at 14 MPa. This is an engineering judgment, or practicality limit. The boiling point at the highest pressure, 300^{0}C at 14 MPa, is well below all maximum allowable material temperatures, T_{struc}^{max} (450^{0}C for SS316). A passive safety feature is ensuring the exit temperatures, T_w^{exit} and T_c^{exit}, will remain below 90% of T_{struc}^{max}. These exit temperatures will always remain below T_{struc}^{max}, under normal operating conditions, since $T_{boil} < T_{struc}^{max}$. The minimization of the coolant temperature at the exit, T_c^{exit}, is necessary because it minimizes T_w^{exit}, and maintains the PFC temperature at lower temperatures. The limit on T_c^{exit} is 300 ^{0}C at 14 MPa, and 235 ^{0}C at 5 MPa. The coolant velocity is 7 m/s at all pressures. An advantage to using water is a low required pumping power. For H_2O, the pumping power remains < 1MW, and accordingly, the pumping power fraction, P_R, is not a limit. The engineering design/practicality limits for H_2O are summarized in Table 2.2.2.1.

2.2.2 Helium

Using water does not require a large amount of pumping power; however, the use of helium for fusion applications requires a high coolant velocity and pumping power. The engineering design/practicality limit is that the maximum allowable pumping power fraction, P_R, is required to remain below 2%. This fraction is defined as the ratio of the amount of pumping power to thermal power for a 1-m toroidal length channel. Selecting P_R to be equal to 2% is an engineering judgement, based upon previous research, with the range of P_R being between 0.5 to a few percent (13), (17). The engineering design/practicality limits are summarized in Table 2.2.2.1.

Table 2.2.2.1 Engineering Design/Practicality Limits for All Material and Coolant Combinations

MATERIAL/ COOLANT	CONSTRAINT ON T_c^{exit} (^{0}C)	P_R(%)	T_c^{exit}(^{0}C)
SS316/5 MPa H_2O	$<T_{boil}$=260	N/A	<235
SS316/14 MPa H_2O	$<T_{boil}$=336	N/A	<300
HT-9/14 MPa	$<T_{boil}$=336	N/A	<300
V-4Cr-4Ti/14 MPa H_2O	$<T_{boil}$=336	N/A	<300
HT-9/15 MPa helium	$<T_{struc}^{max}$	<2	variable
V-4Cr-4Ti/15 MPa helium	$<T_{struc}^{max}$	<2	variable

It is important to minimize the pumping power fraction, which is directly related to the exit coolant tube wall temperature, T_w^{exit}, (which drives the temperature throughout the first wall structure). The pumping power fraction is a constraint for helium limited to 2%. The pumping power fraction is limited to a few percent (13) to not only remove the first wall heat, but at a high efficiency. A pump efficiency of 33% (20) is assumed.

2.3 Physical Limits

2.3.1 Maximum Material Temperatures

Physical limits include maximum material temperatures and the ASME stress limit criterion. Similar to the water design, T_w^{exit}, is limited to 90% of the maximum structural material temperature, T_{struc}^{max}, which is 495 and 675 ^{0}C for HT-9 and V4-Cr-4Ti, respectively. To obtain a common comparison between HT-9 and V-4Cr-4Ti, T_w^{exit} is set equal to 495 ^{0}C for the V-4Cr-4Ti/helium (15 MPa) design. The maximum material temperature, T_w^{exit} for each material is summarized in Table 2.3.1.1.

Table 2.3.1.1 Maximum Allowable Material Temperatures for SS316, HT-9, and V-4Cr-4Ti

Material	Maximum Material Temperature (^{0}C)	T_w^{crit} (^{0}C)
SS316	450 (7)	405
HT-9	550 (9)	495
V-4Cr-4Ti	750 (10)	495

These maximum material temperatures are based on the following. SS316 is limited by swelling-induced irradiation, and degradation of material properties above 450^{0}C (6),(7). The ferritic-martensitic steel, HT-9, has a low ductile-brittle transition temperature (8),(9); however, it encounters less swelling and possesses better thermo-mechanical properties than SS316. A maximum material temperature of 550^{0}C is recommended as the maximum HT-9 temperature (9),(13). Vanadium alloys have the least swelling and activation and have the best thermo-mechanical properties. V-4Cr-4Ti is the primary candidate of all the vanadium alloys being considered for fusion applications. A maximum material temperature of 750 ^{0}C is recommended by (13) and (24). Vanadium alloys are generally better suited for use with Li coolant. However, since the optimum first wall geometry for Li coolant would be quite different than the geometry of this

ststudy, we use vanadium alloys with He and H_2O coolants in order to obtain a consistent comparison with SS316. We note that there are questions about the compatibility of vanadium alloys with He (impurities) and H_2O coolants. The maximum temperature for beryllium was limited to 600^0C, for compatibility with moisture (3). Lack of thermo-mechanical data (complicated trends of properties) above 600^0 C (4) also suggests the use of this limit. However, beryllium may be able to operate at a higher temperature. Two other maximum temperatures for beryllium, 800^0C, and 1200^0C are recommended (5) due to safety and ignition in air, respectively, and these are used in our uncertainty studies.

2.3.2 Stress Limits

2.3.2.1 Limiting Stress

The ASME code criterion limits stress intensities to a multiple of the design stress intensity, S_m (material dependent). The design stress intensity, S_m, is defined as the lesser of 2/3 of the yield stress, σ_y, or 1/3 of the ultimate tensile stress, σ_u. Stress intensities are induced in the first wall structure by thermal loadings, (peak surface heat flux and volumetric heat source), by the coolant, and by plasma disruptions. The entire first wall structure must handle stress intensities induced by temperature gradients (thermal stress intensity).

The coolant tube is designed to withstand stress intensities induced by the coolant pressure, and from plasma disruptions. Thermal stress intensities are *secondary* stress intensities denoted by σ_{th}, and stress intensities induced from the coolant pressure and plasma disruptions are *primary* stress intensities, denoted by σ_p. As discussed in Chapter 3, the maximum allowable primary stress intensity produced by the coolant pressure and plasma disruptions, σ_p, is limited by the design stress intensity of a particular material, S_m. The required coolant tube thickness to accommodate primary stresses was predicted by Roarke's formula (Equation 3.2.1.2) for a thin-shelled vessel. The required thickness is less than 2 mm. We take 2 mm as a practical lower limit for a coolant tube thickness. Table 2.3.2.1 lists the material dependent stress intensity and the ASME code criterion for SS316, HT-9, and V-4Cr-4Ti.

Table 2.3.2.1 Design Stress Intensity and ASME Code Criterion for SS316, HT-9, and V-4Cr-4Ti

MATERIAL	DESIGN STRESS INTENSITIES		ASME CODE CRITERION
	S_m** (MPa)	$3S_m$ (MPa)	
SS316	110	330	$\sigma_p < S_m$ $\sigma_p + \sigma_{th} < 3S_m$
HT-9	132	396	
V-4Cr-4Ti	145	435	

** Calculated from minimum of : 1/3 σ_u, 2/3 σ_y (See Appendix A for material properties)

A second ASME code criteria requires the sum of the primary stress intensity (from plasma disruptions and coolant pressure), σ_p plus the thermal stress intensity, σ_{th}, to remain below three times the design stress intensity of a material, $3S_m$. This corresponds to a limit of 330, 396, and 435 MPa, for SS316, HT-9, and V-4Cr-4Ti, respectively (see Table 2.3.2.1). The thermal stress intensity (or secondary stress intensity) dominates over the primary stress intensity.

2.3.2.2 Calculated Stress

The primary stress intensity, σ_p, in the unit cell geometry is modeled as a radial pressure force, regardless of the coolant type, for an ANSYS structural analysis, and is independent of the thermal loadings (peak surface heat flux or volumetric heat source). Two pressure loadings, 5 and 14 MPa, were studied to assess the effect of the primary stress on the heat flux limit. Only the coolant pressure, and not the plasma disruption pressure, was modeled because the coolant pressure dominates over plasma disruptions (14-15 MPa coolant pressure opposed to ~1 MPa from plasma disruptions). For a coolant pressure of 5 MPa, the primary stress intensity is ~ 20 MPa, and for a coolant pressure of 14-15 MPa, the primary stress intensity is ~60 MPa. The results are independent of the coolant type, and they are only a function of the coolant pressure and first wall geometry.

These values are well below the design stress intensities for SS316, HT-9, and V-4Cr-4Ti, of 110, 132, and 145 MPa, respectively (see Table 2.3.2.1). The secondary stress intensity has more impact on the first wall design than does the primary stress intensity. For a coolant pressure of 14 MPa, the primary stress intensity is only 60/330 = 18% of three times the design stress intensity, $3S_m$, for the SS316 case.

CHAPTER III

MODELING

3.1 Plasma Power Exhaust

Highly energetic particles bombard the beryllium surface of the plasma facing component. The two types of particles that create the heat in the PFC (first wall) include the following. Alpha particles and 14 MeV neutrons created from fusion reactions introduce high surface heat fluxes (0.1-1.0 MW/m^2) and a volumetric heat source (5-50 MW/m^3) in the structural material, respectively (15), (18). The alpha particles are confined in the plasma and give up their energy to heat the ions and electrons. The energy to the wall is a combination of energetic ions and electrons, most of which are magnetically diverted onto the divertor plate, and radiation, which is distributed uniformly to the first wall surrounding the plasma. The alpha particle energy is exhausted from the plasma in the form of intense surface heat fluxes, which are split between two plasma facing components: the first wall and the divertor plate. The fraction of plasma energy exhaust travelling to the divertor is ϖ, and 1-ϖ , the compliment fraction, travels to the first wall.

For the first wall, which is the focus of the study, the fraction of plasma energy exhaust typically ranges from 50-80%, or $1-\varpi$ is between 0.5 and 0.8. A plasma energy exhaust fraction of 0.8 is used in this study. These values of $1-\varpi$ are based upon ITER (15). The fraction of plasma energy exhaust to the first wall, $1-\varpi$, is directly proportional to the surface heat flux induced by these particles. There is a surface heat flux distribution that has an average value and a peak value. The peak surface heat flux, q''_{peak}, may be written as the average surface heat flux multiplied by a peaking factor, $\hat{f}$. The corresponding volumetric heat source, q''', is related to the peak surface heat flux by the fraction of the plasma exhaust energy deposited on the first wall, $1-\varpi$. Following the ITER first wall design procedure, 80% of the plasma power exhaust (excluding the neutron power)is assumed incident on the first wall, or $1-\varpi=0.8$. The following equations (3.1.1-3.1.6) develop the governing equation (3.1.7), which relates the peak surface heat flux and volumetric heat source, and which is used in the heat removal and heat conduction calculations.

The average surface heat flux increases with $1-\varpi$ and fusion power, and decreases with the first wall area (6):

$$q''_{avg} = \frac{P_{fus}}{5\,A_{fw}}(1 - \varpi) \quad 3.1.1$$

where:

q''_{avg} = average surface heat flux (MW/m^2)

P_{fus} = fusion power (MW)

A_{fw} = cross sectional area of the first wall (m^2)

$1-\varpi$ = fraction of plasma exhaust energy particles to the first wall (unitless)

The first wall is analyzed using the peak surface heat flux, q''_{peak}, which is the average surface heat flux, q''_{avg}, multiplied by a peaking factor, $\hat{f}$. This peak surface heat flux is related to the plasma thermal power, the peaking factor, $\hat{f}$, and the first wall cross sectional area (6):

$$q''_{peak} = \frac{P_{fus}}{5\,A_{w}}(1 - \varpi)\,\hat{f} \quad 3.1.2$$

where:

q''_{peak} = surface heat flux (MW/m^2)

P_{fus} = plasma thermal power (MW)

A_w = cross sectional area of the first wall (m^2)

1- ϖ = fraction of particles to the first wall (dimensionless) = 80%

$\hat{f}$ = peaking factor

For this analysis, a conservative assumption is made: the peak surface heat flux is distributed uniformly across a sufficiently large surface area so that the cooling effect of heat conduction parallel to the surface area (axial conduction) can be neglected (see Section 3.2.2 Computational Model). The peak surface heat flux is used as the thermal loading in the heat conduction analysis (see Section 3.2.3 Heat Conduction).

Another thermal loading complementary to the surface heat flux is the 14 MeV neutron flux (MW/m^2), Γ_n, which leads to a volumetric heat source. The average Γ_n is related to the peak surface heat flux, by the peaking factor (6):

$$\Gamma_n = \frac{4P_{fus}}{5A_{fw}} = \frac{4q''_{peak}}{(1-\varpi)\hat{f}} = \frac{4q''_{avg}}{1-\varpi} \quad 3.1.3$$

where:

Γ_n = 14 MeV neutron flux (MW/m^2)

q''_{peak} =peak surface heat flux (MW/m^2)

1- ϖ = fraction of plasma energy exhaust to the divertor

$\hat{f}$ =peaking factor.

This neutron flux creates a volumetric heat source, q''' (MW/m^3), which is generated internally in the beryllium layer and structural material and attenuates roughly exponentially (by $e^{-\mu x}$), in the radial (x direction) into the first wall (6). This neutron volumetric heating is enhanced by a factor, h, which is the ratio of the volumetric heat source from all plasma particles to the volumetric heat source due to the 14 MeV neutrons. The exponential attenuation factor, $e^{-\mu x}$, is neglected, based on the thinness of the first wall, which leads to a conservative result (i.e., a higher neutron volumetric heating, q'''). The following assumptions are made concerning the 14 MeV neutron flux.

Although the 14 MeV neutron flux Γ_n, is not uniform over the first wall, it is unlikely that the peak in Γ_n, which usually occurs at the outboard midplane, and the peak in the surface heat flux, q''_{peak}, occur at identical locations. Therefore, an average neutron flux, Γ_n, (at a particular q''_{peak}) is used.

The governing equation used in the heat removal and heat conduction analyses is the relation between the volumetric heat source in the first wall and the peak surface heat flux:

$$q''' = \frac{4\mu h}{(1-\varpi)\hat{f}} q''_{peak} e^{-\mu x} \qquad 3.1.4$$

where:

μ=material dependent attenuation coefficient (~12.5m^{-1} for all materials) (29)

q''_{peak} =peak surface heat flux (MW/m^2)

h =factor (unitless)

1- ϖ = fraction of plasma energy exhaust which reaches the first wall

$\hat{f}$ =peaking factor

$e^{-\mu x}$ =exponential attenuation factor ~ h^{-1} (15)

These equations lead to the relationship between the volumetric heat source, q''', and the 14 MeV neutron flux:

$$q''' = \Gamma_n \mu \qquad 3.1.5$$

Using Equation 3.1.3, and 3.1.5, the volumetric heat source may be expressed in terms of the fusion power, and the material-dependent coefficient, μ:

$$q''' = \frac{4 P_{fus}}{5 A_{fw}} \mu \qquad 3.1.6$$

Equation 3.1.2 implies that, for a constant $(1-\varpi)$, $\hat{f}$, and first wall area, A_{fw}, the peak surface heat flux, q''_{peak}, varies directly with the fusion power. It is shown from equation 3.1.6 that, for a particular material (μ), and first wall area, the volumetric heat source, q''', varies linearly with fusion power. In this study, it is important to relate the volumetric heat source and peak surface heat flux for a particular material, which will be used as variable thermal loadings in the

ANSYS heat conduction analysis. Canceling the fusion power, P_{fus} from 3.1.2 and 3.1.6 gives the relation between the volumetric heat source and peak surface heat flux, which is based upon the material type, for a constant fraction of plasma

energy exhaust to the first wall:

$$q''' = \frac{4\mu q''_{peak}}{(1-\varpi)\hat{f}} \qquad 3.1.7$$

Table 3.1.1 lists this variation of q''' with q''_{peak}, using the ITER peaking factor, $\hat{f}$ equal to 2.25, and a fraction of plasma energy exhaust, $1-\varpi$, of 0.8. In this study, the volumetric heat source varies with the peak surface heat flux, for a particular material. Fixing the first wall area, A_{fw}, fraction of plasma energy exhaust, and peaking factor, dictates through equations 3.1.2 and 3.1.6, that the volumetric heat source and peak surface heat flux vary with the fusion power. The relation between the volumetric heat source and peak surface heat flux is

used given by equation 3.1.7, for the ANSYS heat conduction analysis, *independent of the fusion power level.*

The 14 MeV volumetric heat source constitutes a thermal loading within the first wall (see Section 3.3.2 on loading and boundary conditions), which is used for the heat conduction analysis. The peaking factor, $\hat{f}$, is based upon ITER and is denoted as $\hat{f}_{ITER}$. From (16), $\hat{f}_{ITER}$ is 2.25, derived from a peak surface heat flux of 0.45 Mw/m^2 and a 14 MeV neutron flux of 1.0 MW/m^2.

Table 3.1.1 Plasma Power Exhaust Parameters for ITER for a Constant A_{fw}, $1-\varpi$, and, $\hat{f}$

VOLUMETRIC HEAT SOURCE	PEAK SURFACE HEAT FLUX	14 MeV NEUTRON FLUX	ITER PEAKING FACTOR	ALPHA PARTICLE FRACTION
q''' (MW/m^3)	q''_{peak} (MW/m^2)	Γ_n (MW/m^2)	$\hat{f}_{ITER}$	$1-\varpi$
13.88	0.50	1.11	2.25	0.8
12.50	0.45	1.00	2.25	0.8
8.30	0.30	0.66	2.25	0.8
5.50	0.20	0.44	2.25	0.8

3.2 Heat Removal

3.2.1 Geometric Heat Removal Configuration

In a tokamak fusion reactor, the plasma facing component, or first wall, absorbs the peak surface heat fluxes generated from the plasma. For this study, only a section (radial-poloidal) of this first wall is analyzed. This section is shown in Figure 3.2.2.1. Within this section are several coolant tubes embedded in a structural plate, or strongback, made of the structural material (identical to the coolant tube material). A 5 mm beryllium sacrificial layer protects the coolant tubes from erosion from plasma particles and the peak surface heat flux. There are several "hot" spots along the first wall due to the peak surface heat flux. A conservative approach is taken, where this peak surface heat flux, is uniformly applied to the plasma facing surface. The section taken from the first wall in Figure 3.2.2.2 shows the radial-poloidal cross section. For further simplification, one coolant tube, or unit cell is analyzed for the heat removal and heat conduction analyses. This unit cell is illustrated in Figure 3.2.2.3. The "coolant tube" for each unit cell is embedded in a solid first wall structure, or strongback, which absorbs the pressure from plasma disruptions (1-3 MPa). The required strongback thickness, t_{sb}, is ~2 cm determined by (22).

The coolant induces a pressure acting radially on the coolant tube wall. The coolant tube wall thickness, t_{min} which is depicted in Figure 3.2.2.3, is designed to handle the stress intensity equivalent up to the design stress intensity, S_m, for a particular material, induced by a coolant pressure P (23):

$$\sigma = \frac{P \cdot r}{t} \qquad 3.2.1.1$$

where,

σ=stress from the coolant pressure (MPa)

P=coolant pressure (MPa)

r =coolant tube radius (5 mm).

A minimum thickness will enable the tube to endure the coolant pressure-induced stress intensity for coolant pressures (ranging from 5-15 MPa). Setting σ equal to the design stress intensity, S_m, for a particular material derives the minimal thickness, t_{min}, required to withstand the stress intensity. SS316 and 14 MPa H_2O require the thickest t_{min} of all material and coolant combinations due to the S_m of only 110 MPa. This results in $t_{min} \sim 0.7$ mm. Following the ITER practice, we use

a lower limit of t_{min} greater than or equal to 2 mm, if this relation leads to $t < 2$ mm.

Equation 3.2.1.1 rearranges to predict the stress induced by the coolant tube, or primary stress intensity:

$$\sigma = \frac{P \cdot r}{t_{min}} = \sigma_p^{theor} \qquad 3.2.1.2$$

Equation 3.2.1.2 is used to estimate the primary stress from the coolant pressure. However, the primary stress used to determine the heat flux limit is calculated using ANSYS. Table 3.2.1 lists predicted primary stress intensities (using equation 3.2.1.2), versus actual calculated stress intensities from ANSYS Revision 5.2 (the radial pressure acting on the coolant tube was modeled), for coolant pressures of 5, 10, and 15 MPa. The difference between the predicted primary stress intensity from equation 3.2.1.2 and the ANSYS calculated stress intensity results from the geometry. Equation 3.2.1.2 is for a circular thin-shelled vessel, whereas the actual geometry of the unit cell is rectangular with an embedded circular tube. The ANSYS calculated primary stress intensity, σ_p^{calc}, is used to determine the heat flux limit, and using this limit meets the

requirement that the primary stress intensity remain below S_m for each material (see Chapter II on limits).

Table 3.2.1 Predicted vs. Calculated Primary Stress Intensity for a Coolant Tube Radius of 5 mm and t_{min} of 2 mm for V-4Cr-4Ti, HT-9, and SS316

Coolant Pressure (MPa)	σ_p^{theor} (MPa) (Equation 3.2.1.2)	σ_p^{calc} (MPa) (ANSYS)	S_m^{**} (SS316 / HT-9 /V-4Cr-4Ti)
5	**12.5**	**~20**	**110 / 132 / 146**
10	**16.7**	**~45***	**110 / 132 / 146**
15	**25.0**	**~60**	**110 / 132 / 146**

* linearly interpolated

** calculated from minimum of : 1/3 σ_u, 2/3 σ_y (See Appendix A for material properties)

3.2.2 Computational Model

The coolant enters and leaves the device radially and flows in the toroidal direction (1 m increments) within the first wall, illustrated by Figure 3.2.2.2. The coolants that were considered are: H_2O (5 and 14 MPa), and helium (15 MPa), and the following cases are studied: SS316 / (5 and 14 MPa H_2O), HT-9 / H_2O (14 MPa), HT-9 / 15 MPa helium, V-4Cr-4Ti / 14 MPa H_2O , and V-4Cr-4Ti / 15 MPa helium.

The first wall model, or unit cell, is selected for the following reasons. Because the first wall is subject to high heat fluxes, it is necessary to have as much coolant as close to the surface as possible. Engineering judgement leads to a minimum thickness of structure between the plasma and the coolant; this thickness must be sufficient to withstand coolant pressure. We also believe there is a minimum practical thickness. We take t_{min} equal to 2 mm and then confirm that this is adequate to withstand coolant pressures. A unit toroidal length of 1 m is selected, which is a typical length for ITER calculations (11), (15). An analysis was performed to verify the non-sensitivity of the toroidal length to coolant pressure (see Chapter IV-Sensitivity Studies).

The exit coolant tube surface temperature, T_w^{exit} is determined by an energy balance on the cell geometry (illustrated in Figure 3.2.2.3) related to the exit coolant temperature:, T_c^{exit} :

$$T_w^{exit} = T_c^{exit} + (q''' A + q''_{peak} \pi D) / h \pi D \qquad 3.2.2.1$$

where:

T_c^{exit} =coolant exit temperature (^{0}C)

T_w^{exit}=coolant tube wall temperature (^{0}C)

q''' =volumetric heat source (MW/m^3)

q''_{peak} =peak surface heat flux (MW/m^2)

A=poloidal-radial surface area of the first wall unit cell (m^2)

D=coolant tube diameter (m)

h =film coefficient (W/m^{2}K)

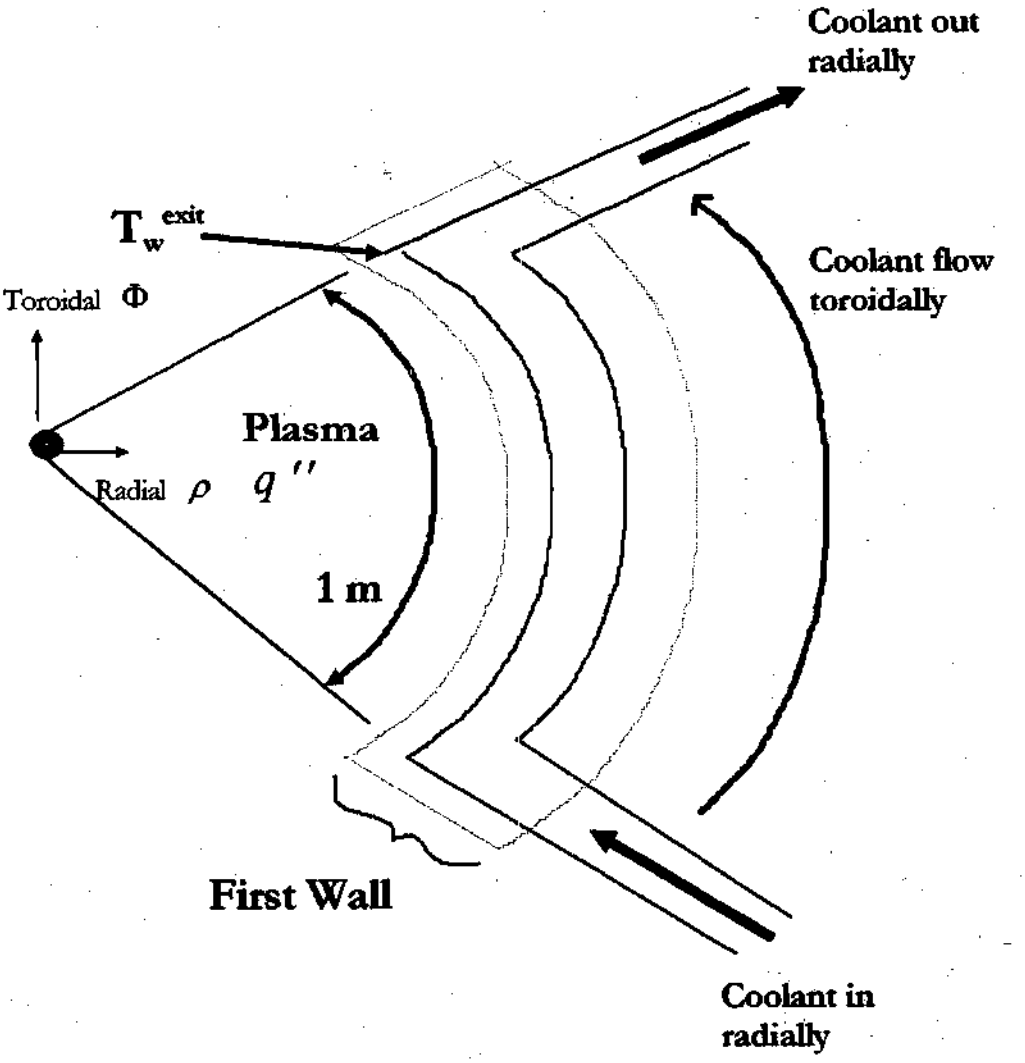

Figure 3.2.2.1
First Wall Section in the
Radial-Toroidal plane

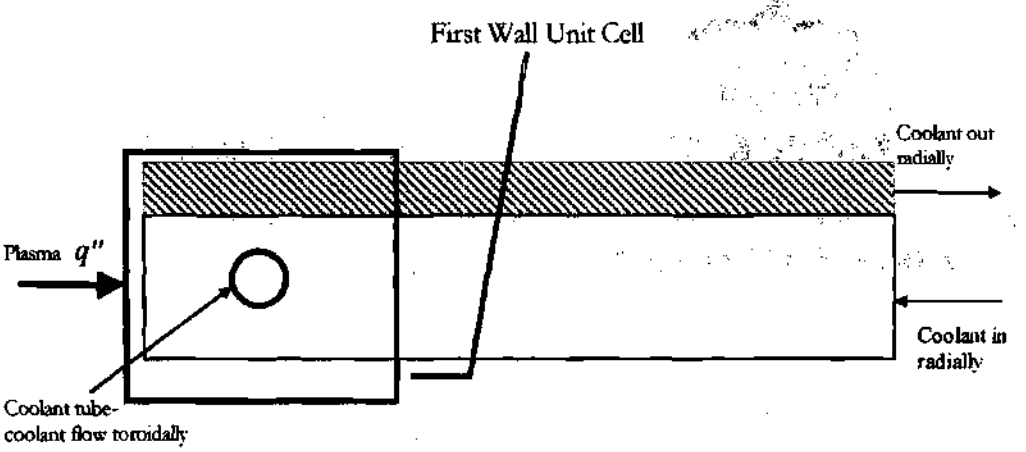

Figure 3.2.2.2
First Wall Section in the
Radial-Poloidal Plane

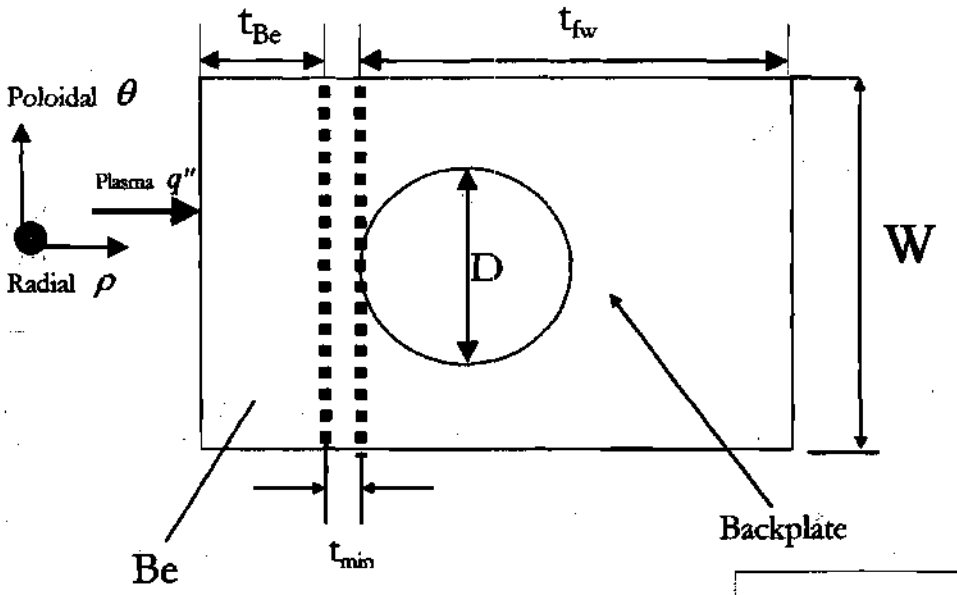

t_{fw}=20 mm
t_{min}=2 mm
t_{Be}=5 mm
W=14 mm

Figure 3.2.2.3
First Wall Unit Cell

The coolant exit temperature is related to the inlet coolant temperature: T_c^{inlet}:

$$T_c^{exit} = T_c^{inlet} + (q''' V + q''_{peak} A) / \dot{m} C_p \qquad 3.2.2.2$$

where:

T_c^{exit}=exit coolant temperature (^{0}C)

T_c^{inlet}=inlet coolant temperature (^{0}C)

$\dot{m}$=mass flow rate (kg/s)

C_p=specific heat of the coolant (kJ/kgK)

V=volume of the first wall unit cell (m^3)

A=surface area of the first wall unit cell (m^2)

q''' =volumetric heat source (MW/m^3)

q''_{peak} =peak surface heat flux (MW/m^2)

The inlet coolant temperatures are set to 200 ^{0}C and 350 ^{0}C (13) for H_2O and helium, respectively. The inlet coolant temperature for H_2O, 200^{0}C, is selected to provide enough margin to ensure that the coolant tube wall temperature at the exit, T_w^{exit}, remains 10% below the boiling point, T_{boil}. The helium inlet

temperature, 350^0C, is selected to compare the results to the benchmark problem from Reference 13. However, to compare the relative heat removal capability for helium versus water, further studies should investigate setting equal the inlet temperatures for each coolant.

A 1 m toroidal section of the first wall, was analyzed for the heat removal and heat conduction calculations. For this cell geometry, the volumetric heat source per unit length, q''' A, and the volume, V, of the first wall are expressed by (18), as depicted in Figure 3.2.2.4:

$$q''' A = q'''_{Be}(Wt_{Be}) + q'''_{struc}\left(Wt_{fw} - \pi\left(\frac{D}{2}\right)^2\right) + q'''_{cool}\,\pi\left(\frac{D}{2}\right)^2 \qquad 3.2.2.3$$

where:

q'''_{Be} = volumetric nuclear heating in the beryllium sacrificial layer (MW/m^3)

q'''_{struc} = volumetric nuclear heating in the structural material (MW/m^3)

q'''_{cool} = volumetric nuclear heating in the coolant (MW/m^3)

W = poloidal first wall thickness (m)

t_{fw} = first wall unit cell thickness (m)

t_{Be} = beryllium sacrificial layer thickness (m)

D = coolant diameter (m)

The volumetric heat source attenuates roughly exponentially throughout the structure. A conservative assumption is made where the volumetric heat source is assumed to be a constant, which is the peak value at the front surface, for every point throughout the first wall structure. Therefore, $q'''_{Be} = q'''_{struc} = q'''_{cool}$, which is the volumetric heat source given by equation 3.1.6 (conservative).

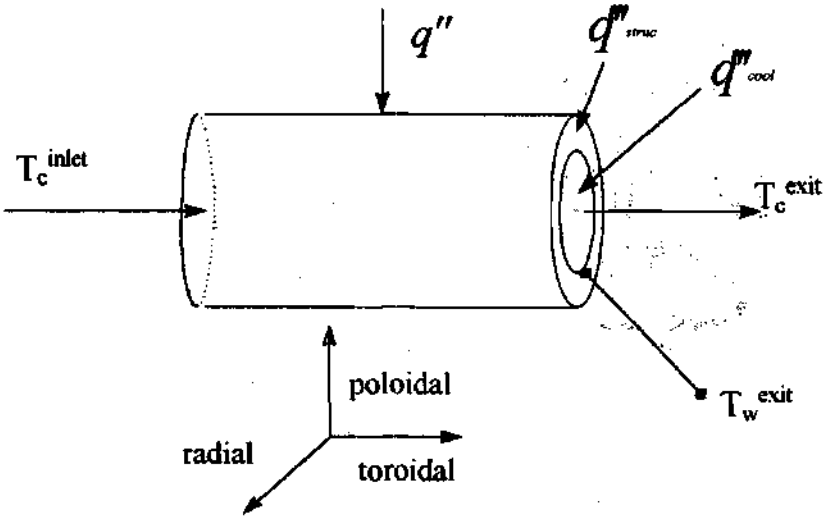

Figure 3.2.2.4 Toroidal 1 m Section of the First Wall

The poloidal width, W, is a function of the coolant tube thickness, t_{min}, and the coolant diameter, D:

$$W = 2*t_{min}+D \qquad 3.2.2.4$$

where:

L_{tor}= toroidal length of the channel = 1m

W = poloidal width (y direction) = 14 mm

t_{min}= coolant tube thickness = 2 mm

D = coolant tube diameter = 10 mm

Similarly, the volume of the cell geometry is approximately (18):

$$V = W*L_{tor}*H \qquad 3.2.2.5$$

where:

W = poloidal width (y direction)=14 mm

L_{tor} = toroidal length of the channel=1m

H = (t_{fw}+t_{Be} in Figure 3.2.2.3) radial length (x direction)=25 mm

The film coefficient, h, is calculated for helium and water, based upon the coolant thermal conductivity and the cell geometry (19):

$$h = \frac{k}{D_h} Nu \qquad 3.2.2.6$$

where:

k = thermal conductivity of the coolant (W/mK)

D_h = coolant tube diameter (m)

Nu = Nusselt number

The hydraulic diameter relates to the wetted perimeter, Z and the cross-sectional area of the coolant channel, S (20):

$$D_h = \frac{4S}{Z} \qquad 3.2.2.7$$

$$D_h = \frac{4\pi D^2}{4\pi D} = D \text{ for circular coolant tube} = 10 \text{ mm}$$

The Nusselt number, Nu, is given by (20):

$$Nu = 0.023 Pr^{0.4} Re^{0.8} \qquad 3.2.2.8$$

where: Re is the Reynolds number ($>10^4$), and Pr is the Prandtl number. They are calculated by (25):

$$Pr = \frac{\mu Cp}{k} \qquad 3.2.2.9$$

$$Re = \frac{\rho v D}{\mu} \qquad 3.2.2.10$$

where:

μ = coolant viscosity (Pa-s)

C_p = specific heat (kJ/kgK)

k = coolant thermal conductivity (W/mK)

v = average coolant velocity (m/s)

D = coolant tube diameter (m)

ρ = density (kg/m^3)

The required pumping power to move the coolant through the 1 m cell geometry with a corresponding friction pressure drop, ΔP (20):

$$P_{pump} = \Delta P \, v A_c \qquad 3.2.2.11$$

where:

ΔP = friction pressure drop (MPa)

v = average coolant velocity (m/s)

A_c = cross-sectional area of fluid flow (m^2)

$=\pi r^2 = \pi(0.000025) = 7.8e\text{-}05$ m^2

The friction pressure drop is related to the coolant type and cell geometry (20):

$$\Delta P = f\left(L/D\right)\frac{\rho v^2}{2} \qquad 3.2.2.12$$

where:

L= toroidal length (1 m)

D = coolant tube diameter (m)

ρ = coolant density (kg/m^3)

v = average coolant velocity (m/s)

f = friction factor

The friction factor , f, is given by the McAdams relation, for a Reynolds number between 30,000 and 1,000,000 (used for helium or water) (20):

$$f=0.184Re^{-0.2} \qquad 3.2.2.13$$

The pumping power fraction, which is the ratio between the pumping power required to remove the thermal power from the 1m cell geometry (depicted in Figure 3.2.2.4) is given by:

$$P_R = \frac{P_{pump}}{\dot{Q}} \leq 2\% \qquad 3.2.2.14$$

where P_{pump} is the pumping power (MW), and $\dot{Q}$ is the thermal power removed

and,

$$\dot{Q} = \dot{m} C_p \Delta T_c \qquad 3.2.2.15$$

where, $\Delta T_c = T_c^{out} - T_c^{inlet}$

T_c^{exit}=coolant exit temperature (at 1 m toroidal length)

T_c^{inlet}=inlet coolant temperature

3.2.3 Limits

Two cases of water, (5 and 14 MPa), are studied to observe the effects of the stress intensity induced by the fluid on the coolant tube, or primary stress intensity (see section 3.2.1, Geometric Heat Removal Configuration, for discussion on primary stress intensity). The temperature of the water, at the exit, T_c^{exit}, is a variable, but it is required to remain 10% below the boiling point of water, which is 260 ^{0}C and 336 ^{0}C, for 5 and 14 MPa, respectively. The coolant tube wall temperature at the end of the channel, T_w^{exit} , is also required to remain 10% below the boiling point for each coolant pressure, which provides a safety margin. This requirement determines T_c^{exit} to be below 300^{0}C at 14 MPa, and below 235^{0}C at 5 MPa. The maximum material temperature T_{struc}^{exit}, is not a limiting factor when using water since T_{boil} is the limiting temperature. The exit tube wall temperature T_w^{exit} (300^{0}C & 235^{0}C), are well below all maximum allowable material temperatures: 450^{0}C, 550^{0}C, 600^{0}C, and 750^{0}C, for SS316,

HT-9, Beryllium, and V-4Cr-4Ti, respectively. All water coolant velocities are set to 7 m/s.

When using helium (15 MPa) as a first wall coolant, a limit on T_w^{exit} is the maximum material temperature, T_{struc}^{max}. A safety margin of 10% requires T_w^{exit} to remain below the values given in Table 2.3.1.1 for the corresponding coolant tube material. In the case of HT-9, T_w^{exit} is 495 ^{0}C obtained by reducing T_{struc}^{max} (550^{0}C) by 10%. For V-4Cr-4Ti, constraining T_w^{exit} to 10% below T_{struc}^{max} (750 ^{0}C), results in 675 ^{0}C, which exceeds the maximum temperature for beryllium: 600 ^{0}C. This further requires T_w^{exit} to remain below 495 ^{0}C to ensure the temperature in the sacrificial layer (beryllium) does not exceed 600 ^{0}C. To remain competitive to the HT-9 / helium design, T_w^{exit} is fixed to 500 ^{0}C (when using V-4Cr-4Ti/helium). These limits are presented in Table 3.2.3.1. It is a calculational strategy to minimize T_w^{exit}, which is the lowest temperature in the first wall, and drives the temperature in the structural material and the beryllium sacrificial layer. Therefore, minimizing T_w^{exit} lowers the thermal stress intensity and material temperatures.

The helium design is not competitive with the water due to the high pumping power requirement. For helium, the pumping power is a limitation in the form of the pumping power fraction, P_R, which is the ratio between the pumping power and the thermal power removed from the first wall, assuming a pump efficiency

of 33% (see Equation 3.2.2.14). This pumping power fraction is kept to 2% (13), (17). This requirement limits T_w^{exit} for helium to temperatures of 495 ^{0}C, making it non-competitive to the first wall water design. The helium inlet coolant temperature, T_c^{inlet}, may be decreased from 350 ^{0}C to the water inlet coolant temperature, 200^{0}C, to lower the required pumping power to achieve a lower T_w^{exit}.

Table 3.2.3.1
Engineering/Practicality and Physical Limits for All Material/Coolant Combinations

MATERIAL	T_{struc}^{max} (^{0}C)	T_w^{exit} (^{0}C)	P_R (%)
SS316/5 MPa H_2O	450	variable	N/A
SS316/14 MPa H_2O	450	variable	N/A
HT-9/14 MPa H_2O	550	variable	N/A
V-4Cr-4Ti/14 MPa H_2O	750	variable	N/A
HT-9/15 MPa helium	550	495	2
V-4Cr-4Ti/15 MPa helium	750	495	2

3.3 Heat Conduction

3.3.1 Overview

Heat conduction calculations are performed for a 2D (radial-poloidal) cross-section of the first wall at the location of the coolant outlet, which determines the coolant tube wall temperature at the exit, T_w^{exit}. This exit wall temperature is the interface between the heat removal and heat conduction analyses. The tube wall exit temperature, T_w^{exit}, is specified as an isothermal boundary condition on the simulated coolant tube of the cell model (see 3.3.2 Boundary Conditions), for the heat conduction analysis. A peak surface heat flux and volumetric heat source are input into the heat conduction analysis, and temperature and thermal stress intensity profiles are obtained. The heat conduction analysis is steady-state, with constant energy generation (constant volumetric heat source from the 14 MeV neutrons). The maximum surface heat flux, $(q''_{peak})_{max}$, is then determined by increasing q''_{peak}, until one of the limiting design constraints (maximum allowable structural temperature, maximum allowable beryllium temperature, or maximum allowable thermal stress is exceeded.

3.3.2 Boundary Conditions

To perform ANSYS heat conduction analyses, the unit cell model of Figure 3.2.2.3 is partitioned into ~53 axisymmetric shell elements on the x-y (radial-poloidal surface), illustrated in Figure 3.3.2.1. Because the unit cell model is symmetric about the radial line passing through the center of the coolant tube, half of the coolant tube is used for the analysis. The five boundaries are shown in Figure 3.3.2.2, with the corresponding boundary condition. Two types of boundary conditions are necessary: thermal and structural. Thermal boundary conditions include: the peak surface heat flux (uniform) on surface 1, an adiabatic condition on surface 4, a coupled (u_y=0) constraint on surface 3, planar symmetry on surface 2, and an isothermal T_w^{exit} on surface 5. By placing an adiabatic condition on surface 4, it is assumed that all the heat is rejected to the coolant tube. This implies that the peak heat flux, q''_{peak}, is incident over a toroidal and poloidal extent of the first wall, and that there is no heat flow across the back surface of the backplate, which are conservative assumptions. ITER calculations also show that a negligible amount of heat conducts through surface 4 (15). The 14 MeV neutron heat source, q''', is applied to every element in the finite-element model. The coolant tube wall temperature at the exit, T_w^{exit}, is an isothermal boundary condition on surface 5.

A second type of boundary condition is structural. A structural analysis is performed to obtain stress intensity profiles throughout the unit cell, due to the coolant pressure loading and to temperature gradients. This models the expansion and contraction (tension and compression) of the unit cell. Thermal stress is a result of temperature gradients from the coolant tube (lowest temperature in the structure), to the plasma-facing surface (highest temperature in the structure). The compression stress is generated internally from the coolant tube to the surface. The outside surface of the first wall unit cell (surface 1 in Figure 3.3.2.2), is at lower temperatures than the interior body of the structure, resulting in tension. This combination of tension-compression on the structure may cause a rotation. This phenomenon explains the position of the highest thermal stress intensities being located in the interior of the structure, near the coolant tube surface. A tension-compression area will cause the unit cell to rotate. To apply appropriate structural boundary conditions, a coupled boundary condition is placed on surface 3. Restraining surface 2 from swelling in the y direction simulates planar symmetry in the y direction. Surfaces 1 and 4 are free surface boundaries, which is appropriate due to the assumption that all stresses are interior to the structure. No assumption is made for the material type or design for a blanket that is attached to surface 4. If the blanket material is

identical to the unit cell structural material, a negligible amount of stress will occur due to different material types (different coefficients of thermal expansion).

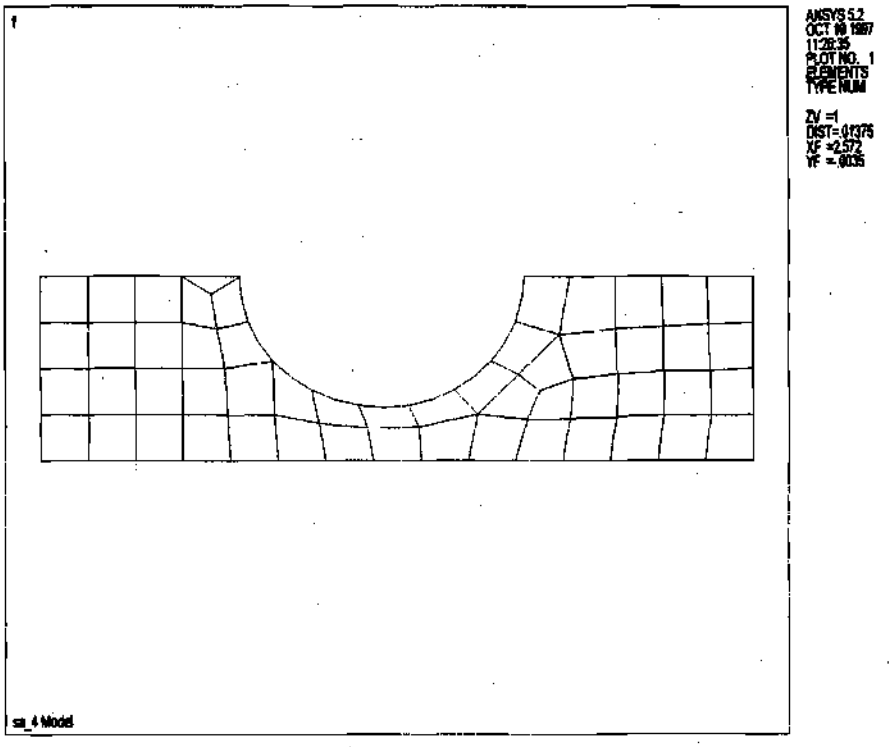

Figure 3.3.2.1
Finite Element Model

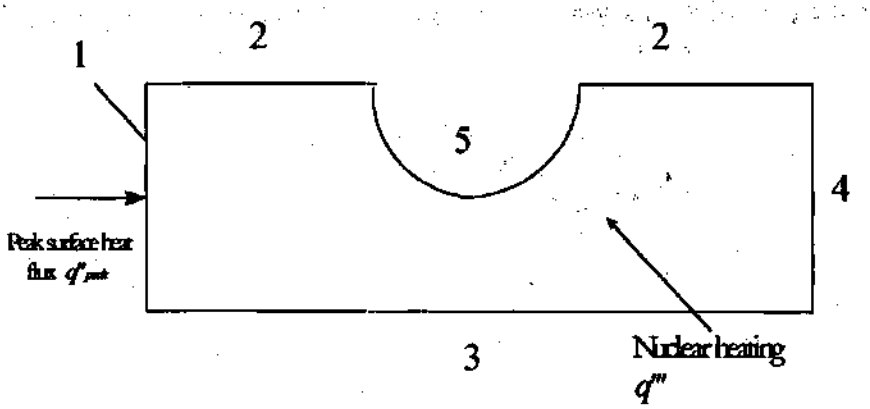

Figure 3.3.2.2
Finite Element Boundary Conditions

CHAPTER IV

RESULTS

4.1 Overview

The heat flux limits are determined for the following material and coolant combinations: SS316/(5 and 14 MPa H_2O); HT-9/ 14 MPa H_2O; HT-9/15 MPa helium; V-4Cr-4Ti/14 MPa H_2O; and V-4Cr-4Ti/15 MPa helium, using the first wall cell geometry. Subject to heat removal and heat conduction limits (discussed in Chapter II), the heat flux limit is determined, consistent with model assumptions described earlier. The coolant tube wall temperature at the end of the 1 m channel, T_w^{exit}, is used as a temperature boundary condition in the ANSYS Revision 5.2 heat conduction analysis.

The heat flux limit is determined in two stages: heat removal and heat conduction. It is the goal to achieve the maximum surface heat flux that satisfies the various maximum temperature and stress limits. A calculational strategy is to minimize T_w^{exit}, which is the lowest temperature in the cell geometry and drives the temperature in the structural material and the beryllium sacrificial layer.

Therefore, minimizing T_w^{exit} lowers the thermal stress intensity and maximum temperature in the cell geometry. Using this coolant tube wall temperature at the exit, thermal stress intensity and temperature profiles are generated and analyzed. The heat flux limit is determined when the [1] maximum allowable beryllium temperature, [2] maximum allowable structural material temperature, or [3] the stress intensity limits is exceeded. The following sections summarize the heat flux limit for each structural material/coolant combination and the limiting constraint. Each case is analyzed and suggestions for improving the heat flux limit are provided. Sensitivity studies involve ranges for improving the heat flux limit for applicable designs. A concluding chapter compares the results for each structural material type against recent fusion research.

4.2 Summary of Results

The heat flux limits for all material / coolant combinations are shown in Table 4.2.1. These heat flux limits are for the first wall cell geometry which is held fixed for all combinations, including a fixed 1m length, for the coolant flow between the inlet and outlet.

The maximum material temperatures occur in the beryllium sacrificial layer in the lower corner (see Figure 4.2.1). The thermal stress intensity is plotted for SS316, with a peak surface heat flux of 0.5 MW/m^2 in Figure 4.2.1. The highest thermal stress intensity occurs near the coolant tube surface (large thermal gradient) along the beryllium/structural material interface (see Appendices B-D). Thermal stress is a result of temperature gradients from the coolant tube (lowest temperature in the structure), to the plasma-facing surface (highest temperature in the structure). The stress is generated internally from the coolant tube to the surface, which creates a compression stress. The outside surface of the first wall unit cell is at lower temperatures than the interior, resulting in tension. This tension-compression on the structure may cause a rotation, which is not allowed. This phenomenon explains the position of the highest thermal stress intensities being located in the interior of the structure, near the coolant tube surface along the beryllium/structural material interface.

The designs with the highest heat flux limits use low-pressure water. Helium limits the designs via the pumping ratio, which is required to remain below 2%. It is a goal to minimize T_w^{exit}, which will lower the temperature in the structure and the beryllium sacrificial layer. With low-pressure water, a T_c^{exit} of 235^{0}C is attainable. Coolant pressure is a significant factor of the resulting heat flux limit. The ASME code criterion states that the thermal stress intensity and the primary stress intensity (due to the coolant pressure) are required to remain below $3S_m$. Even though the primary stress intensity is only ~20-60 MPa/330 MPa=6-18% of the contributed stress, decreasing the coolant pressure from 14 to 5 MPa reduces the primary stress by a factor of three (60 to 20 MPa), and increases the heat flux limit.

The design with the highest heat flux limit, (see Table 4.2.1), is the V-4Cr-4Ti/14 MPa water combination, with a heat flux limit of 2.0 MW/m^2, limited by the maximum beryllium temperature, T_{Be}^{max}. This heat flux limit is higher than the V-4Cr-4Ti/He (15MPa) design, which is less than 0.5 MW/m^2 and limited by the pumping power. If the pumping power fraction were allowed to exceed 2%, the next limiting factor would be the maximum allowable beryllium temperature (600 ^{0}C), which results in a heat flux limit of 0.65 MW/m^2 (see Table 4.2.1), for the V-4Cr-4Ti/He design. The maximum allowable V-4Cr-4Ti temperature (750 ^{0}C) and the stress intensity limits are the least limiting factors on the design,

which yield heat flux limits of 1.8 and 2.3 MW/m^2, respectively. A sensitivity study is performed to determine the effect of increasing the heat flux limit when relaxing T_{Be}^{max}.

The second highest heat flux limit is for the HT-9/H_2O (14 MPa) design, 1.23 MW/m^2, which is limited by the ASME code. This is higher than the HT-9/He (15 MPa) design, which is less than 0.5 MW/m^2, limited by the pumping power. The design with the smallest heat flux limit is SS316/H_2O (5 and 14 MPa), which corresponds to ~0.45 and 0.36 MW/m^2, respectively, which is limited by the ASME code. The SS316/H_2O (5 MPa) design yields a slightly higher heat flux limit than the SS316/H_2O (14 MPa) design, because the ASME code is the limiting criteria. The water pressure is a factor for determining the heat flux limit. The primary stress σ_p, for low-pressure water, is lower than the primary stress when using high-pressure water (by a factor 3). The ASME code requires that the thermal stress and primary stress intensities remain below $3S_m$. The corresponding heat removal parameters for the heat flux limits are listed in Table 4.2.2.

Table 4.2.1 Heat Flux Limit for ITER Candidate Materials

MATERIAL	COOLANT PRESSURE (MPa)	HEAT FLUX LIMIT (MW/M^2)	LIMITING FACTOR
SS316	**5 (H_2O)**	**~0.45**	**ASME**
SS316	5 (H_2O)	0.90	T_{struc}^{max}
SS316	5 (H_2O)	1.2	T_{Be}^{max}
SS316	**14 (H_2O)**	**0.36**	**ASME**
SS316	14 (H_2O)	1.0	T_{struc}^{max}
SS316	14 (H_2O)	1.2	T_{Be}^{max}
HT-9	**14 (H_2O)**	**1.23**	**ASME**
HT-9	14 (H_2O)	2.0	T_{Be}^{max}
HT-9	14 (H_2O)	2.1	T_{struc}^{max}
HT-9	**15 (He)**	**<0.5**	**2% Pumping Power**
HT-9	15 (He)	0.5	T_{struc}^{max}
HT-9	15 (He)	0.6	T_{Be}^{max}
HT-9	15 (He)	1.1	ASME
V-4Cr-4Ti	**14 (H_2O)**	**2.0**	T_{Be}^{max}
V-4Cr-4Ti	14 (H_2O)	2.0	ASME
V-4Cr-4Ti	14 (H_2O)	4.0	T_{struc}^{max}
V-4Cr-4Ti	**15 (He)**	**<0.5**	**2% Pumping Power**
V-4Cr-4Ti	15 (He)	0.65	T_{Be}^{max}
V-4Cr-4Ti	15 (He)	1.80	ASME
V-4Cr-4Ti	15 (He)	2.3	T_{struc}^{max}

Table 4.2.2
Heat Removal Parameters for Heat Flux Limit Corresponding to Most Limiting Factor

Material	Coolant pressure (MPa)	q''_{peak} (MW/m^2)	Limiting Factor	v (m/s)	P_{pump} (MW)	h (W/m^{2}K)	T_c^{exit} (^{0}C)	T_w^{exit} (^{0}C)
SS316	5 H_2O	~0.45	ASME	7	<1	~49,000	~210	~216
SS316	14 H_2O	0.36	ASME	7	<1	~48,000	~205	~215
HT-9	14 H_2O	1.23	ASME	7	<1	~48,000	~210	~230
HT-9	15 He	<0.5	Heat removal	~50	~9	~7360	~425	~495
V-4Cr-4Ti	14 H_2O	2.0	T_{Be}^{max}	~6.0	<1	~48,000	~220	~260
V-4Cr-4Ti	15 He	<0.5	Heat removal	~50	~690	~7360	~414	~495

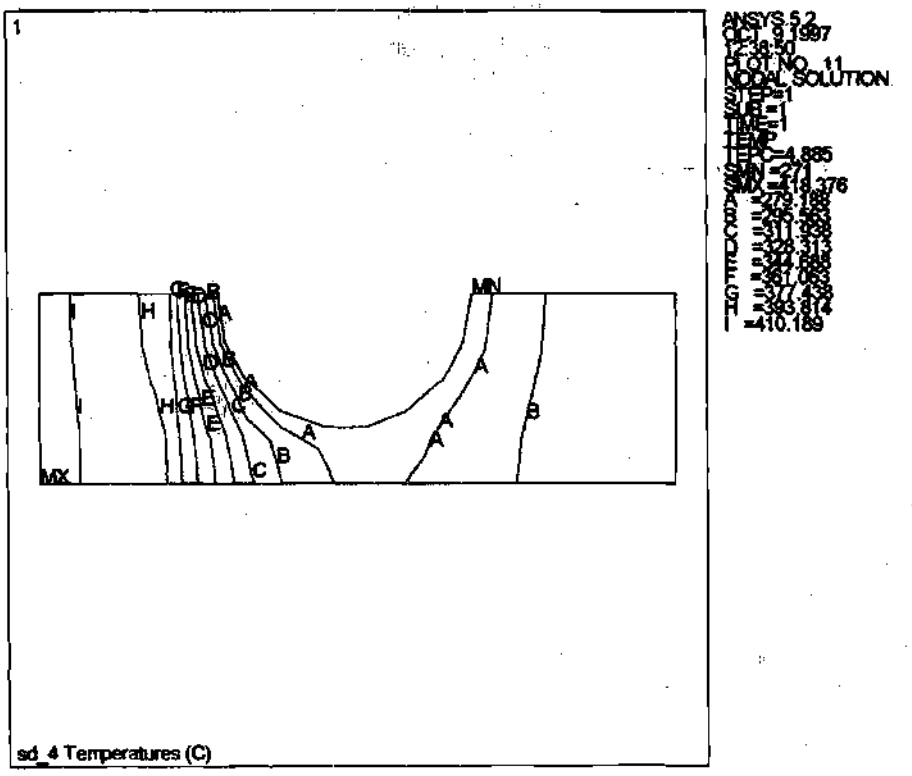

Figure 4.2.1
Temperature Profile (^{0}C) for SS316/H_2O (5 MPa),
Peak Surface Heat Flux of 0.5 MW/m^2; T_w^{exit}=271^{0}C

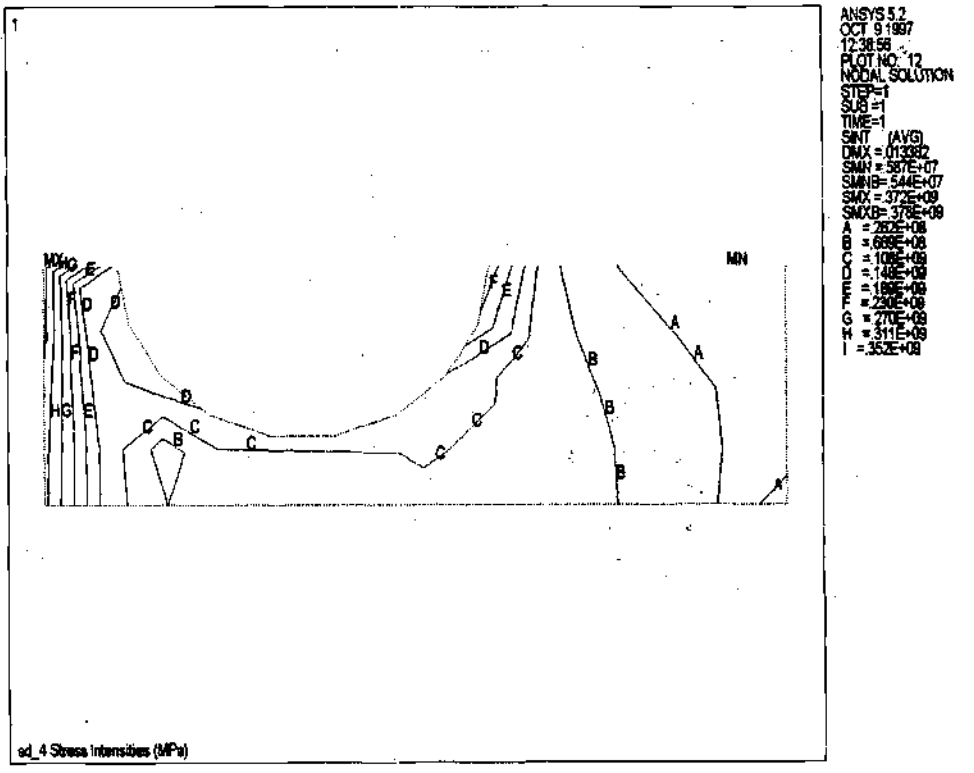

Figure 4.2.2
Thermal Stress Profile (MPa) for SS316/H_2O (5 MPa), (beryllium sacrificial layer removed for clarity), Peak Surface Heat Flux of 0.5 MW/m^2; T_w^{exit}=271^{0}C

4.3 Case Studies-Results

4.3.1 SS316 / H_2O (5 MPa)

As shown in Figure 4.3.1.1 and Table 4.3.1.1, the limiting constraint is stress, yielding a heat flux limit of ~0.45 MW/m^2. The two stress intensity components, σ_{th}, (thermal or secondary), and σ_p, (primary) are required to remain below three times the design stress intensity, $3S_m$. The thermal stress dominates over the primary stress. For a 5 MPa coolant, the primary stress intensity is ~20 MPa, which is only a 6% contribution to $3S_m$. The thermal stress intensity may be reduced by decreasing the temperature gradients in the first wall structure. A calculational procedure to decrease this temperature profile is to lower the coolant tube wall temperature at the exit, T_w^{exit}, by lowering T_c^{exit}. This will drive the required performance for heat removal (i.e., the coolant velocity and pumping power will increase). Another strategy includes lowering the inlet coolant temperature, T_c^{inlet}. For all water cases, the velocity is fixed to 7 m/s.

Depicted in Figure 4.3.1.1, the second limiting constraint is the structural material temperature, which is fixed at 450 ^{0}C. The resulting heat flux limit is ~0.9 MW/m^2. Beyond this temperature, swelling and loss of ductility occur in stainless steels. The least limiting factor is the maximum beryllium temperature, which enables the SS316 design to handle 1.2 MW/m^2 at 600^{0}C, and ~2.0

MW/m^2 at 800^0C. Using beryllium as a sacrificial layer with SS316 is highly beneficial and necessary for obtaining higher heat flux limits.

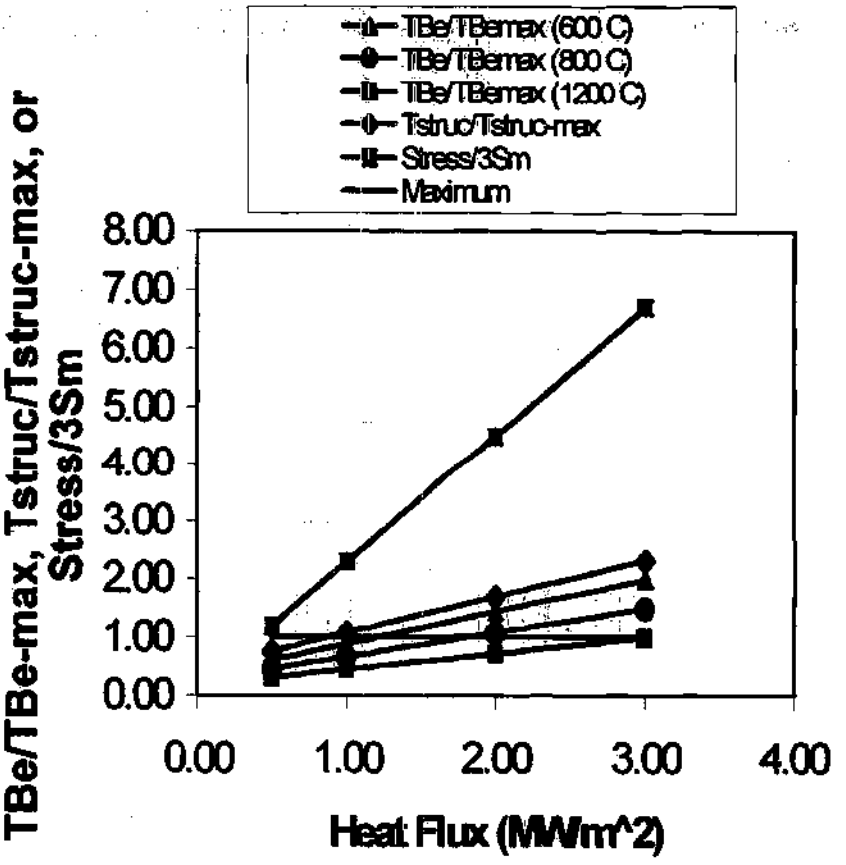

Figure 4.3.1 1 Heat Flux Limit (MW/m^2) Determination Using the TBe/TBe-max, Tstruc/Tstruc-max, or Stress/3Sm Criteria for SS316 (5 MPa H_2O)

The heat removal parameters for varying surface heat fluxes, are presented in Table 4.3.1.2 All water cases have the same flow rate of 7 m/s, and a T_c^{exit} below 235 ^{0}C up to 1.0 MW/m^2. The coolant tube exit temperature, T_w^{exit}, increases with the amount of surface heat flux incident on the PFC.

Table 4.3.1.1
Heat Flux Limit (MW/m^2) Determination Using the T_{Be}/T_{Be}^{max}, $T_{struc}/T_{struc}^{max}$, or Stress/3$S_m$ Criteria for SS316 (5 MPa H_2O)

q" (MW/m^2)	0.50	1.00	2.00	3.00
T_{Be}/T_{Be}^{max} (600 ^{0}C)	0.61	0.88	1.42	1.97
T_{Be}/T_{Be}^{max} (800 ^{0}C)	0.45	0.66	1.07	1.48
T_{Be}/T_{Be}^{max} (1200 ^{0}C)	0.30	0.44	0.71	0.98
$T_{struc}/T_{struc}^{max}$	0.75	1.06	1.69	2.31
Stress/3S_m	1.18	2.28	4.50	6.71

Table 4.3.1.2
Heat Flux Limits and Heat Removal Parameters
for SS316 Using 5 MPa H_2O (v = 7 m/s)

q''_{peak} (MW/m^2)	0.5	1.0	2.0	3.0
T_c^{exit} (^{0}C)	207	238	275	314
T_w^{exit} (^{0}C)	216	260	320	380
v/L	7	7	7	7
h (W/m^{2}K)	~49,000	~49,000	~49,000	~49,000
T_{Be}/T_{Be}^{max}(600 ^{0}C)	0.61	0.88	1.42	1.97
$T_{struc}/T_{struc}^{max}$(450 ^{0}C)	0.75	1.06	1.69	2.31
stress/3S_m	1.18	2.28	4.50	6.71
Factor	$q''_{peak}{}^{max}$ (MW/m^2)			
T_{Be}^{max} (600 ^{0}C)	1.2			
T_{struc}^{max} (450 ^{0}C)	0.90			
stress	~0.45			

4.3.2 SS316 / H_2O (14 MPa)

Similar to the low-pressure design, the limiting constraint using high-pressure water is stress. For to the SS316 / low pressure water case, the heat flux limit is only ~0.45 MW/m^2, and 0.36 MW/m^2 for the high pressure design. The heat flux limits are given in Table 4.3.2.1 and Figure 4.3.2.1. Not only does the poor thermo-mechanical properties of SS316 impose restrictions on the level of tolerable stress, but the design includes high pressure water which adds to the primary stress intensity, σ_p. The thermal stress intensity, σ_{th}, is a function of a minimum achievable T_c^{exit} (235 ^{0}C). Minimizing T_c^{exit} decreases the temperature profile and lowers the thermal stress in the PFC, which leads to an increased heat flux limit.

The other stress contribution, primary stress intensity (due to the fluid pressure) is higher due to an increase in coolant pressure by a factor of 3 (60 MPa stress opposed to 20 MPa). It is the 60 MPa primary stress, for high-pressure water, which yields a heat flux limit of 0.36 MW/m^2 instead of ~0.45 MW/m^2 for the low-pressure design. The advantage to using high-pressure water, compared to low- pressure water is the ability to remove the same amount of heat for a longer channel (see Sensitivity section). The disadvantage to using 14 MPa water is the high primary stress due to the coolant pressure. Decreasing the thermal or primary stress intensity may further increase the heat flux limit. The thermal

stress intensity, σ_m, may be decreased by decreasing T_c^{inlet}. Another strategy for increasing the heat flux limit is decreasing the coolant pressure to 5 MPa, which lowers the primary stress intensity from 60 MPa to 20 MPa. In the case where T_{Be}^{max} is the limiting factor, the heat flux limit is 1.20 MW/m^2, (at 600 ^{0}C), and it is 0.9 MW/m^2 when T_{struc}^{max} is the limiting criterion. Relaxing T_{Be}^{max} to 800 ^{0}C, and 1200 ^{0}C, increases the heat flux limit to ~ 2.0 and ~3.0 MW/m^2, respectively.

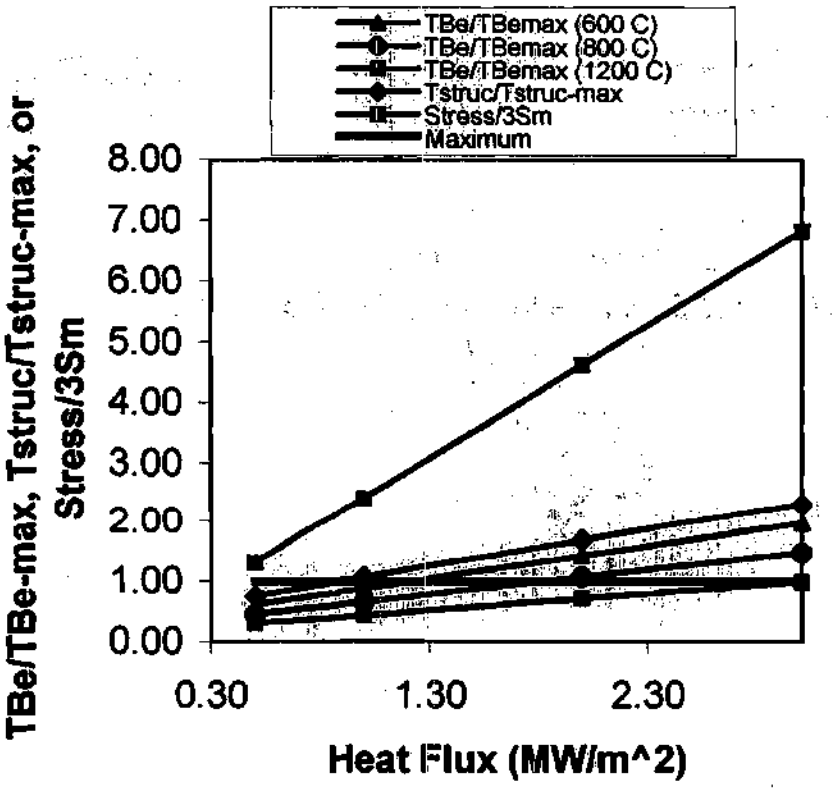

Figure 4.3.2.1 Heat Flux Limit (MW/m^2) Determination Using the T_{Be}/T_{Be}^{max}, $T_{struc}/T_{struc}^{max}$, or Stress/$3S_m$ Criteria for SS316 (14 MPa H_2O)

Table 4.3.2.1
Heat Flux Limit (MW/m^2) Determination Using the T_{Be}/T_{Be}^{max}, $T_{struc}/T_{struc}^{max}$, or Stress/$3S_m$ Criteria for SS316 (14 MPa H_2O)

q''_{peak} (MW/m^2)	0.50	1.00	2.00	3.00
T_{Be}/T_{Be}^{max} (600 ^{0}C)	0.60	0.87	1.42	1.96
T_{Be}/T_{Be}^{max} (800 ^{0}C)	0.45	0.66	1.06	1.47
T_{Be}/T_{Be}^{max} (1200 ^{0}C)	0.30	0.44	0.71	0.98
$T_{struc}/T_{struc}^{max}$ (450 ^{0}C)	0.75	1.06	1.68	2.30
Stress/$3S_m$	1.30	2.41	4.62	6.82

Table 4.3.2.2
Heat Flux Limits and Heat Removal Parameters for SS316 Using 14 MPa H_2O (v = 7 m/s)

q''_{peak} (MW/m^2)	0.5	1.0	2.0	3.0
T_c^{exit} (^{0}C)	205	210	222	232
T_w^{exit} (^{0}C)	215	230	260	290
v/L	7	7	7	7
h (W/m^2K)	~48,000	~48,000	~48,000	~48,000
T_{Be}/T_{Be}^{max} (600 ^{0}C)	0.60	0.87	1.42	1.96
$T_{struc}/T_{struc}^{max}$ (450 ^{0}C)	0.75	1.06	1.68	2.30
Stress/$3S_m$	1.30	2.41	4.62	6.82
Factor	$q''_{peak}{}^{max}$ (MW/m^2)			
T_{Be}^{max} (600 ^{0}C)	1.2			
T_{struc}^{max} (450 ^{0}C)	0.9			
stress	0.36			

4.3.3 HT-9 / H_2O (14 MPa)

Similar to SS316, stress is the limiting constraint, and limits the heat flux to 1.23 MW/m^2. This value of the heat flux limit is higher than for SS316, and lower than V-4Cr-4Ti, which results from the thermophysical properties of SS316, HT-9,, and V-4Cr-4Ti. Since all water designs operate at the same velocity and T_c^{exit}, the resulting heat flux limit is a function of the ability for a structural material to conduct the heat, and not a function of the heat removal capability of the coolant. Decreasing the thermal or primary stress intensity may increase the heat flux limit. The primary stress intensity is dependent on the coolant pressure. By decreasing the coolant pressure to 5 MPa, the primary stress intensity decreases by a factor of 3.

The second most limiting constraint is the maximum beryllium temperature, T_{Be}^{max}, at 600 ^{0}C, which limits the heat flux to ~2.0 MW/m^2. The heat flux limit, as a function of T_{Be}^{max}, is depicted in Figure 4.3.3.1. If T_{Be}^{max} is allowed to exceed 600 ^{0}C to 800 ^{0}C, and to 1200 ^{0}C, the heat flux limits are 3 and >5 MW/m^2, respectively, opposed to 2.0 MW/m^2 at 600 ^{0}C. Table 4.3.3.1 provides the tabular format of Figure 4.3.3.1. As for the 600 ^{0}C T_{Be}^{max} limiting the heat flux to 2.0 MW/m^2, the maximum structural material temperature, T_{struc}^{max}, also limits the heat flux to 2.1 MW/m^2. The heat flux limit is determined by using

Table 4.3.3.1. The corresponding heat removal parameters are presented in Table 4.3.3.2.

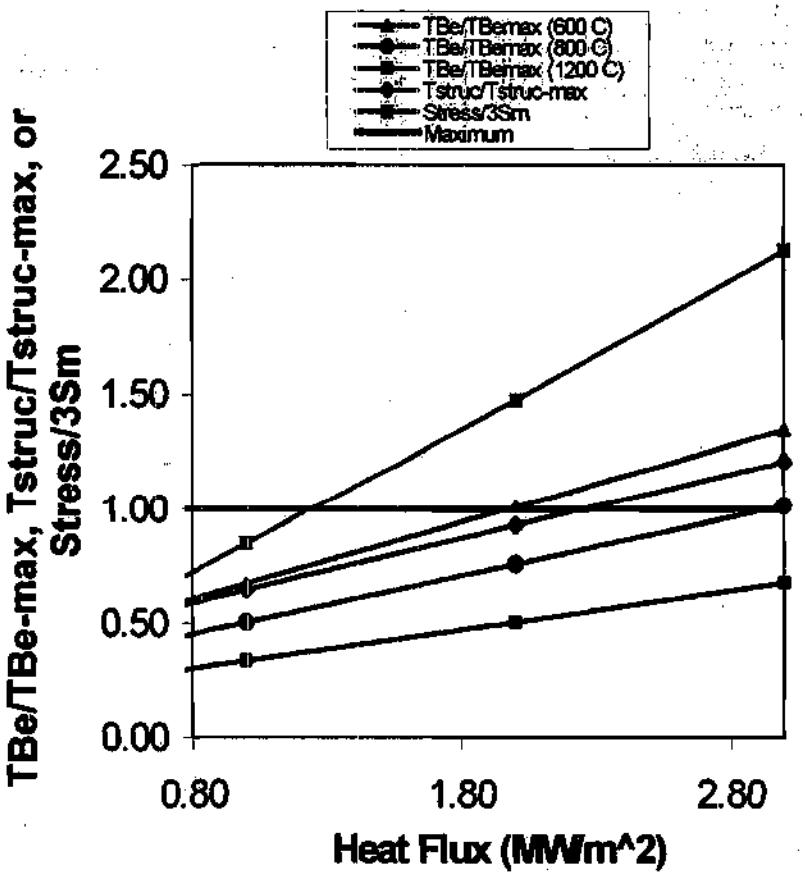

Figure 4.3.3.1 Heat Flux Limit (MW/m^2) Determination Using the T_{Be}/T_{Be}^{max}, $T_{struc}/T_{struc}^{max}$, or Stress/$3S_m$ Criteria for HT-9 (14 MPa H_2O)

Table 4.3.3.1
Heat Flux Limit (MW/m^2) Determination Using
the T_{Be}/T_{Be}^{max}, $T_{struc}/T_{struc}^{max}$, or Stress/$3S_m$ Criteria
for HT-9 (14 MPa H_2O)

q''_{peak} (MW/m^2)	0.50	1.00	2.00	3.00
T_{Be}/T_{Be}^{max} (600 ^{0}C)	0.50	0.67	1.01	1.35
T_{Be}/T_{Be}^{max} (800 ^{0}C)	0.38	0.50	0.76	1.01
T_{Be}/T_{Be}^{max} (1200 ^{0}C)	0.25	0.34	0.51	0.68
$T_{struc}/T_{struc}^{max}$ (550 ^{0}C)	0.50	0.65	0.93	1.21
Stress/$3S_m$	0.53	0.85	1.48	2.13

Table 4.3.3.2 Heat Flux Limits and Heat Removal Parameters
for HT-9 Using 14 MPa H_2O (v = 7 m/s)

q''_{peak} (MW/m^2)	0.5	1.0	2.0	3.0
T_c^{exit} (^{0}C)	205	210	222	232
T_w^{exit} (^{0}C)	215	230	260	290
v/L	7	7	7	7
h (W/m^2K)	~48,000	~48,000	~48,000	~48,000
T_{Be}/T_{Be}^{max} (600 ^{0}C)	0.50	0.67	1.01	1.35
$T_{struc}/T_{struc}^{max}$ (550 ^{0}C)	0.50	0.65	0.93	1.21
stress/$3S_m$	0.53	0.85	1.48	2.13
Factor	$q''_{peak}{}^{max}$ (MW/m^2)			
T_{Be}^{max} (600 ^{0}C)	2.0			
T_{struc}^{max} (550 ^{0}C)	2.1			
stress	1.23			

4.3.4 HT-9 / He (15 MPa)

Compared to the HT-9-high pressure water design, the HT-9-helium design has a lower heat flux limit of less than 0.5 MW/m^2 (compared to 1.23 MW/m^2), limited by pumping power. At 0.5 MW/m^2, a high velocity of 50 m/s is required to remove the heat and obtain a T_w^{exit} of 495 ^{0}C (see Table 4.3.4.2). The total pumping power is ~9 MW, which exceeds that for the water designs (~1 MW). The second most limiting factor is T_{struc}^{max}, yielding a heat flux limit of 0.5 MW/m^2. The PFC temperature remains elevated due to a high T_w^{exit} (495 ^{0}C). Decreasing this exit coolant temperature from 495 ^{0}C would result in an excessive pumping power. Stress is the least limiting factor, which results in a heat flux limit 1.1 MW/m^2. The corresponding total pumping power is ~80 MW, and a velocity of over 100 m/s. The PFC temperatures and stresses may be decreased, without increasing the pumping power, by decreasing the inlet coolant temperature, T_c^{inlet} from 350 ^{0}C.

The maximum beryllium temperature at 600 ^{0}C limits the heat flux to 0.6 MW/m^2. As depicted in Figure 4.3.4.1, relaxing T_{Be}^{max} to 800 ^{0}C and 1200 ^{0}C, increases the heat flux limit to 2 and 4 MW/m^2, respectively. The corresponding heat removal parameters are presented in Table 4.3.4.2.

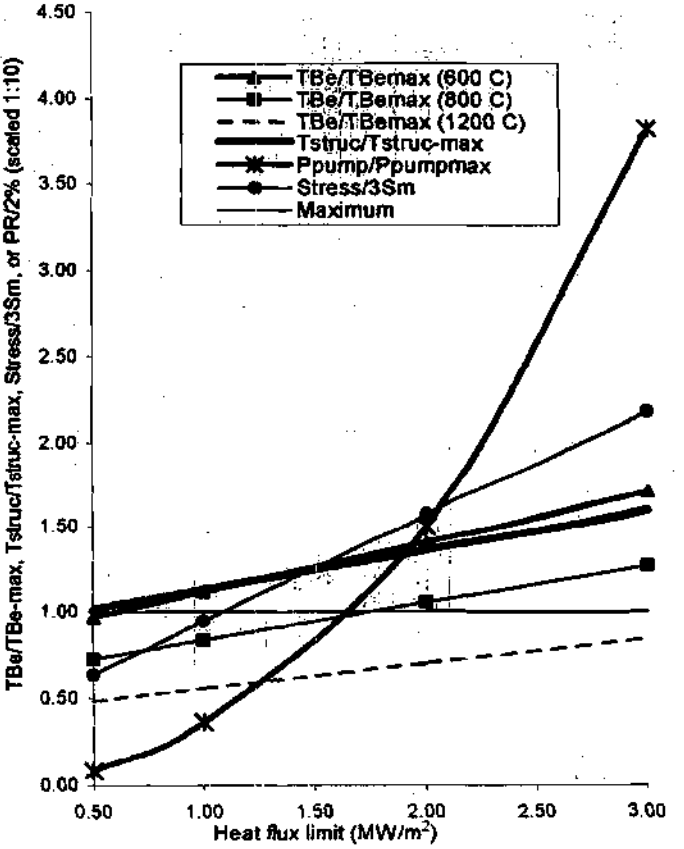

Figure 4.3.4.1 Heat Flux Limit (MW/m^2) Determination Using the T_{Be}/T_{Be}^{max}, $T_{struc}/T_{struc}^{max}$, Stress/$3S_m$, or $P_R/2\%$ (scaled 1:10) Criteria for HT-9 (15 MPa Helium)

Table 4.3.4.1
Heat Flux Limit (MW/m^2) Determination Using the
T_{Be}/T_{Be}^{max}, $T_{struc}/T_{struc}^{max}$, Stress/$3S_m$, or P_R/2% (scaled 1:10)
Criteria for HT-9 (15 MPa Helium)

q''_{peak} (MW/m^2)	0.50	1.00	2.00	3.00
T_{Be}/T_{Be}^{max} (600 ^{0}C)	0.97	1.12	1.41	1.69
T_{Be}/T_{Be}^{max} (800 ^{0}C)	0.73	0.84	1.05	1.27
T_{Be}/T_{Be}^{max} (1200 ^{0}C)	0.48	0.56	0.70	0.85
$T_{struc}/T_{struc}^{max}$	1.01	1.13	1.36	1.59
P_R/2% (scaled 1:10)	0.08	0.36	1.5	3.82
Stress/$3S_m$	0.64	0.95	1.57	2.18

Table 4.3.4.2
Heat Flux Limits and Heat Removal Parameters for HT-9
(T_w^{exit}=495^{0}C) Using 15 MPa Helium

q''_{peak} (MW/m^2)	0.5	1.0	2.0	3.0
T_c^{exit} (^{0}C)	425	420	414	411
T_w^{exit} (^{0}C)	495	495	495	495
v/L	50	109	236	374
h (W/m^{2}K)	7360	13,600	25,400	36,600
P_{pump} (MW)	9.1	78.0	690	2,487
T_{Be}/T_{Be}^{max}(600 ^{0}C)	0.97	1.11	1.4	1.69
T_{struc}/T_{sruc}^{max}(550 ^{0}C)	1.01	1.13	1.36	1.59
stress/3S_m	0.64	0.95	1.57	2.2
Factor	$q''_{peak}{}^{max}$ (MW/m^2)			
T_{Be}^{max}(600 ^{0}C)	0.60			
T_{struc}^{max}(550 ^{0}C)	0.50			
stress	1.1			
2%Pumping power	<0.5			

4.3.5 V-4Cr-4Ti /He (15 MPa)

The most limiting factor for the vanadium and helium design is heat removal, or the pumping power fraction remaining below 2%. The corresponding heat flux limit is less than 0.5 MW/m^2. This heat flux limit is close to the heat flux limit for SS316 and 5 MPa H_2O, ~0.45 MW/m^2. SS316 has poor thermo-mechanical properties, specifically a low yield and ultimate tensile stress and low thermal conductivity. This affects the heat flux limit in the form of a maximum allowable stress and maximum material temperatures. Vanadium alloys, on the other hand, have excellent thermo-mechanical properties, and the heat flux limit should be significantly *greater* than the heat flux limit when using SS316. However, the use of helium hinders the heat removal capability due to the limit on pumping power (or pumping power fraction). Sensitivity studies are performed to examine the effect of relaxing the requirement on P_R (see Section 4.4.1). The required total pumping power is ~9MW, with a corresponding velocity of 50 m/s. The second limiting factor is the maximum beryllium temperature (600 ^{0}C), with a heat flux limit of 0.65 MW/m^2, and stress, which limits the heat flux to 1.8 MW/m^2. As illustrated in Table 4.3.5.1, the total pumping power is excessive, (~80 MW), and removing the heat from the PFC requires high velocities (over 100 m/s). Decreasing the inlet coolant temperature and relaxing the maximum beryllium temperature to

800 ^{0}C and 1200 ^{0}C, would increase the heat flux limit to 2 and 4.5 MW/m^{2}, respectively, without requiring an excessive pumping power.

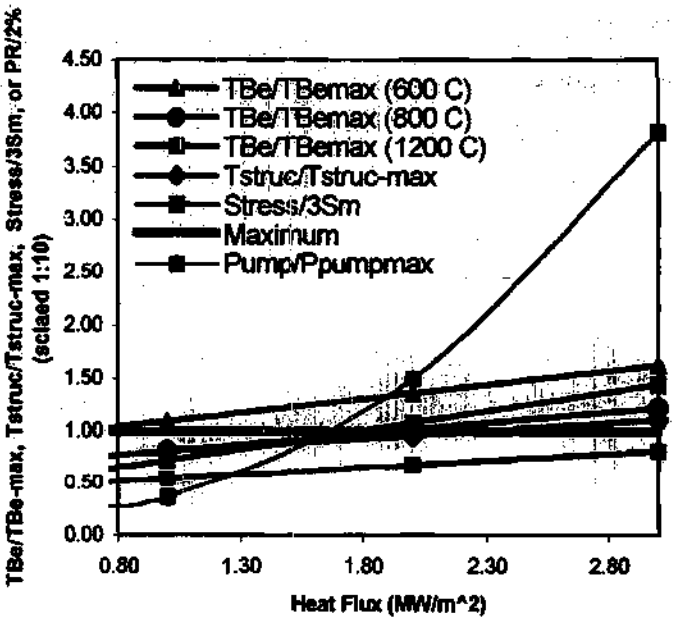

Figure 4.3.5.1 Heat Flux Limit (MW/m^2) Determination Using the T_{Be}/T_{Be}^{max}, $T_{struc}/T_{struc}^{max}$, $Stress/3S_m$, or $P_R/2\%$ (scaled 1:10) Criteria for V-4Cr-4Ti (15 MPa Helium)

Table 4.3.5.1
Heat Flux Limit (MW/m^2) Determination Using the
TBe/TBe-max, Tstruc/Tstruc-max, or Stress/3Sm Criteria
for V-4Cr-4Ti (15 MPa Helium)

q''_{peak} (MW/m^2)	**0.50**	**1.00**	**2.00**	**3.00**
T_{Be}/T_{Be}^{max} (600 ^{0}C)	0.96	1.09	1.36	1.63
T_{Be}/T_{Be}^{max} (800 ^{0}C)	0.72	0.82	1.02	1.22
T_{Be}/T_{Be}^{max} (1200 ^{0}C)	0.48	0.55	0.68	0.81
$T_{struc}/T_{struc}^{max}$ (750 ^{0}C)	0.73	0.81	0.96	1.11
P_R/2% (scaled 1:10)	0.08	0.36	1.5	3.82
Stress/$3S_m$	0.55	0.72	1.08	1.44

Table 4.3.5.2
Heat Flux Limits and Heat Removal Parameters for V-4Cr-4Ti
(T_w^{exit}=495^{0}C) Using 15 MPa Helium

q''_{peak} (MW/m^2)	0.5	1.0	2.0	3.0
T_c^{exit} (^{0}C)	425	420	414	411
T_w^{exit} (^{0}C)	495	495	495	495
v/L	50	109	236	374
h (W/m^{2}K)	7360	13,600	25,400	36,600
P_{pump} (MW)	9.1	78.0	690	2,487
$T_{struc}/T_{struc}^{max}$(750 ^{0}C)	0.73	0.81	0.96	1.11
T_{Be}/T_{Be}^{max} (600 ^{0}C)	0.96	1.09	1.36	1.63
stress/3S_m	0.55	0.72	1.08	1.44

Factor	$q''_{peak}{}^{max}$ (MW/m^2)
T_{Be}^{max} (600 ^{0}C)	0.65
T_{struc}^{max} (750 ^{0}C)	2.3
stress	1.8
2% Pumping power	<0.5

4.3.6 V-4Cr-4Ti / H_2O (14 MPa)

Neglecting material compatibility, the vanadium alloy, V-4Cr-4Ti, and high-pressure water is studied to observe the effect of increasing the heat flux limit, and the results are compared to the vanadium and high-pressure helium design. Using vanadium alloys with helium results in reduced heat flux limits compared to using H_2O.

The maximum beryllium temperature of 600 ^{0}C limits the high pressure H_2O and V-4Cr-4Ti design. This corresponds to a heat flux limit of 2.0 MW/m^2 opposed to only 0.5 MW/m^2 for V-4Cr-4Ti high-pressure helium design. The heat flux limit is increased to 3 and > 4 MW/m^2, for a T_{Be}^{max} of 800 ^{0}C and 1200 ^{0}C, respectively (see Figure 4.3.6.1). The corresponding coolant velocity (7 m/s) with the heat flux limit (and factor) for the V-4Cr-4Ti and high-pressure water, are illustrated in Table 4.3.6.2. Low coolant velocities is another advantage when using H_2O opposed to helium. Helium velocities are greater than H_2O (>20 m/s). The maximum material temperature for V-4Cr-4Ti is an advantage for PFC applications. The greatest heat flux limit is 4.0 MW/m^2 when considering T_{struc}^{max}. Therefore, vanadium alloys may be used without beryllium, however, the effects of vanadium on the plasma should be studied.

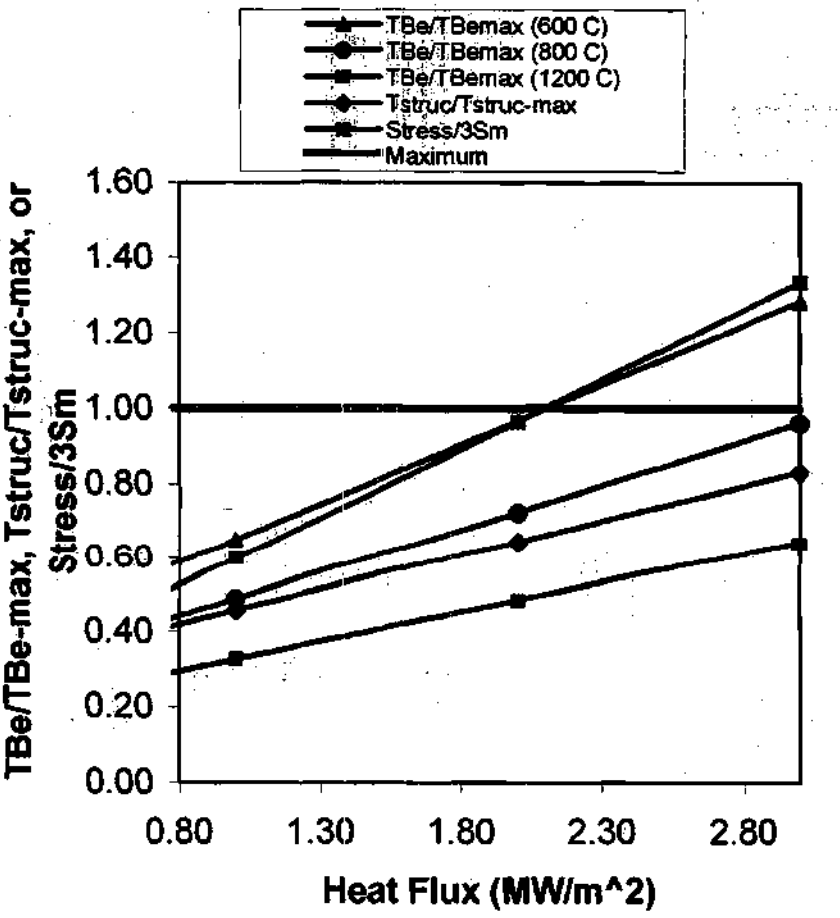

Figure 4.3.6.1 Heat Flux Limit (MW/m^2) Determination Using T_{Be}/T_{Be}^{max}, $T_{struc}/T_{struc}^{max}$, or stress/$3S_m$, Criteria for V-4Cr-4Ti (14 MPa H_2O)

Table 4.3.6.1
Heat Flux Limit (MW/m^2) Determination Using the T_{Be}/T_{Be}^{max}, $T_{struc}/T_{struc}^{max}$, or Stress/$3S_m$ Criteria for V-4Cr-4Ti (14 MPa H_2O)

q''_{peak} (MW/m^2)	0.50	1.00	2.00	3.00
T_{Be}/T_{Be}^{max} (600 ^{0}C)	0.49	0.65	0.97	1.28
T_{Be}/T_{Be}^{max} (800 ^{0}C)	0.37	0.49	0.73	0.96
T_{Be}/T_{Be}^{max} (1200 ^{0}C)	0.25	0.33	0.48	0.64
$T_{struc}/T_{struc}^{max}$	0.36	0.45	0.65	0.83
Stress/$3S_m$	0.41	0.60	0.97	1.34

Table 4.3.6.2 Heat Flux Limits and Heat Removal Parameters for V-4Cr-4Ti Using 14 MPa H_2O (v = 7 m/s)

q''_{peak} (MW/m^2)	0.5	1.0	2.0	3.0
T_c^{exit} (^{0}C)	205	210	222	232
T_w^{exit} (^{0}C)	215	230	260	290
v/L	7	7	7	7
h (W/m^2K)	~48,000	~48,000	~48,000	~48,000
T_{Be}/T_{Be}^{max} (600 ^{0}C)	0.49	0.65	0.97	1.28
$T_{struc}/T_{struc}^{max}$ (750 ^{0}C)	0.36	0.45	0.65	0.83
Stress/$3S_m$	0.41	0.60	0.97	1.34
Factor	$q''_{peak}{}^{max}$ (MW/m^2)			
T_{Be}^{max} (600 ^{0}C)	2.0			
T_{struc}^{max} (750 ^{0}C)	4.0			
stress	2.0			

4.4 Sensitivity Studies

4.4.1 Maximum Allowable Pumping Power Fraction (V-4Cr-4Ti / He (15 MPa))

Observing the fact that heat removal inhibits the performance of the V-4Cr-4Ti / He design, a sensitivity study was performed to observe the effect of the relaxation of the pumping power design parameter, P_R. Like all cases using helium, this pumping power fraction, P_R, is required to remain below 2%, which limits the heat removal capability, which yields a heat flux limit of <0.5 MW/m^2. Other research presents P_R in a range of 0.5 to a few percent (11), (15). The heat flux limit, varying with P_R is presented in Figure 4.4.1.1. The heat flux limit varies non-linearly with the P_R to 2 % ratio. An increase in the P_R to 2% ratio from 1 to 25 only increases the heat flux form 0.8 to ~2.0 MW/m^2. Comparing the V-4Cr-4Ti / He design with the SS316/H_2O (14 MPa) design, the heat flux limits are close (0.50 MW/m^2) with a P_R of 2%. Relaxing P_R increases the heat flux limit, but increases the pumping power. Another method of increasing the heat flux limit when using vanadium alloys without excessive pumping power requirements is to use high-pressure water as a coolant. Neglecting material compatibility, the vanadium alloy, V-4Cr-4Ti and high-pressure water case is studied to observe the effect of increasing the heat flux limit.

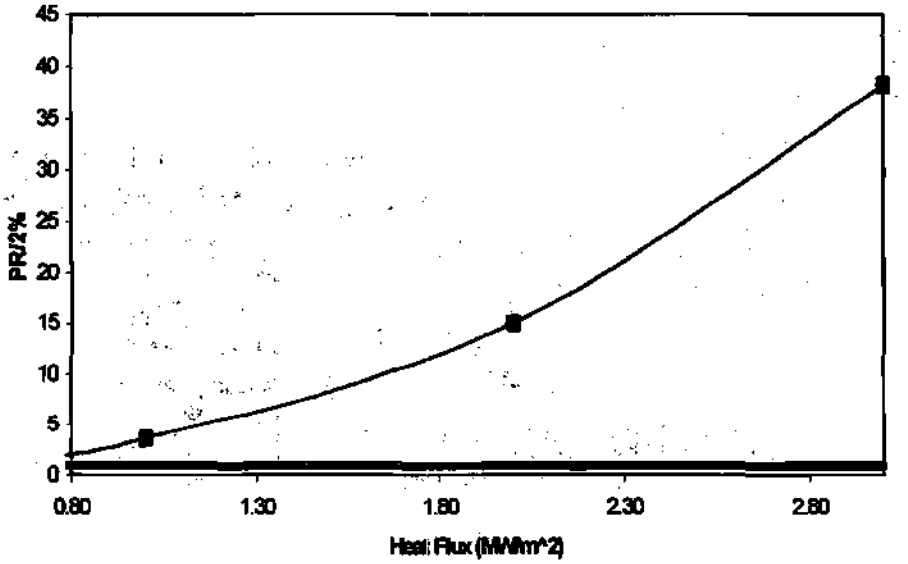

Figure 4.4.1.1 Heat Flux Limit (MW/m^2) Determination Using the $P_R/2\%$ Criteria for V-4Cr-4Ti (15 MPa Helium)

4.4.2 Maximum Allowable Beryllium Temperature (V-4Cr-4Ti / He (15 MPa))

The limiting factor (given in Table 4.2.1) for vanadium and high pressure helium is heat removal (pumping power fraction of 2%), yielding a heat flux limit of <0.5 MW/m^2. The second most limiting factor is the maximum beryllium temperature, T_{Be}^{max}, which gives a heat flux limit of 0.64 MW/m^2. Sensitivity studies are performed to observe the effect of increasing the heat flux limit by relaxing T_{Be}^{max}. Even relaxing T_{Be}^{max} to 1200 ^0C, the maximum beryllium temperature still limits the design more than do stress or T_{struc}^{max}. This suggests that, due to a high T_{struc}^{max} for V-4Cr-4Ti, the helium and H_2O designs should not include a beryllium sacrificial layer. Instead, this sacrificial layer should be replaced with V-4Cr-4Ti, giving a PFC made entirely of V-4Cr-4Ti. However, further studies must be performed to assess the effect of using V-4Cr-4Ti as a PFC (i.e., assess any negative effects on the plasma). The results are presented in Table 4.4.2.1.

Table 4.4.2.1 Heat Flux Limit for V-4Cr-4Ti/He (15 MPa)
Limited by T_{Be}^{max} for T_w^{exit}=495 ^{0}C

Heat flux limit (MW/m^2)	T_{Be}^{max} (^{0}C)
0.65	600
~2.0	800
>3.0	1200

4.4.3 Coolant Pressure (SS316/ H_2O)

Sensitivity studies are performed to determine the effect of increasing the coolant pressure, which would increase the toroidal length cooled. For a peak surface heat flux, q''_{peak}, of 0.5 MW/m^2 and a T_w^{exit} of 235 ^{0}C, the high pressure water cools 1.2 m, as opposed to 1.0 m for low pressure water. There is little benefit for using high-pressure water when maximizing the toroidal channel length. The benefit to using high-pressure water is to allow higher coolant tube exit temperatures. However, when using stainless steel or ferritic steel (HT-9), stress is the limiting factor, and minimizing the primary stress would increase the heat flux limit. Since T_w^{exit} and primary stress are a function of coolant pressure, using low-pressure water is more suitable than high-pressure water

CHAPTER V

COMPARISON WITH PREVIOUS RESULTS

5.1 Literature Review

Several technical reports/journals were studied to derive a basic geometry and material/coolant database for the ITER first wall. The ITER divertor designs are similar to the first wall design, and are required to handle higher peak surface heat fluxes. Therefore, divertor designs were reviewed (in addition to first wall designs).

In the Mogahed and Sviatoslasky study, (11), a 3-D block model (similar to the design of this study), was analyzed. The design was constructed of a 1cm-beryllium sacrificial layer, 1.9 cm Glidcop A125 Cu structural/coolant tube material, and a 1-cm diameter channel. Low-pressure water (4 MPa) was used to cool the first wall. ANSYS Revision 5.2 software performed the heat removal and heat conduction calculations. Structural boundary conditions included planes of symmetry and free rotation/translation of the structure. For a coolant tube wall temperature, T_w^{exit}, of 140^0C, the design accommodated peak surface heat fluxes

ranging from 3-5 MW/m^2. Compared to the design used in this study, these peak surface heat fluxes are very high. The contributing factor is (1) the use of copper as the structural material and heat sink, and (2) the use of a 13-mm groove depth in the radial direction along the beryllium-Cu interface. Copper has a thermal conductivity ~30 times the value for SS316, and ~10 times the conductivity for V-4Cr-4Ti. However, copper alloys are more radioactive than vanadium alloys or stainless steels. The design presented in this study does not take credit for any heat transfer from a surface via a groove or fin. In the Mogahed and Sviatoslasky study, the use of a 13 mm groove reduced the thermal stress from ~1600 MPa to ~300 MPa, for a surface heat flux of 3 MW/m^2. The thermal stress for the Be-SS316, in this study, is ~300 MPa for a surface heat flux of 0.5 MW/m^2.

Hechanova and Kazimi (5) designed a divertor plate (similar to the first wall design). Circular coolant tubes directly faced the plasma. These coolant tubes consisted of a beryllium sacrificial layer and a copper alloy structural/coolant tube material. The system was cooled with single-phase, low pressure (3.5 MPa) water, with a low inlet temperature, 50 ^0C, and high velocity, 10 m/s (the coolant velocity may be lowered by increasing the coolant pressure to ~ 15 MPa). The design consisted of an inner tube diameter of 1.5 cm, and an outer tube diameter of 1.8 cm. Heat removal analyses determined the heat removal parameters,

which were input into HEATING3H, to evaluate the temperature/stress intensity profiles throughout the structure. The design handled peak surface heat fluxes of 10-15 MW/m^2, although the beryllium temperature was within a high range: 800-1200 ^{0}C. This design handles higher heat fluxes mainly due to (1) a larger value for the maximum beryllium temperature, T_{Be}^{max}, (2) a higher coolant velocity, (3) a lower coolant inlet temperature (50 ^{0}C opposed to 200 ^{0}C used in this study), and (4) the geometry of the tube. The geometry of the tube is circular, without additional material due to a rectangular shape, which lowers the overall structure. The use of a twisted tape geometry, in the toroidal direction, enhanced the heat transfer coefficient. Our design incorporated a simple, smooth geometry, in the toroidal direction.

Austenitic stainless steels, particularly SS316, with water as the coolant, is commonly used as a structural material due to the known data. Tavassoli and Touboul (1) studied SS316LN-IG for a 1500 MW ITER design. SS316LN-IG was the structural base coupled with a Cu alloy heat sink, protected by a beryllium sacrificial layer. The first wall coolant was low-pressure (3 MPa) water, which removed the heat induced by a neutron wall load of ~1.0 MW/m^2. Grossbeck, Gibson, and Jitsukawa (12) not only considered austenitic, but also ferritic steels, for first wall applications. It was shown that the advantage of using ferritic steels over austenitic steels is the lower irradiation creep rates. A study by

Wang et al benchmarked the heat removal calculations and the resulting heat flux limit, based upon material temperatures for V-4Cr-4Ti and the ferritic-martensitic steel, HT-9. (13). Circular coolant tubes, with only a few millimeters between the plasma and the coolant, did not consist of a beryllium sacrificial layer, which current ITER designs incorporate. A constant volumetric heat source of 10 MW/m^3 did not vary with the peak surface heat flux (non-conservative). Our study accounts for the increase of the volumetric heat source with increasing peak surface heat flux. For example, for a peak surface heat flux of 2 MW/m^2, the corresponding volumetric heat source is ~55 MW/m^3, which is 5 times higher than the 10 MW/m^3 value. This will over-predict the heat flux limit. Based on maximum material temperatures of 750 ^0C, and 550 ^0C for lithium-cooled V-4Cr-4Ti and helium-cooled HT-9, respectively, the heat flux limits were 2.3 and 0.5 MW/m^2, respectively. For SS316, several studies conclude a heat flux limit of 0.5 MW/m^2 (14).

CHAPTER VI

CONCLUSION

A series of heat conduction and heat removal calculations have been performed for a tube bank PFC model with a beryllium sacrificial layer. With the type being developed in the ITER design, different combinations of structural materials and coolants were used for the purpose of comparing maximum allowable heat fluxes for SS316/H_2O, HT-9/ H_2O, HT-9/helium, and V-4Cr-4Ti/helium.

SS316/H_2O is limited to 0.45-0.5 MW/m^2 by the ASME code criterion. Stress, and not material temperature, limits all SS316 designs. Either the pumping power fraction or material temperature limits the helium designs. This arises from a lowest achievable T_w^{exit} of 495^{0}C, and results in a larger overall unit cell temperature. The maximum allowable heat flux for HT-9/helium is <0.5 MW/m^2, limited by pumping power, as opposed to 1.23 MW/m^2 for the water design. V-4Cr-4Ti/helium is limited to <0.5 MW/m^2 by pumping power, and to 0.65 MW/m^2 by the maximum temperature of 600 ^{0}C in the beryllium. Replacing the beryllium sacrificial layer with 5 mm of V-4Cr-4Ti would result in

a higher allowable T_w^{exit}, which lowers the required pumping power, and the temperature of the structure would be allowed to exceed 600 ^{0}C (750 ^{0}C limit for V-4Cr-4Ti opposed to 600 ^{0}C for beryllium).

The calculations presented were all performed for the same geometrical PFC model, which is being developed for SS316/H_2O. As such, they provide a measure of the relative heat removal capabilities of the different structural/coolant combinations. A comparison based on different geometrical designs optimized to the different structural/coolant combinations would be expected to show even larger differences.

CHAPTER VII

REFERENCES

1. Tovassouli, A.a and Touboul, F., "Austenitic Stainless Steels, Status of the Properties Database and Design Rule Development," Journal of Nuclear Materials, 233-237 (1996) 51-61.

2. American Society of Mechanical Engineers, ASME, SECTION II-D, 1995 Edition.

3. Billone, M.C., Dienst, W., Fament, T., Lorenzetto, P., Noda, K., "ITER Solid Breeder Blanket Materials Database," work supported by US DOE under contract W-31-109-Eng 38, November, 1993.

4. Dombrowski, D.E., et al, "Thermomechanical Properties of Beryllium," JET-IR(94)07, Dec. 1994.

5. Hechanova, A.E., and Kazimi, M.S., "Thermo-mechanical Performance of Beryllium Coated Copper Divertors," Fusion Technology, 21.3(1992):1880-1886.

6. Stacey, W.M., Fusion, John Wiley& Sons, 1981.

7. Merola, M., et al, "The Design of the Low Activation Steels for a New Austenitic Alloy," First Wall Technology, 21 Mar(1992):129-141.

8. Igata, N., "Ferritic/Martensitic Dual-Phase Steel As Fusion Reactor Material," Fusion Reactor Materials, Proceedings of the First International Conference, Tokyo, Japan, p. 141-148.

9. Asakura, Kentaro, and Fujita, Toshio, "Elevated Temperature Strength and Toughness of Ferritic Steels," Journal of the Atomic Energy Society of Japan, v28 n3 Mar 1986, p.222-231.

10. Matsui, H., Fkumoto, K., Smith, D.L., Chung, H.M., van Witzenberg, W. Votino, S.N., "Status of Vanadium Alloys for Fusion Reactors," Journal of Nuclear Materials, v233-237 Pt A Oct 1996, Elsevier Science, p. 92-99.

11. Mogahed, E.A., and Sviatoslavsky, I.N., "ITER Limiter First Wall 3-D Thermo-Mechanical Analysis," 12th Topical Meeting on the Technology of Fusion Power, 16-20 June 1996, Reno, NV.

12. Grossbeck, M.L., Gibson, L.T., Jetsukawa, S.., "Irradiation Creep in Austenitic and Ferritic Steels Irradiated in a tailored neutron spectrum to induce fusion reactor levels of helium," Journal of Nuclear Materials, 233-237(1996)148-151.

13. Wang, X.R., Sze, D.K., Tillack, M.S., Wong, C.P.C., "Heat Flux Limits on the Plasma-Facing Components for a Commercial Fusion Reactor," IEEE 1995 Conference on Fusion Engineering.

14. Rebut, P.H., "ITER: The First Experimental Fusion Reactor," Fusion Engineering and Design, 20 (1995)85-118.

15. Personal communication, W.M. Stacey, August 1996.

16. Stacey, W.M., et al., "A Tokamak Tritium Production Reactor", Georgia Tech report GTFR-132 (1996); also, Fusion Technology., to be published (1997).

17. Baxi, Chandu B., "Helium-cooled divertor module for fusion devices," Proceedings of SPIE-The International Society for Optical Engineering, v1997, 1993, p. 108-117.

18. Karditsas, P.J., "Thermal and Structural Behavior of Various First Wall Concepts, Fusion Engineering and Design, 25(1994)273-287.

19. Duderstadt, James J. and Hamilton, Louis J., Nuclear Reactor Analysis, John Wiley & Sons, 1976.

20. Todreas, Neil E. and Kazimi, M.S., Nuclear Systems I-Thermal Hydraulic Fundamentals, Hemisphere Publishing Corp., 1990.

21. ANSYS User's Manual Revision 5.2, August 31, 1995 ANSYS Inc., 275 Technology Drive, Canonsburg, PA.

22. Stacey, W.M., "Tokamak Demonstration Reactors," Nuclear Fusion, Vol. 35, No.11 (1995).

23. Young, Warren C., Roark's Formulas for Stress and Strain, Sixth Edition, McGraw-Hill, Inc., Table 28, pg. 518.

24. Ehst, D., et al, "Tokamak Power Systems Studies-FY 1986: A Second Stability Power Reactor," Argonne National Laboratory, March 1987, pg. 6-39.

25. Incropera, Frank P., and DeWitt, David P., Fundamentals of Heat and Mass Transfer, Third Edition, John Wiley & Sons, 1990, pg.345.

26. Sychev, V.V et al, Thermodynamic Properties of Helium, Hemisphere Publications, Co., 1987.

27. Vargattik, Natan B., et al, Handbook of Thermal Conductivity of Liquids and Gases, CRC Press, 1994.

28. Fetter, S.A., "Radiological Hazards of Fusion Reactors: Models and Comparisons," Ph.D dissertation, UC-Berkeley, 1985.

29. Hoffman, E.A., et al, "Radioactive Waste Disposal Characteristics of Candidate Tokamak Demonstration Reactors", GTFR-019, August 1995.

Appendix A
Coolant and Material Properties

HELIUM

TABLE I PROPERTIES OF HELIUM AT 15 MPa

Property	Table value	Interpolated value	Table value
Specific heat[26] C_p (kJ/kgK)	5.189 (700 K)	5.189 (673 K)	5.188 (600K)
Density ρ^{26} (kg/m^3)	10.04 (700 K)	10.47 (673 K)	11.65 (600K)
Thermal conductivity k[27] (W/mK)	0.2837 (700 K)	0.2835 (673 K)	0.2828 (500 K)

WATER

TABLE II PROPERTIES OF SATURATED WATER AT 5 AND 14 MPa

Property	5 MPa*	14 MPa*
Specific heat[20] C_p (kJ/kgK)	5038	7880
Viscosity μ^{20} (Pa-s)	1.03E-04	7.68E-05
Density ρ^{20} (kg/m^3)	777.7	623.3
Thermal conductivity k^{20} (W/mK)	0.5973	0.4676
Saturation temperature (K/^{0}C)	533/260	609/336

*Interpolated from saturated water tables

TABLE III THERMOPHYSICAL PROPERTIES OF ITER CANDIDATE MATERIALS

Property	**Beryllium (4)**	**SS316 (29)**	**HT-9 (29)**	**V-4Cr-Ti (29)**
Expansion Coefficient α (1/K)	16.0E-06	1.8E-05	1.22E-05	1.04E-05
Elongation Modulus E (MPa)	48.0	166.0	181.0	112.0
Thermal Conductivity k (W/mK)	100.0	14.8	26.2	34.0
Poisson Ratio ν (dimensionless)	0.08	0.27	0.3	0.37
Ultimate Tensile Stress S_u (MPa)	----------	485	396	440
Yield Stress S_y (MPa)	85.0	165	307	270
Design Stress Intensity* S_m (MPa)	----------	110	132	146
Attenuation coefficient μ (m^{-1})	12.5	12.5	12.5	12.5
Temperature (^{0}C)	1000	400	500	600

*Calculated from minimum of $2/3S_y$ of $1/3S_u$

APPENDIX B

ANSYS 5.2 MODEL, TEMPERATURE, AND THERMAL STRESS PROFILES FOR SS316 AND 4 MPa WATER

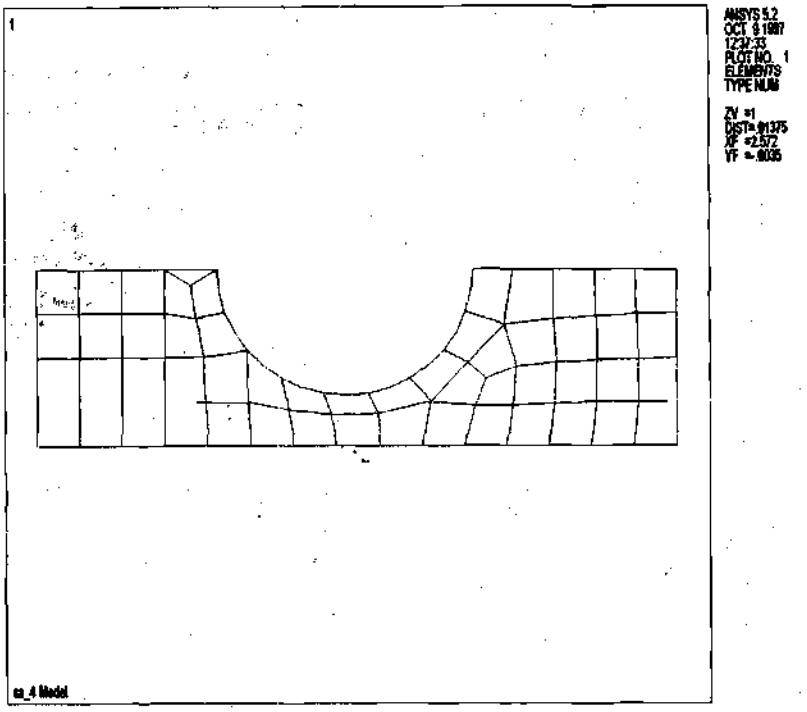

Figure 1 Finite Element Model of PFC for SS316 with q''_{peak} = 3.0 MW/m^2 and T_w^{exit}=286 ^{0}C (5 MPa water)

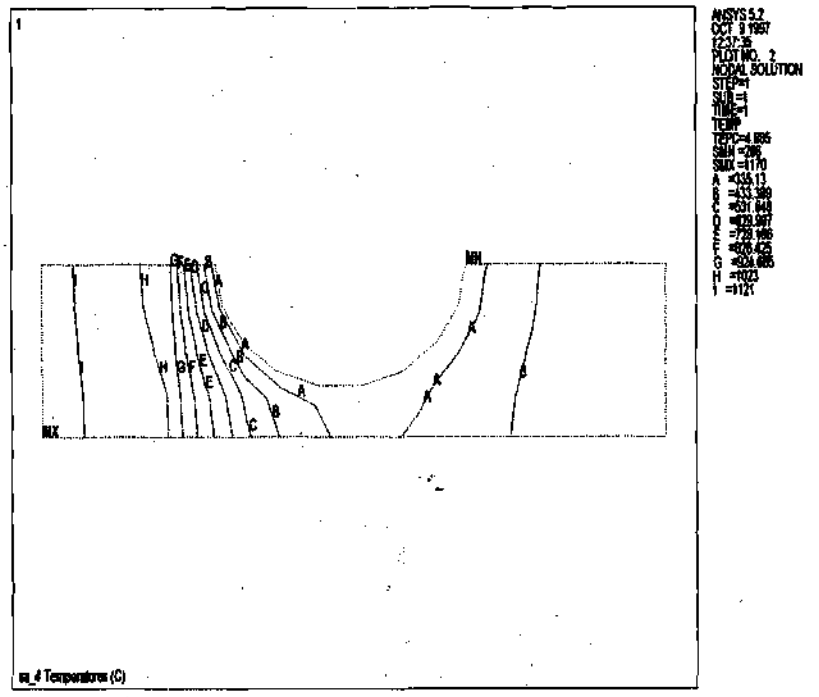

Figure 2 Temperature distribution in PFC for SS316 with q''_{peak} = 3.0 MW/m^2 and T_w^{exit}=286 ^{0}C (5 MPa water)

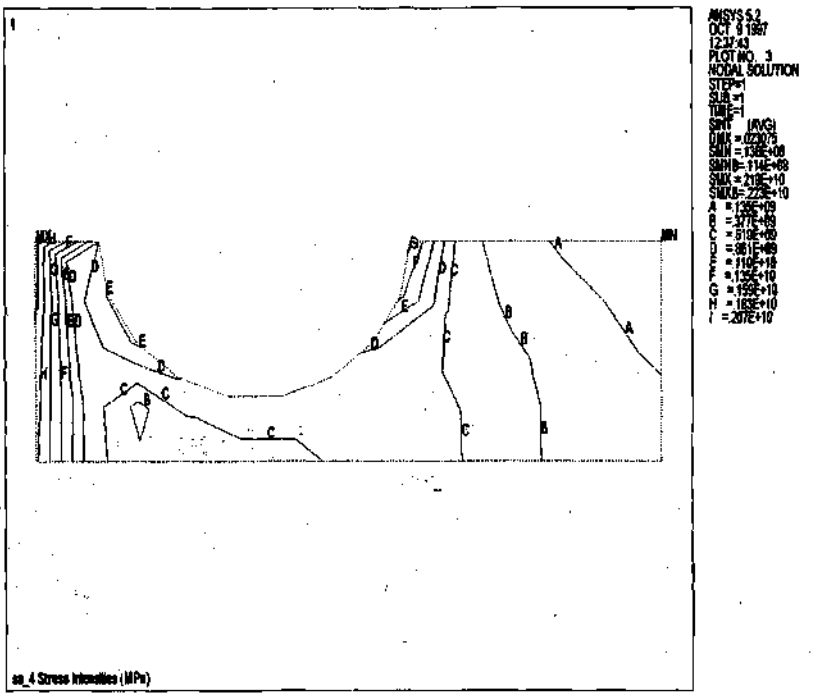

Figure 3 Thermal stress distribution in PFC for SS316 with q''_{peak} = 3.0 MW/m^2 and T_w^{exit}=286 ^{0}C (5 MPa water)

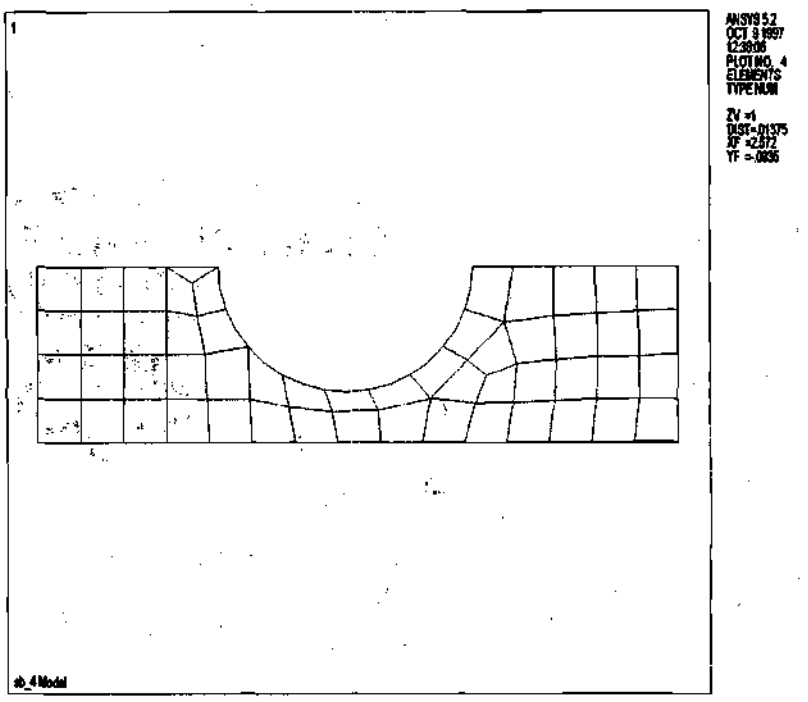

Figure 4 Finite Element Model of PFC for SS316 with q''_{peak} = 2.0 MW/m^2 and T_w^{exit}=367 ^{0}C (5 MPa water)

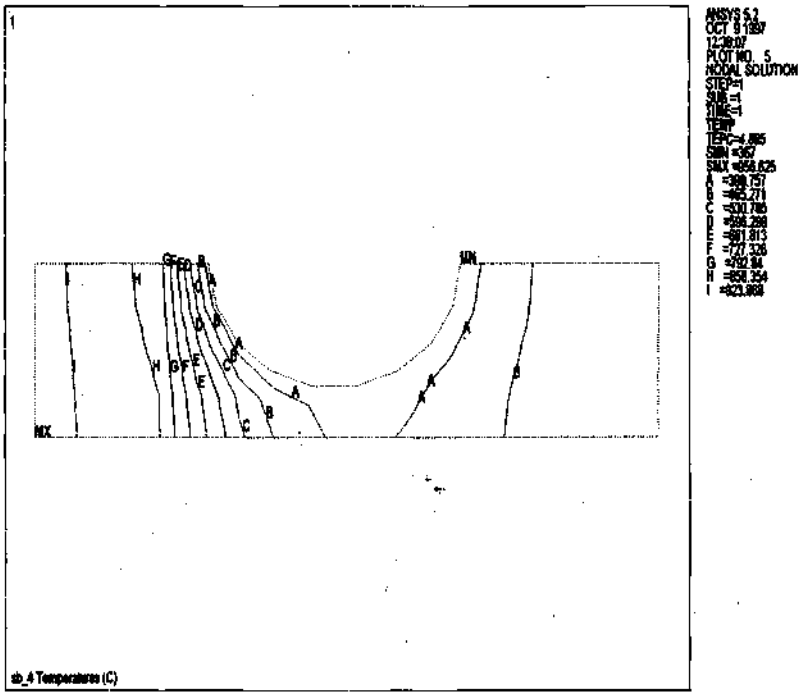

Figure 5 Temperature distribution in PFC for SS316 with q''_{peak} = 2.0 MW/m^2 and T_w^{exit}=367 ^{0}C (5 MPa water)

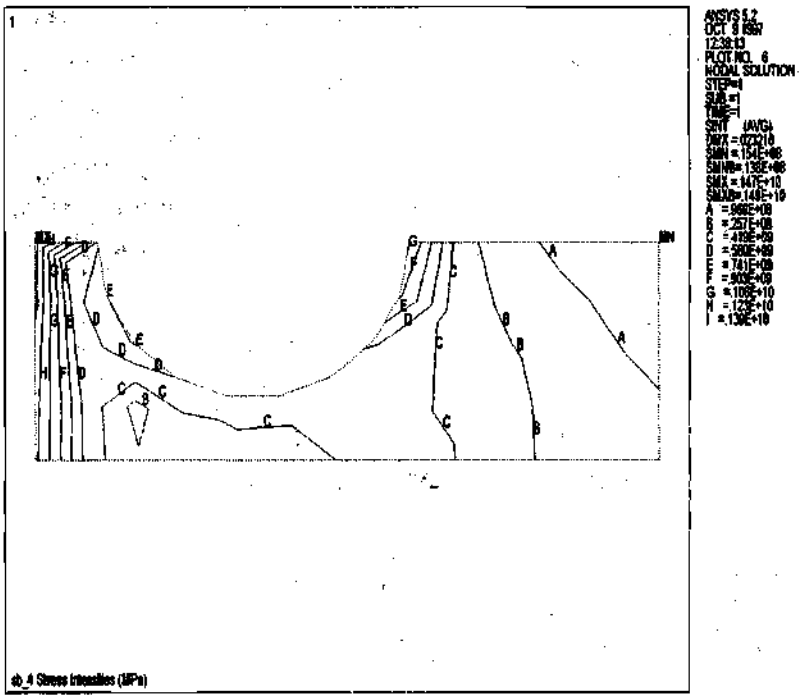

Figure 6 Thermal stress distribution in PFC for SS316 with q''_{peak} = 2.0 MW/m^2 and T_w^{exit}=367 ^{0}C (5 MPa water)

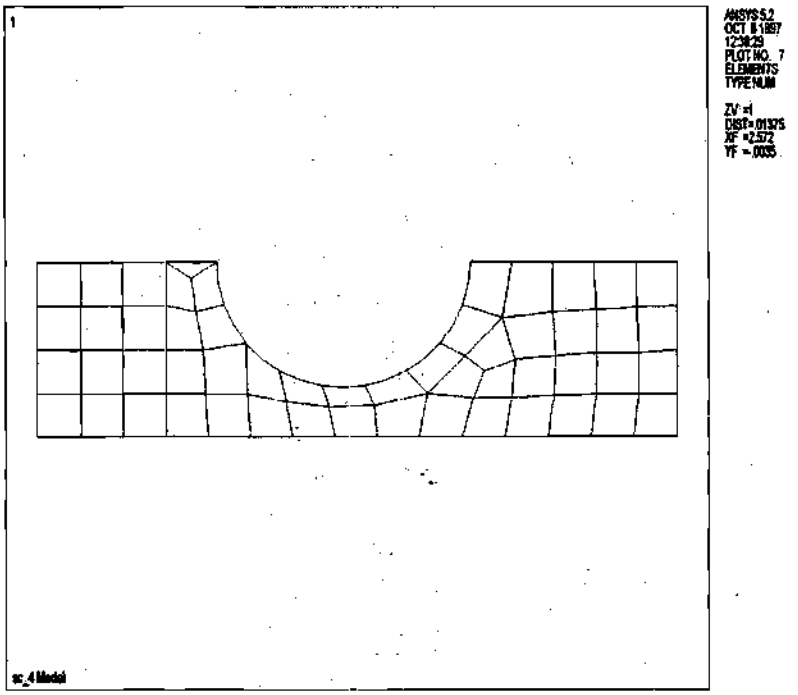

Figure 7 Finite Element Model of PFC for SS316 with q''_{peak} = 1.0 MW/m^2 and T_w^{exit}=276 ^{0}C (5 MPa water)

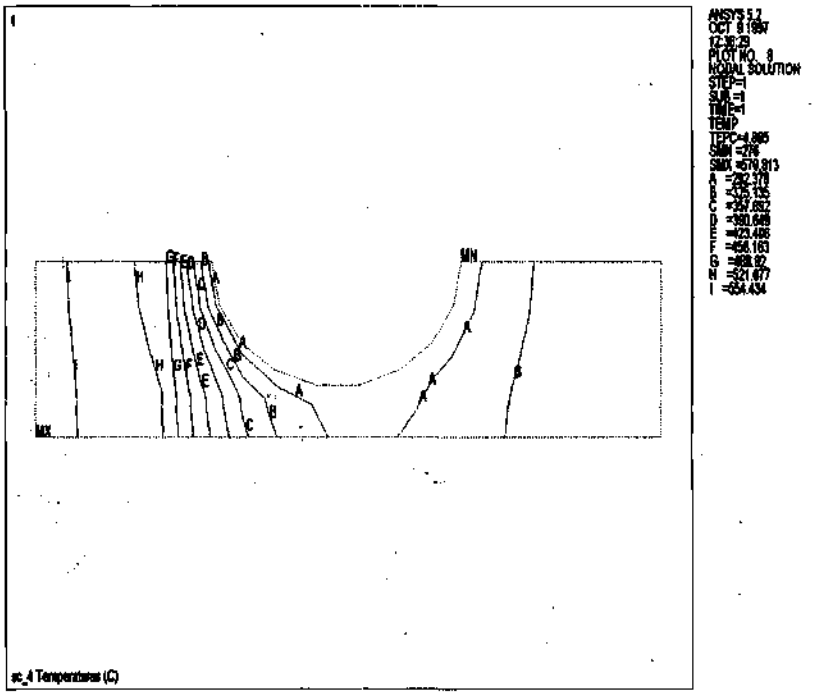

Figure 8 Temperature distribution in PFC for SS316 with q''_{peak} = 1.0 MW/m^2 and T_w^{exit}=276 ^{0}C (5 MPa water)

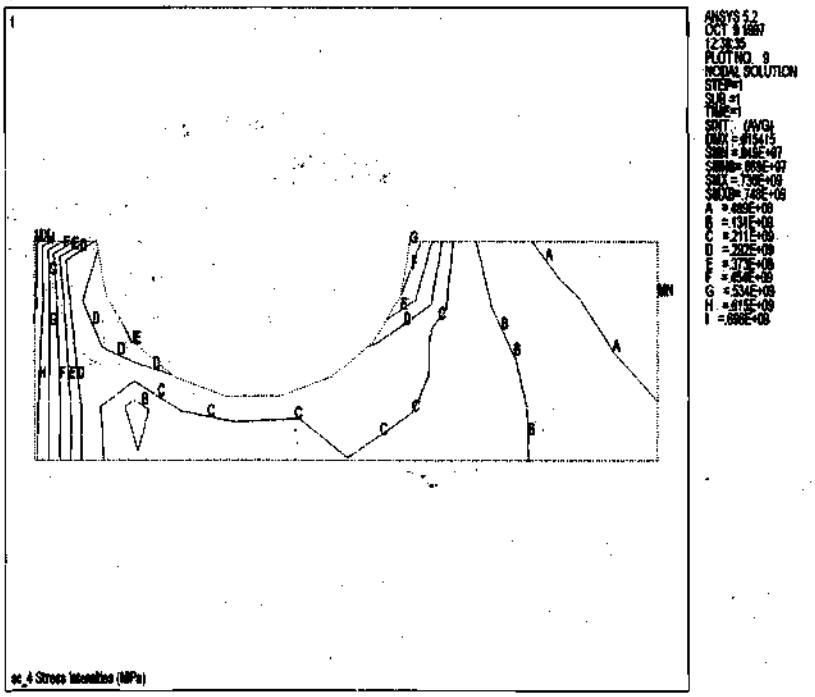

Figure 9 Thermal stress distribution in PFC for SS316 with q''_{peak} = 1.0 MW/m^2 and T_w^{exit}=276 ^{0}C (5 MPa water)

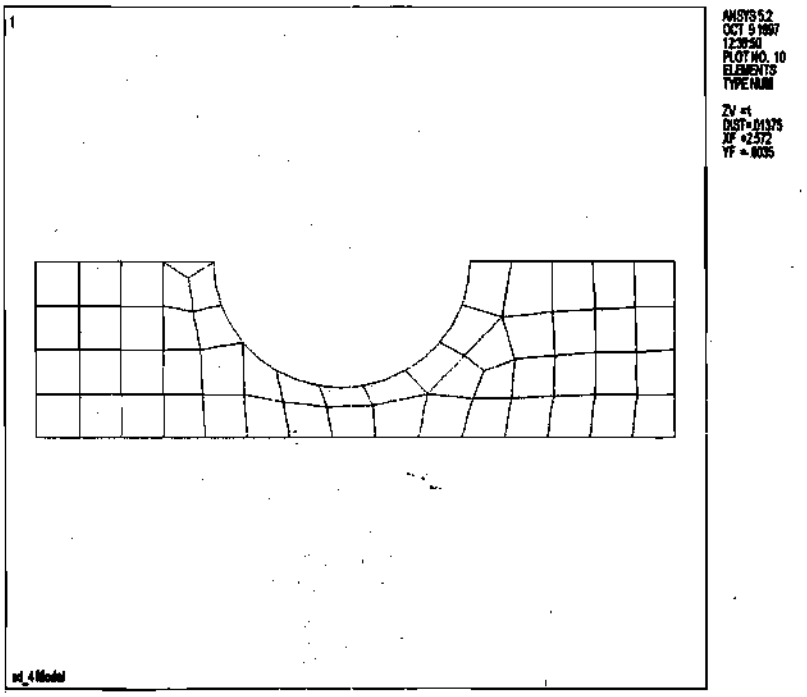

Figure 10 Finite Element Model of PFC for SS316 with $q''_{peak} = 0.5$ MW/m^2 and T_w^{exit}=271 ^{0}C (5 MPa water)

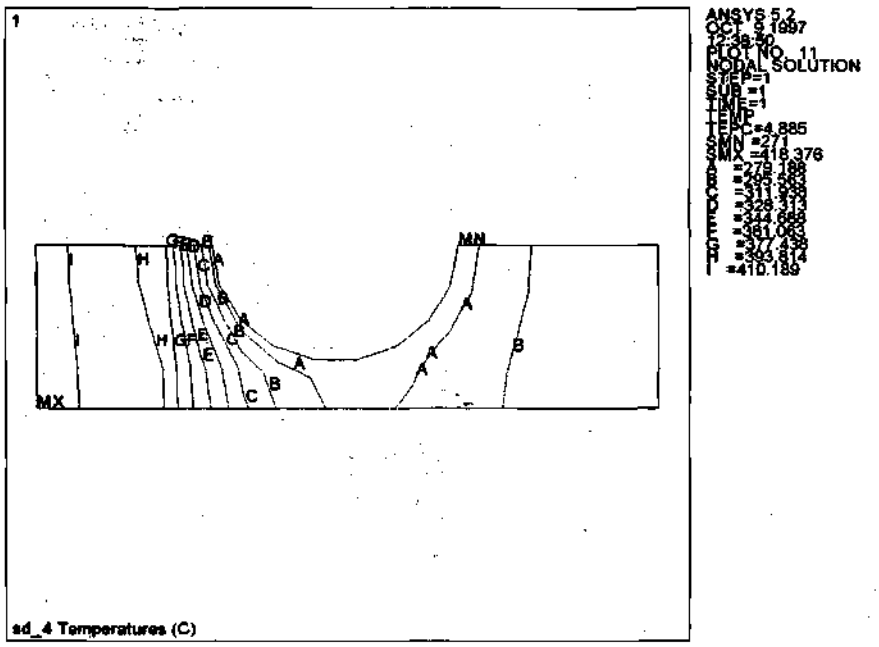

Figure 11 Temperature distribution in PFC for SS316 with q''_{peak} = 0.5 MW/m^2 and T_w^{exit}=271 ^{0}C (5 MPa water)

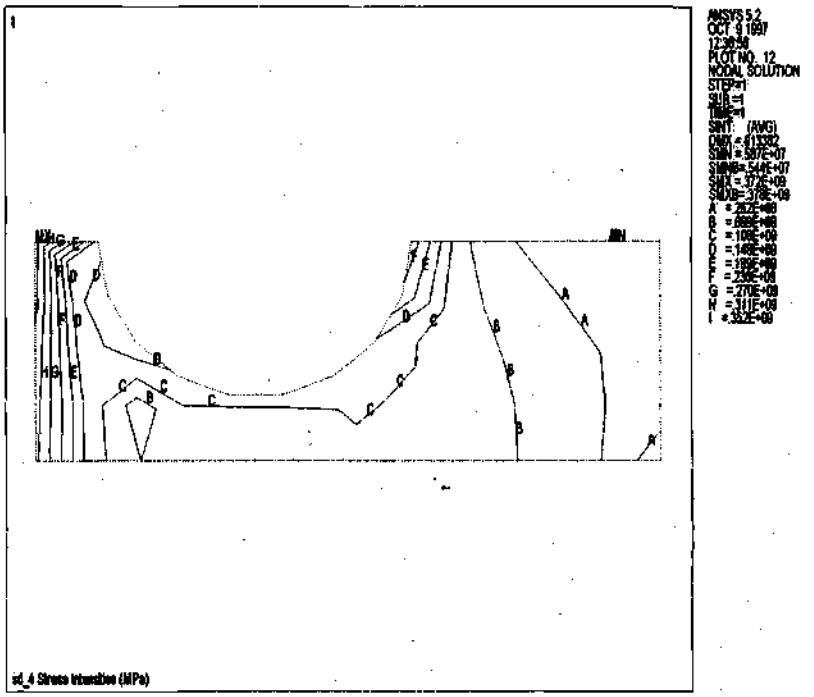

Figure 12 Thermal stress distribution in PFC for SS316 with q''_{peak} = 0.5 MW/m^2 and T_w^{exit}=271 ^{0}C (5 MPa water)

Appendix C

ANSYS 5.2 MODEL, TEMPERATURE, AND THERMAL STRESS PROFILES FOR SS316, HT-9, AND V-4Cr-4Ti FOR 14 MPa WATER

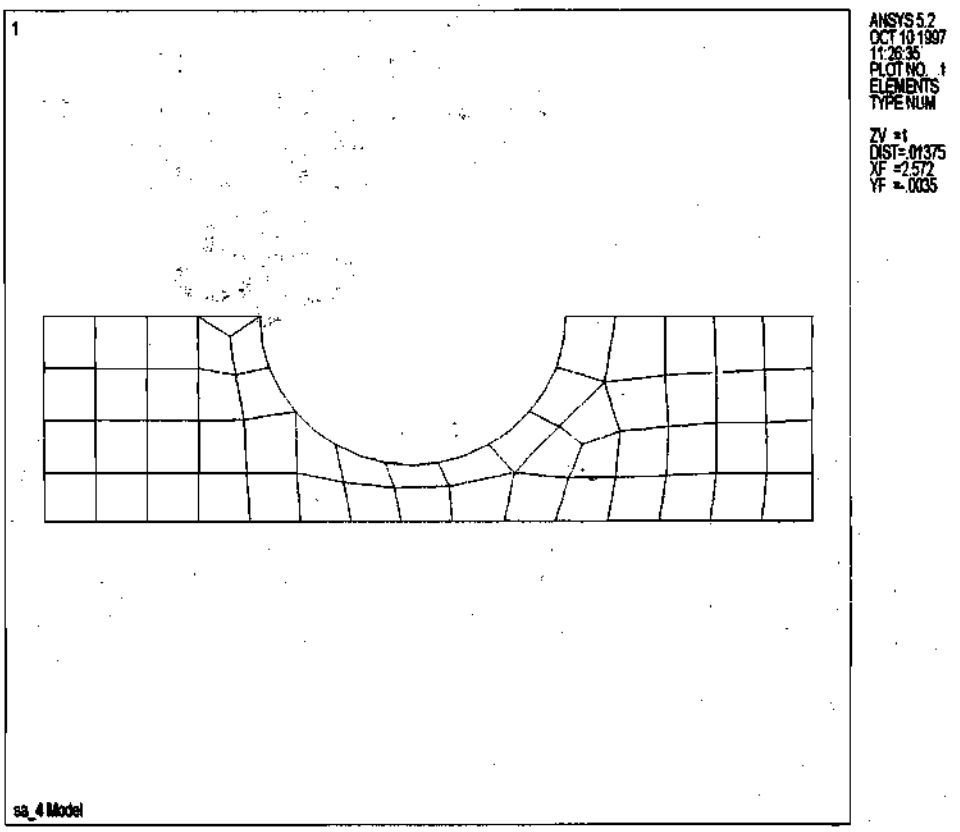

Figure 1 Finite Element Model of PFC for SS316 with q''_{peak} = 3.0 MW/m^2 and T_w^{exit}=281 ^{0}C (14 MPa water)

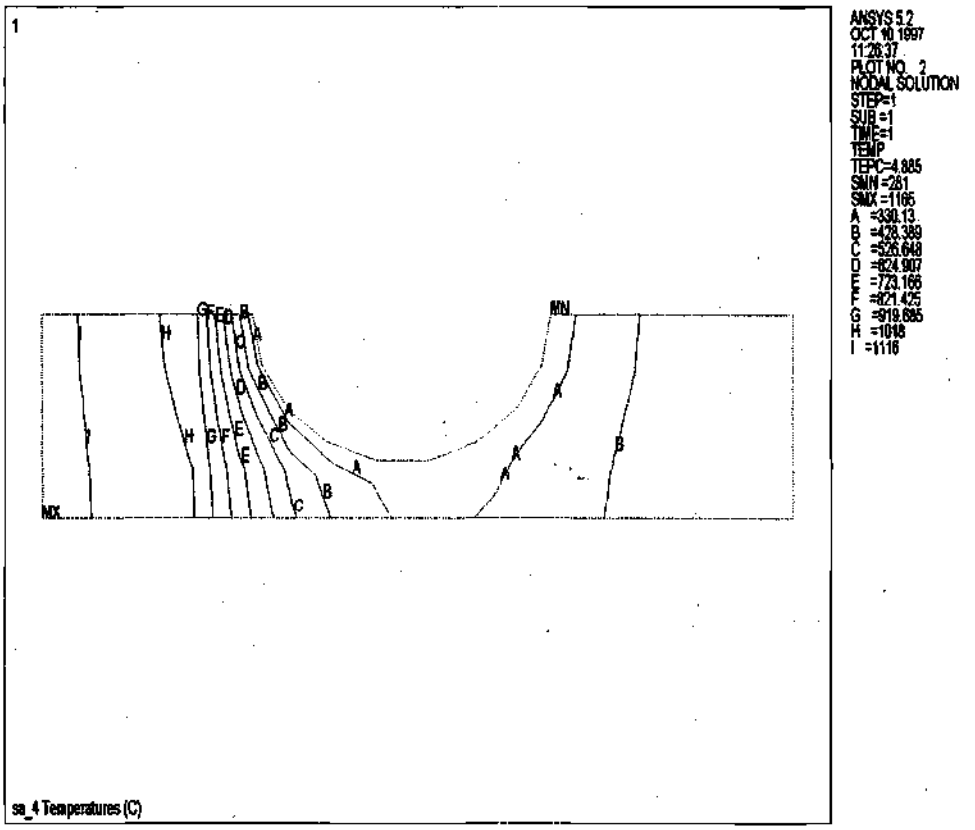

Figure 2 Temperature distribution in PFC SS316 with q''_{peak} = 3.0 MW/m^2 and T_w^{exit}=281 ^{0}C (14 MPa water)

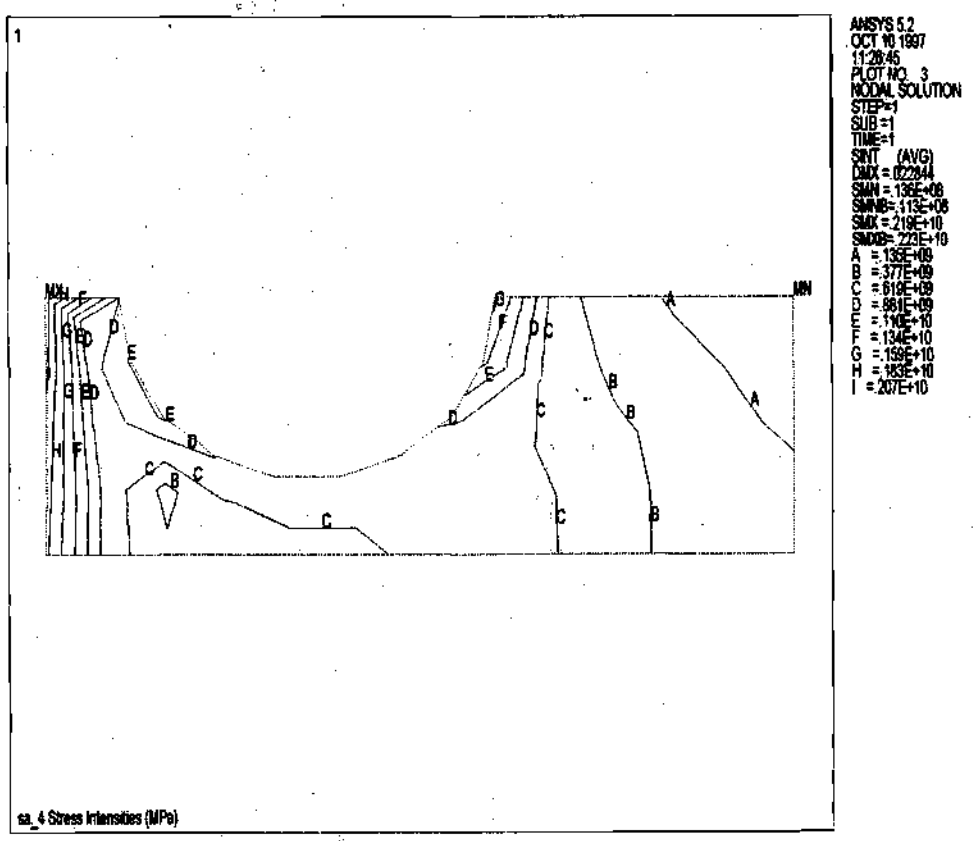

Figure 3 Thermal stress distribution in PFC SS316 with q''_{peak} = 3.0 MW/m^2 and T_w^{exit}=281 ^{0}C (14 MPa water)

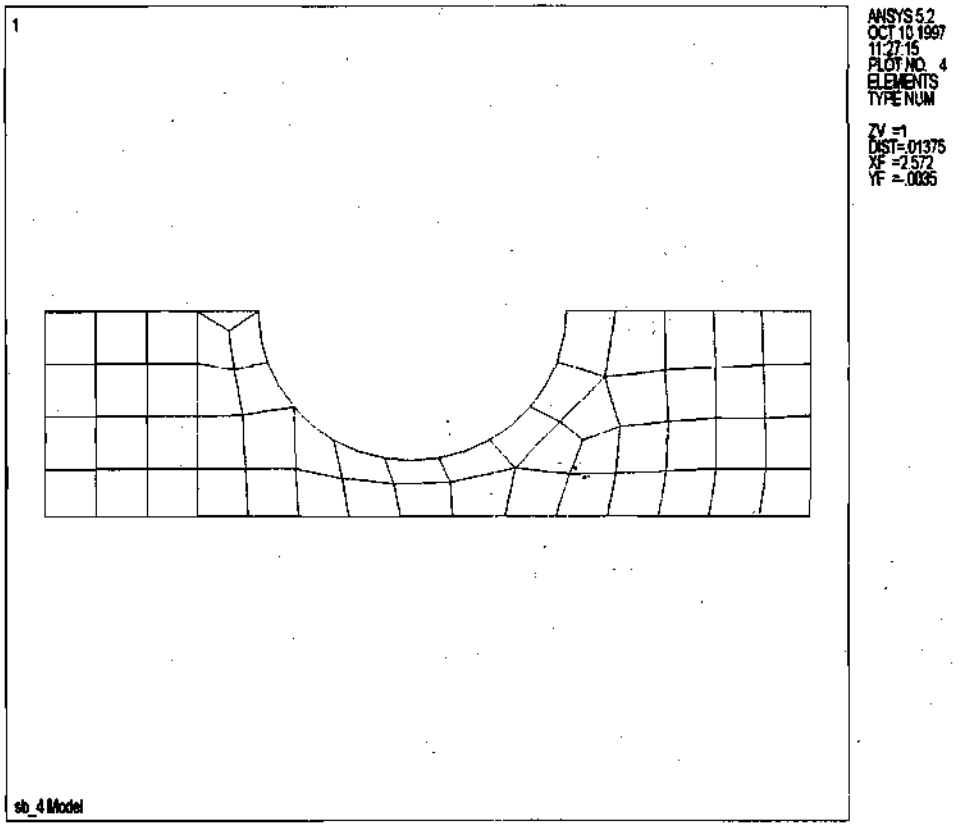

Figure 4 Finite Element Model of PFC
SS316 with q''_{peak} = 2.0 MW/m^2 and
T_w^{exit}=277 ^{0}C (14 MPa water)

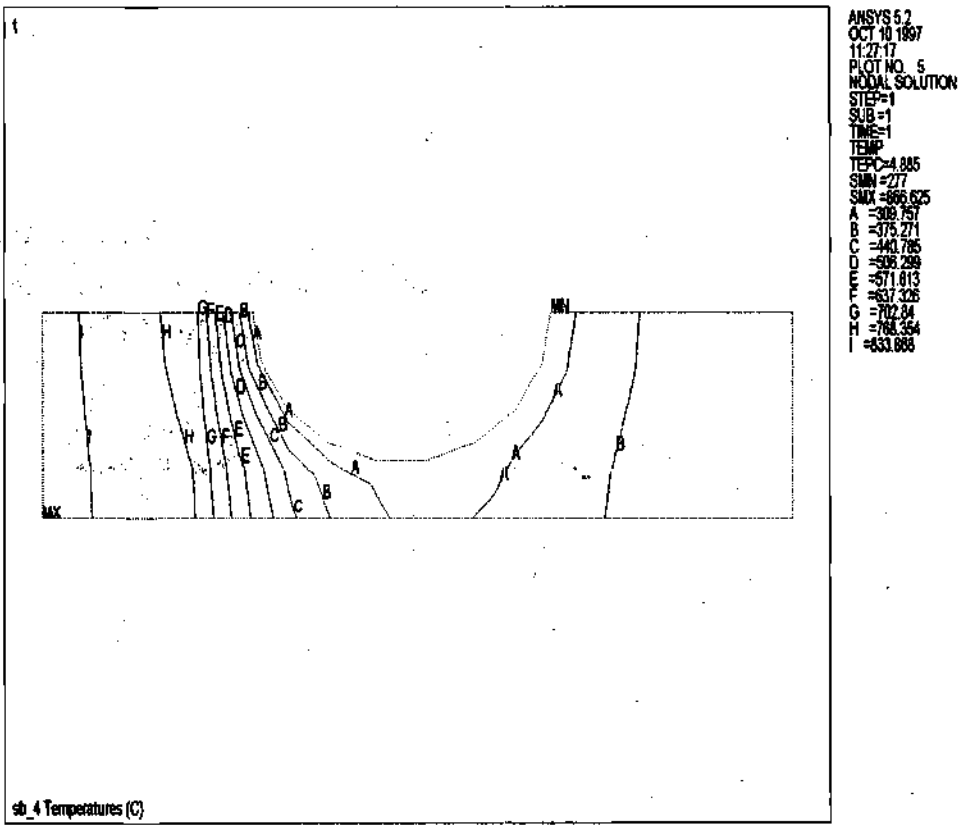

Figure 5 Temperature distribution in PFC SS316 with q''_{peak} = 2.0 MW/m^2 and T_w^{exit}=277 ^{0}C (14 MPa water)

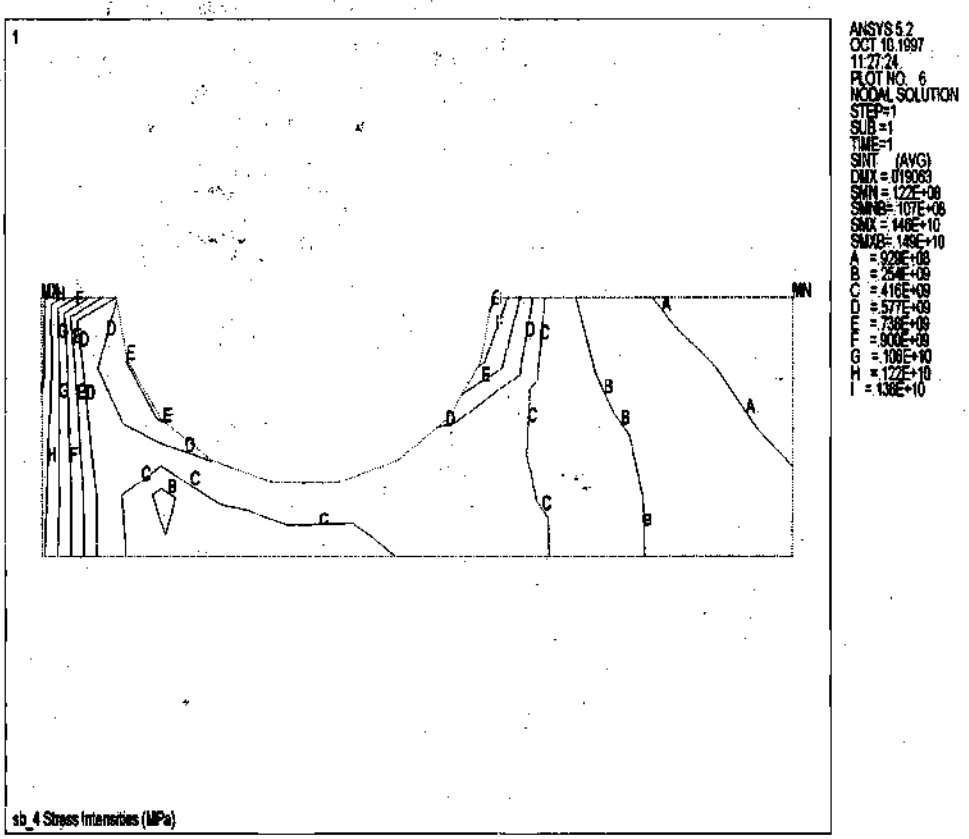

Figure 6 Thermal stress distribution in PFC SS316 with q''_{peak} = 2.0 MW/m^2 and T_w^{exit}=277 ^{0}C (14 MPa water)

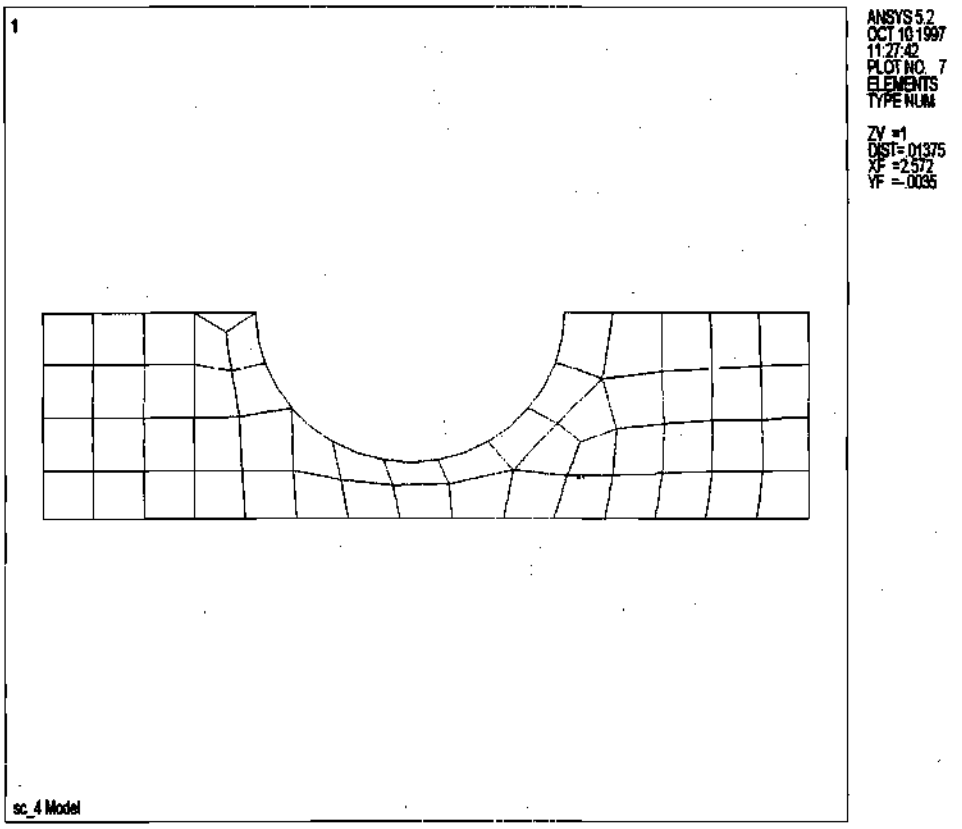

Figure 7 Finite Element Model of PFC SS316 with q''_{peak} = 1.0 MW/m^2 and T_w^{exit}=270 ^{0}C (14 MPa water)

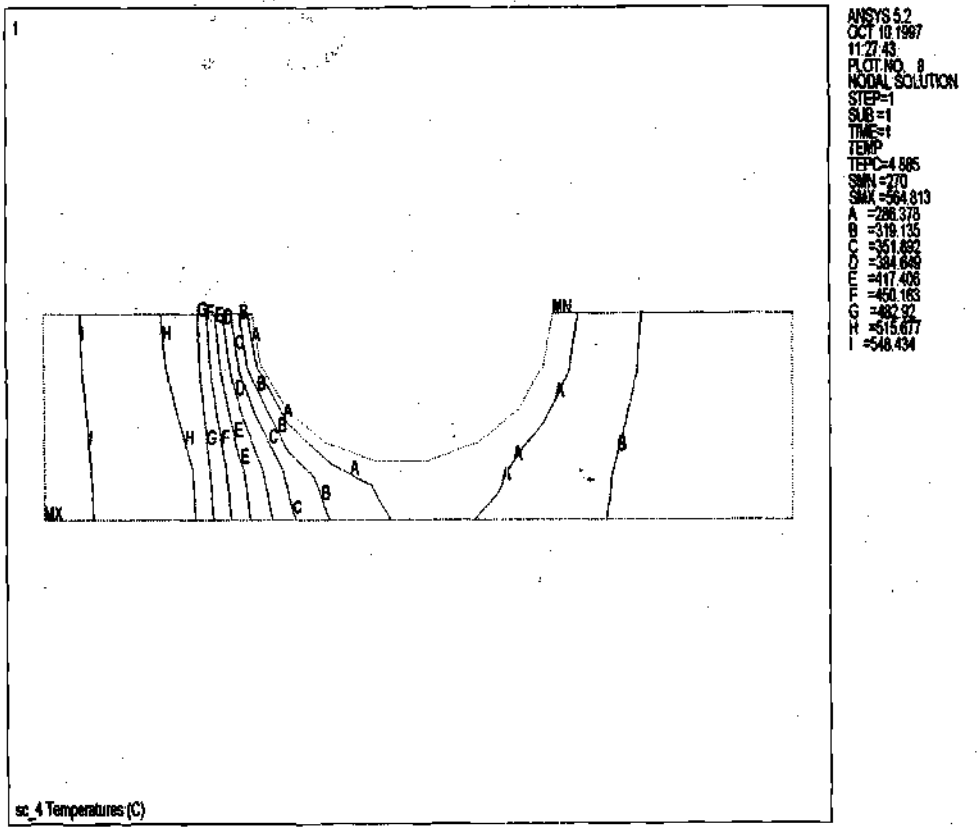

Figure 8 Temperature distribution in PFC SS316 with q''_{peak} = 1.0 MW/m^2 and T_w^{exit}=270 ^{0}C (14 MPa water)

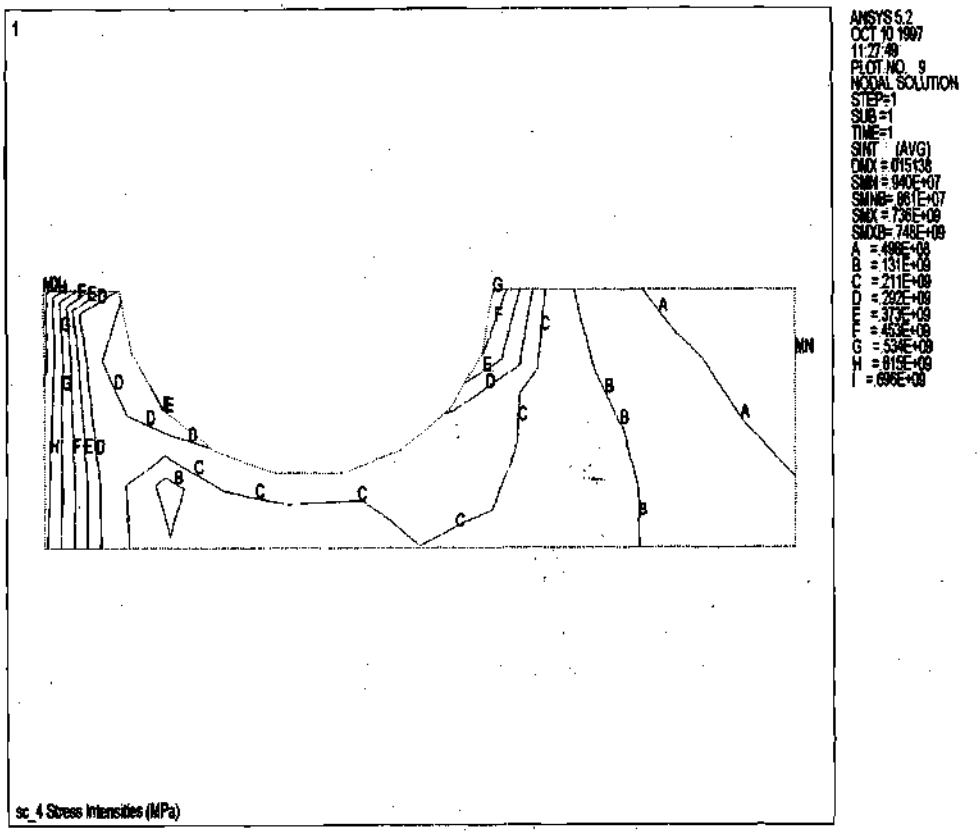

Figure 9 Thermal stress distribution in PFC SS316 with q''_{peak} = 1.0 MW/m^2 and T_w^{exit}=270 ^{0}C (14 MPa water)

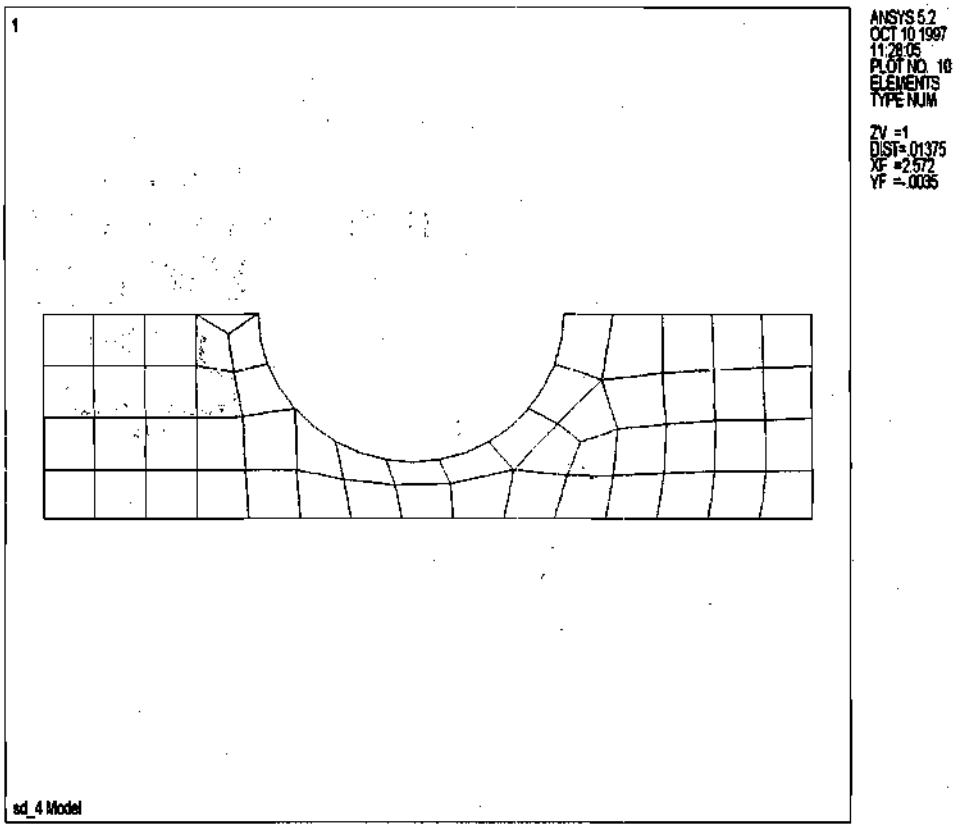

Figure 10 Finite Element Model of PFC SS316 with q''_{peak} = 0.5 MW/m^2 and T_w^{exit}=265 ^{0}C (14 MPa water)

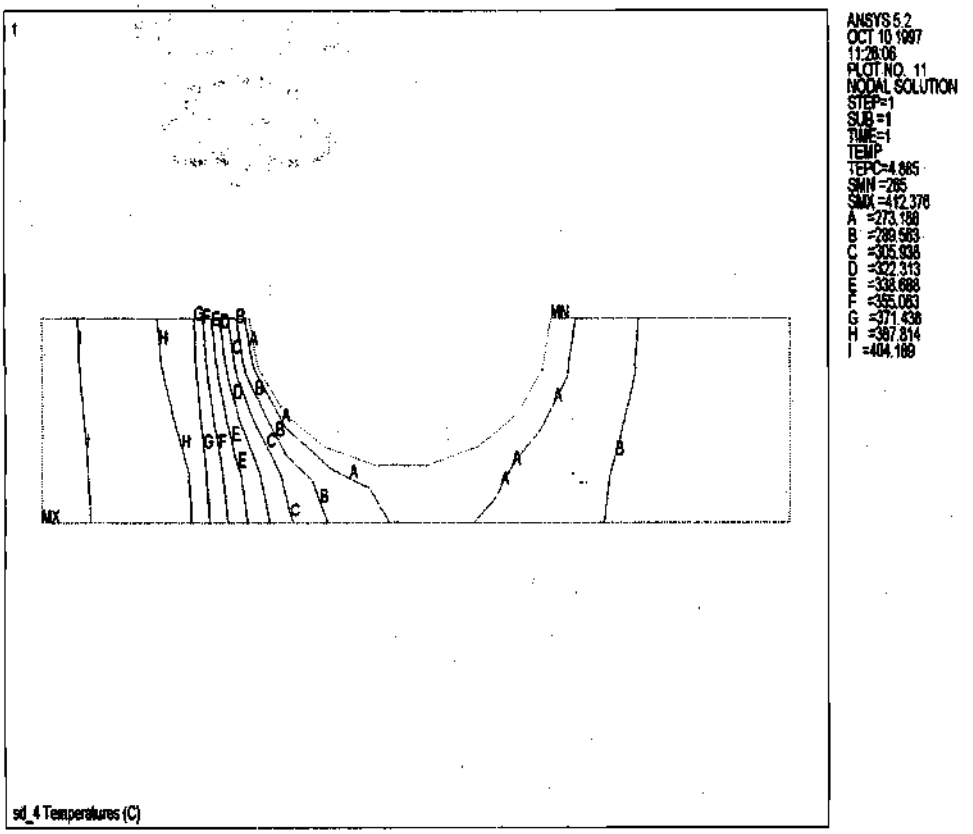

Figure 11 Temperature distribution in PFC SS316 with q''_{peak} = 0.5 MW/m^2 and T_w^{exit}=265 ^{0}C (14 MPa water)

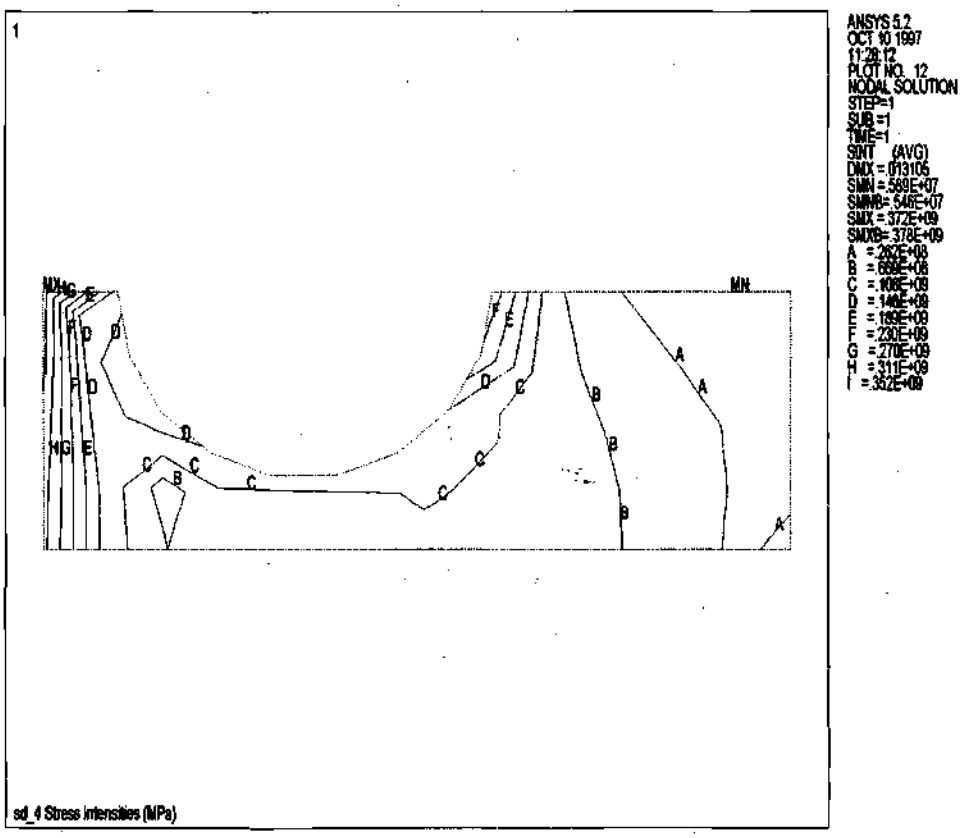

Figure 12 Thermal stress distribution in PFC SS316 with q''_{peak} = 0.5 MW/m^2 and T_w^{exit}=265 ^{0}C (14 MPa water)

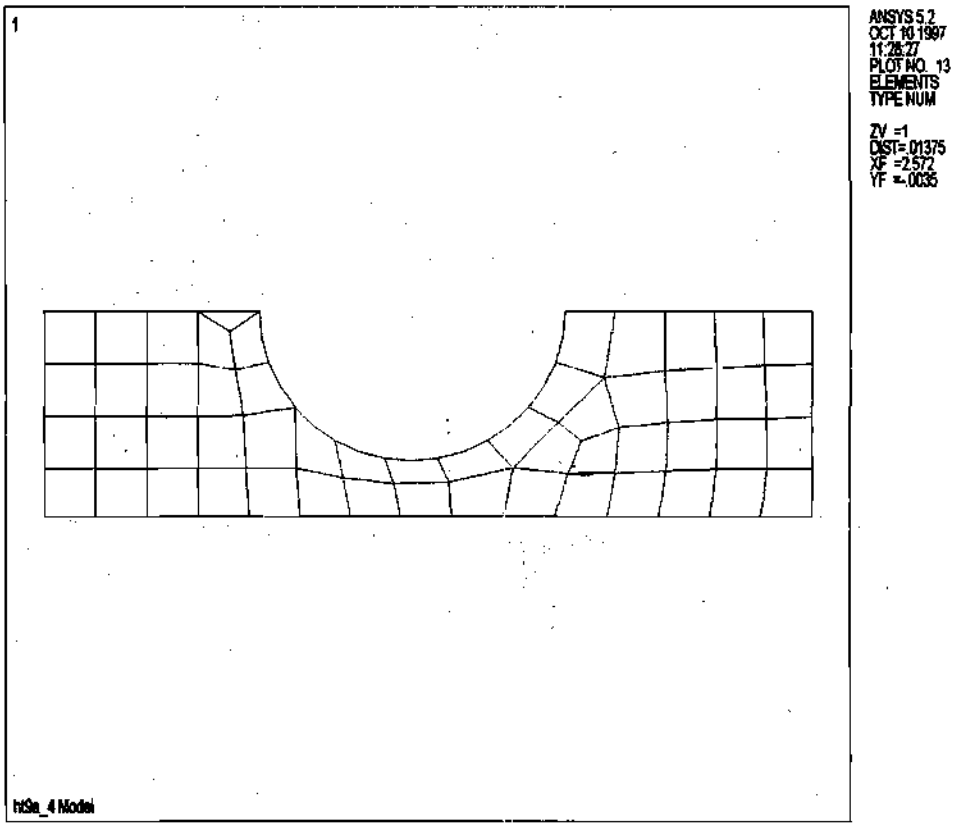

Figure 13 Finite Element Model of PFC for HT-9 with q''_{peak} = 3.0 MW/m^2 and T_w^{exit}=281 ^{0}C (14 MPa water)

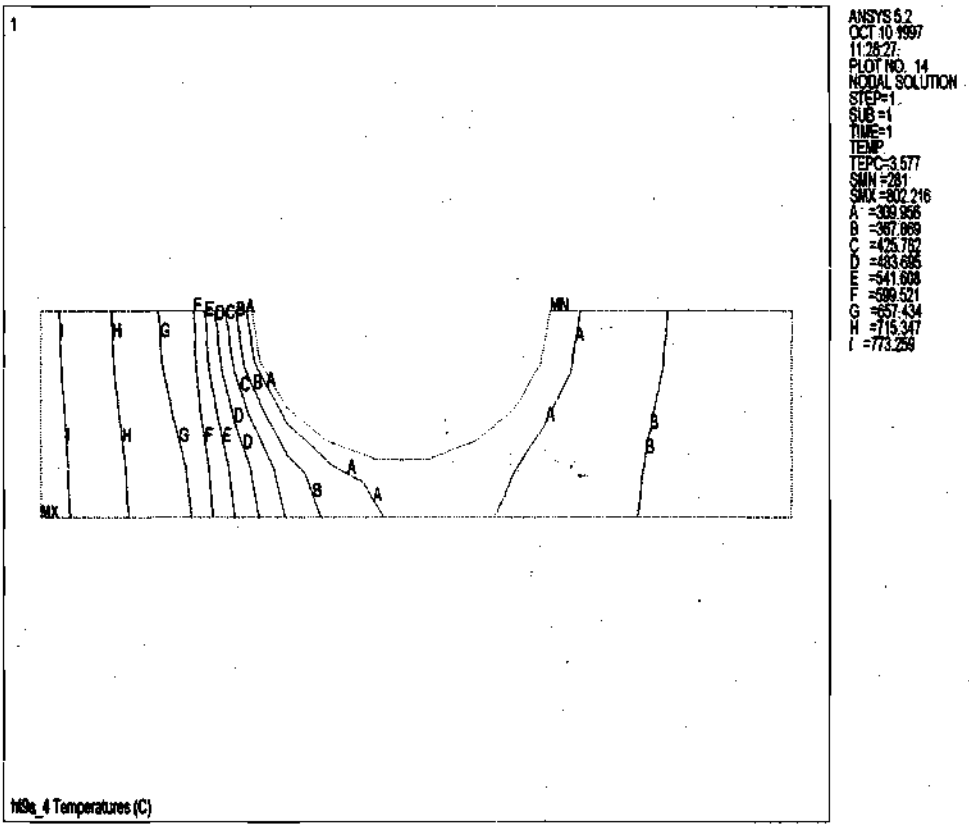

Figure 14 Temperature distribution in PFC for HT-9 with q''_{peak} = 3.0 MW/m^2 and T_w^{exit}=281 ^{0}C (14 MPa water)

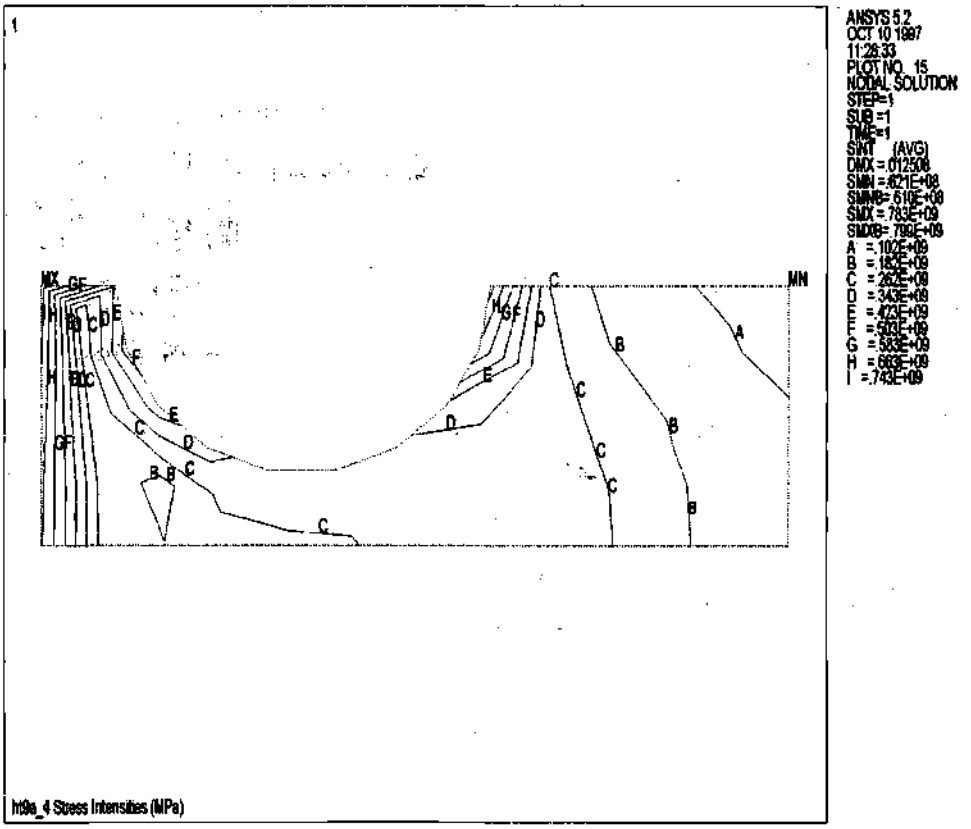

Figure 15 Thermal stress distribution in PFC for HT-9 with q''_{peak} = 3.0 MW/m^2 and T_w^{exit}=281 ^{0}C (14 MPa water)

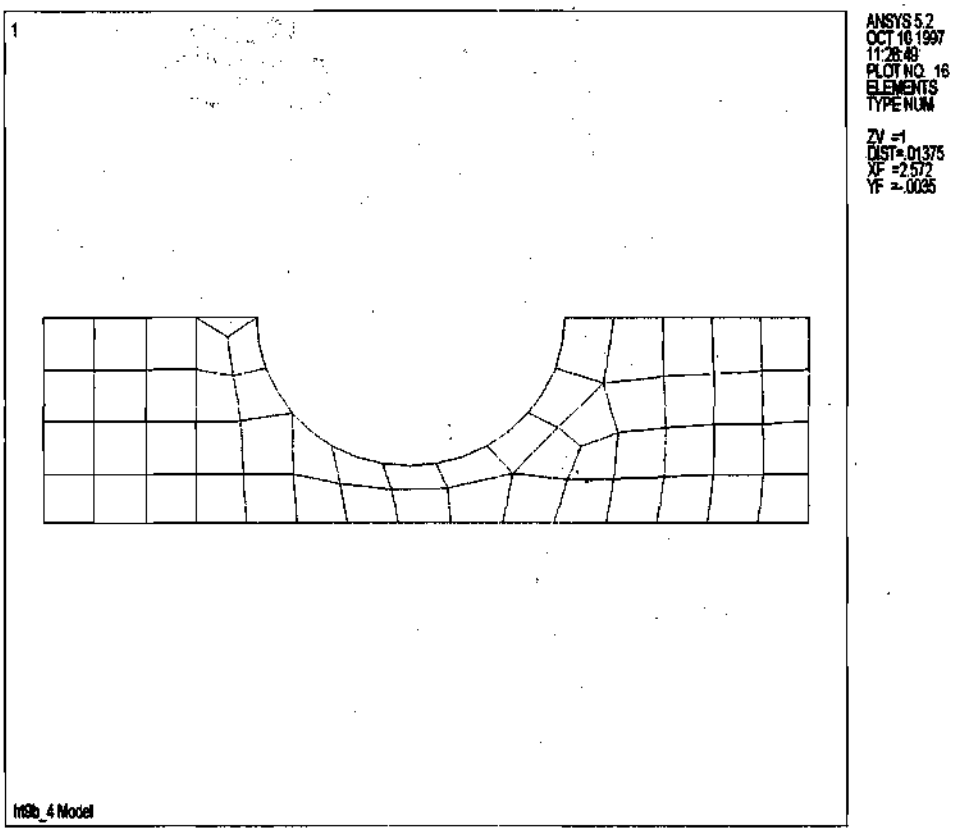

Figure 16 Finite Element Model of PFC for HT-9 with q''_{peak} = 2.0 MW/m^2 and T_w^{exit}=277 ^{0}C (14 MPa water)

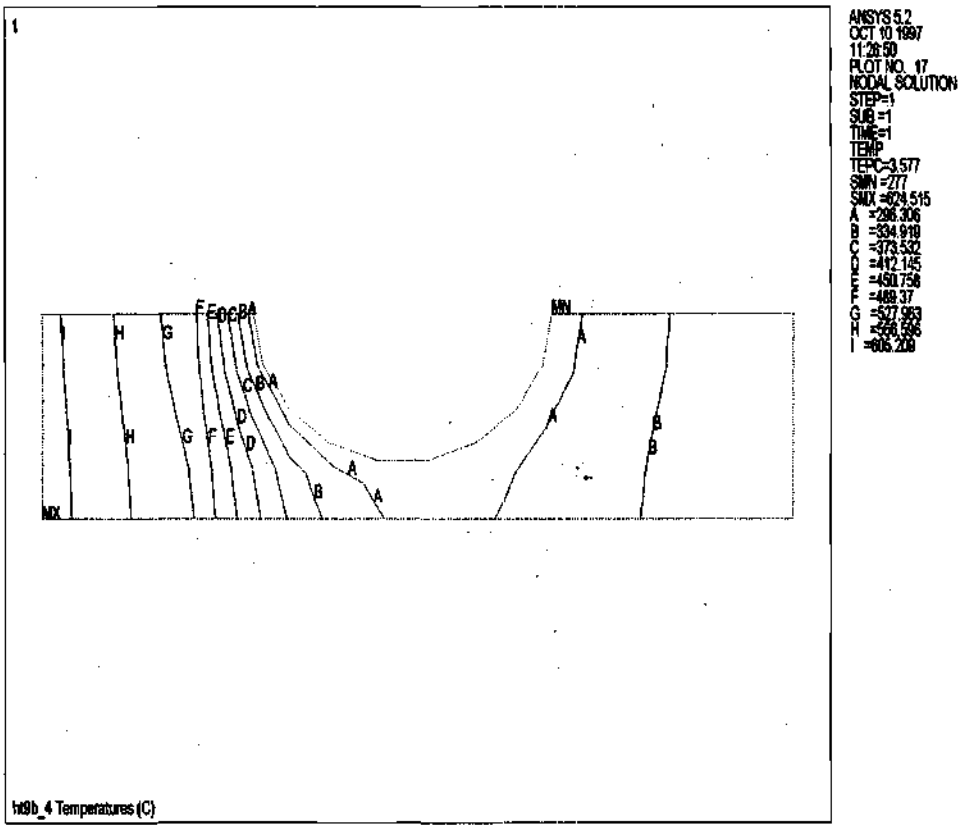

Figure 17 Temperature distribution in PFC for HT-9 with $q''_{peak} = 2.0$ MW/m^2 and T_w^{exit}=277 ^{0}C (14 MPa water)

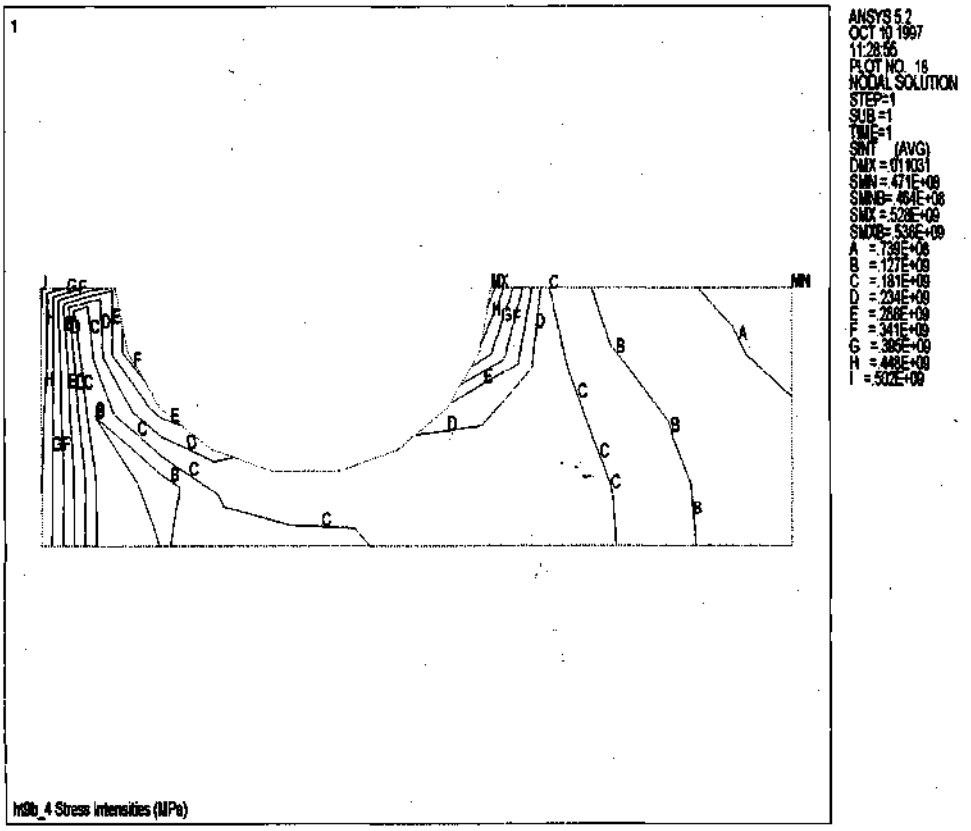

Figure 18 Thermal stress distribution in PFC for HT-9 with q''_{peak} = 2.0 MW/m^2 and T_w^{exit}=277 ^{0}C (14 MPa water)

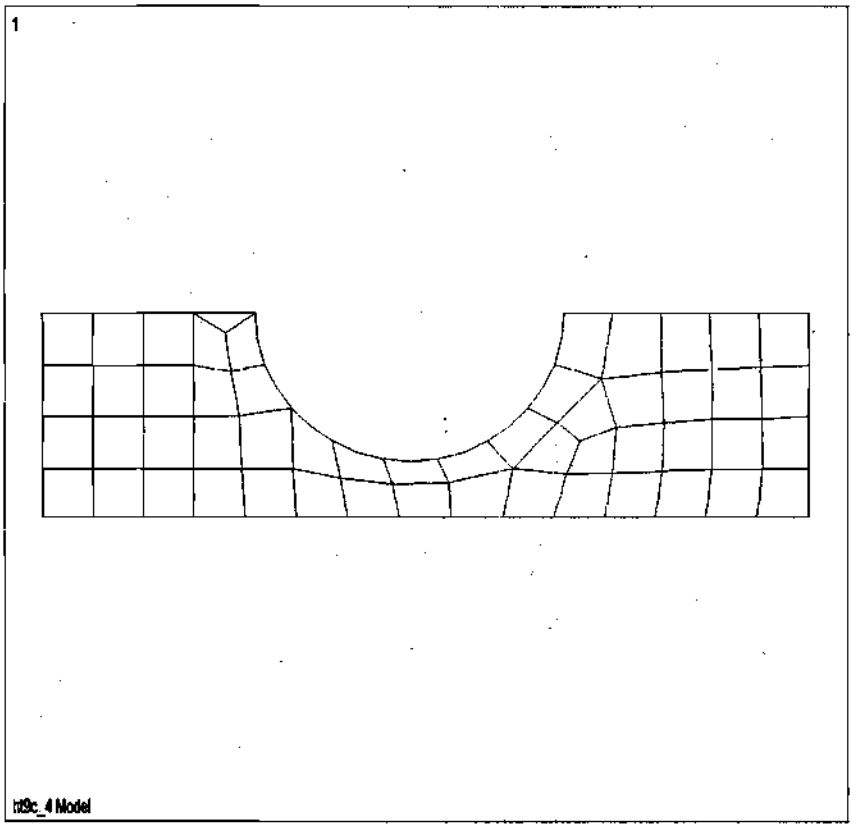

Figure 19 Finite Element Model of PFC for HT-9 with q''_{peak} = 1.0 MW/m^2 and T_w^{exit}=270 ^{0}C (14 MPa water)

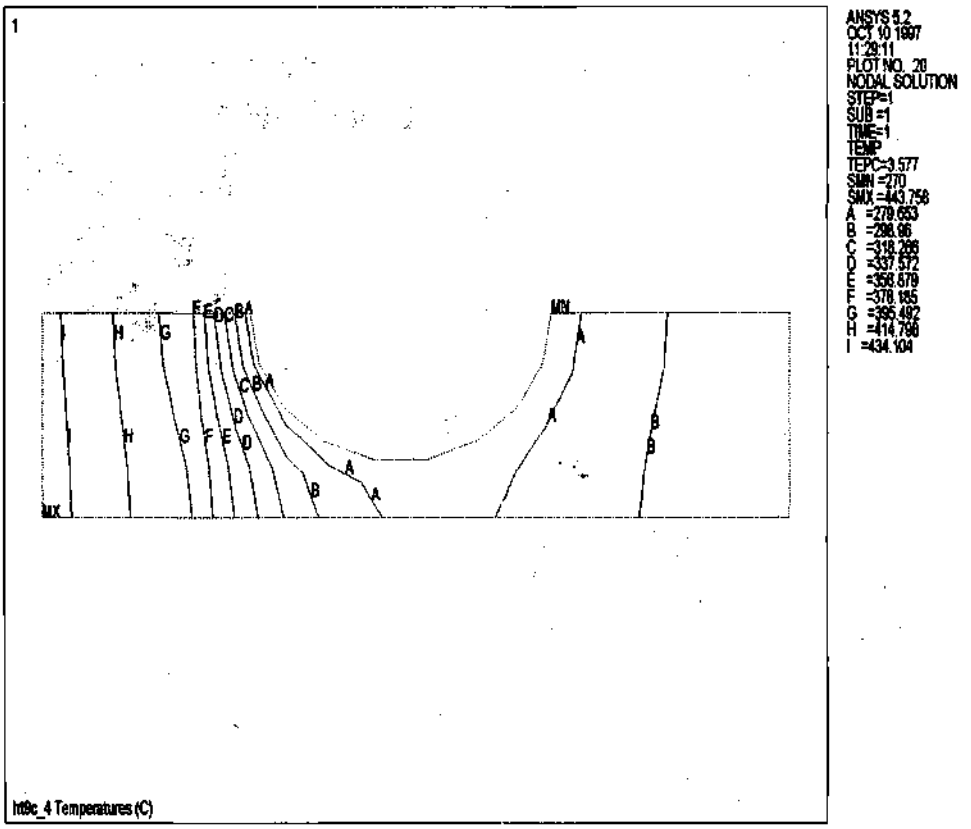

Figure 20 Temperature distribution in PFC for HT-9 with q''_{peak} = 1.0 MW/m^2 and T_w^{exit}=270 ^{0}C (14 MPa water)

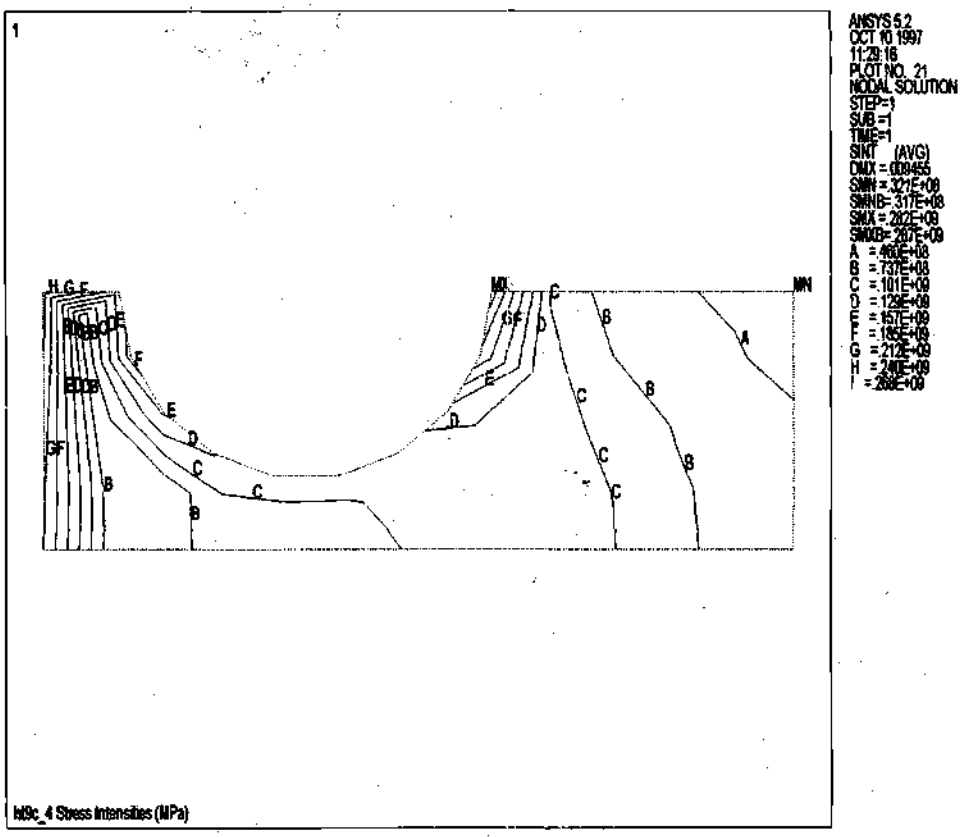

Figure 21 Thermal stress distribution in PFC for HT-9 with q''_{peak} = 1.0 MW/m^2 and T_w^{exit}=270 ^{0}C (14 MPa water)

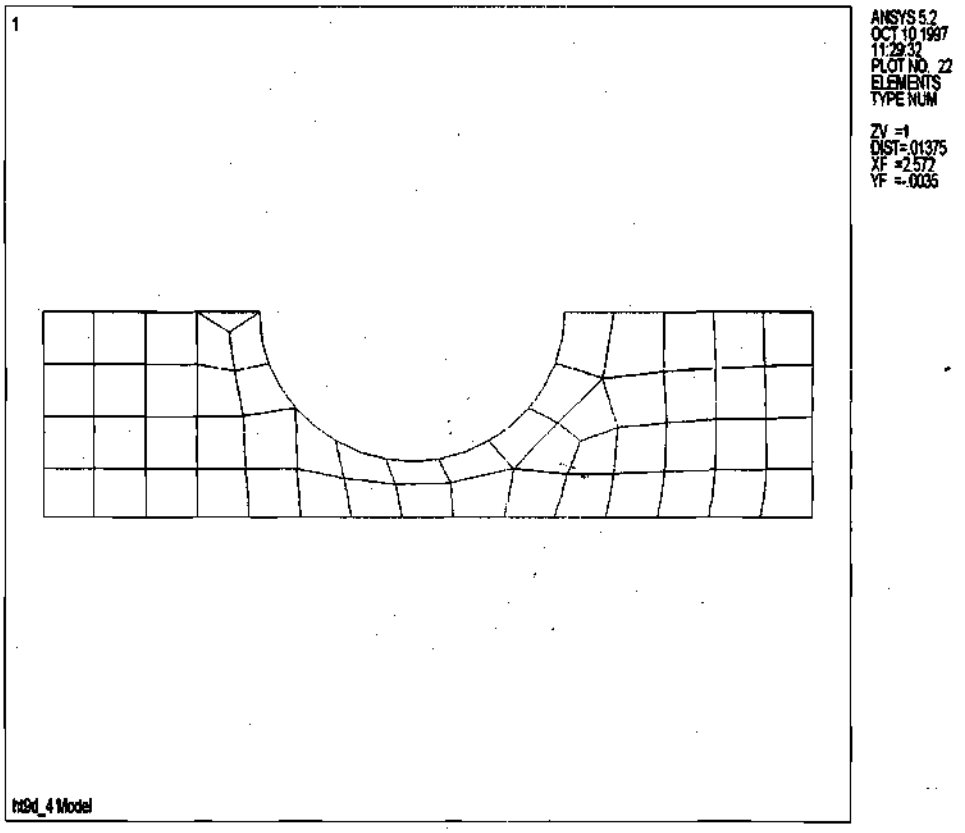

Figure 22 Finite Element Model of PFC for HT-9 with q''_{peak} = 0.5 MW/m^2 and T_w^{exit}=265 ^{0}C (14 MPa water)

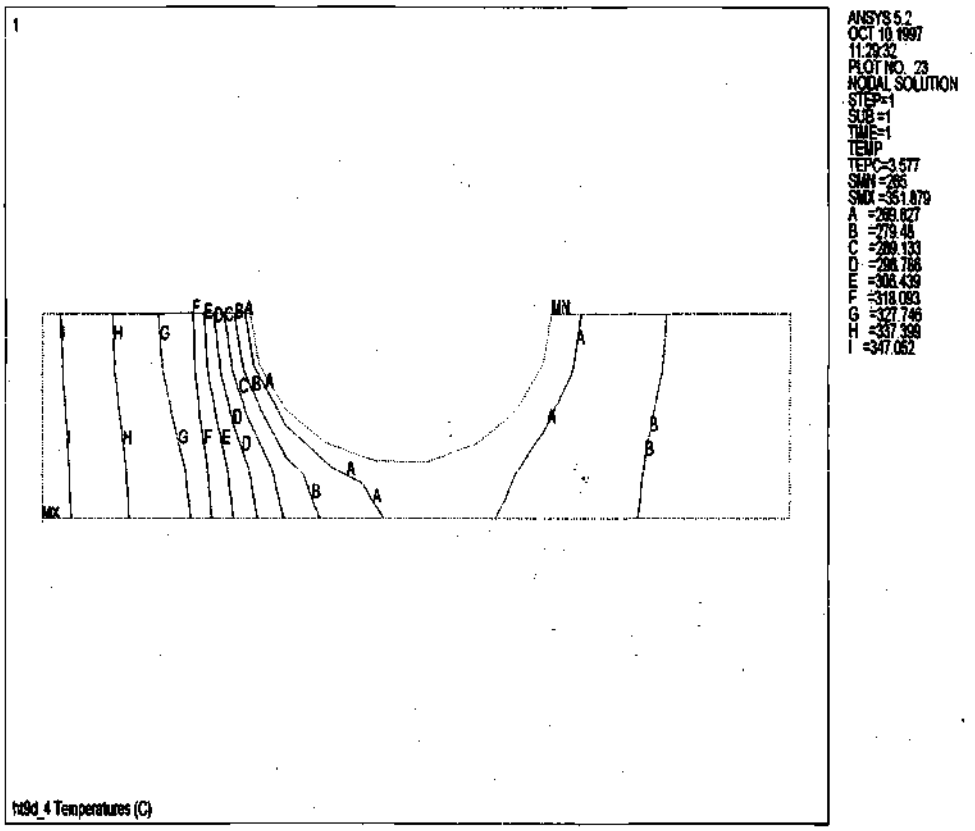

Figure 23 Temperature distribution in PFC for HT-9 with $q''_{peak} = 0.5$ MW/m^2 and T_w^{exit}=265 ^{0}C (14 MPa water)

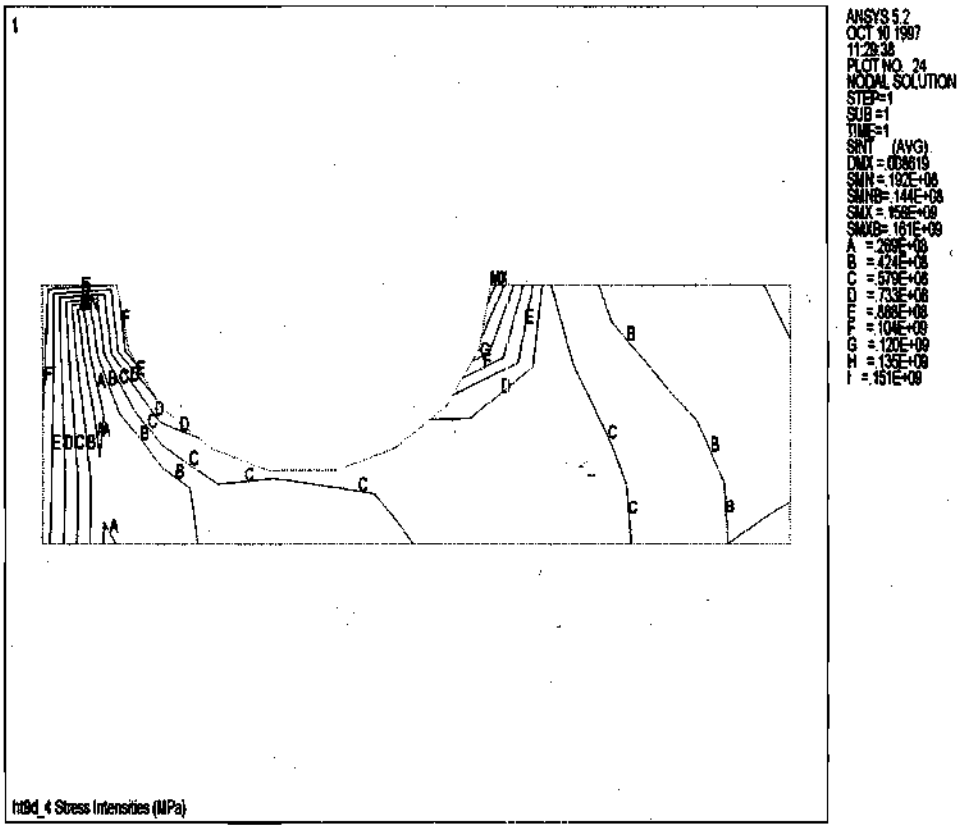

Figure 24 Thermal stress distribution in PFC for HT-9 with $q''_{peak} = 0.5$ MW/m^2 and T_w^{exit}=265 ^{0}C (14 MPa water)

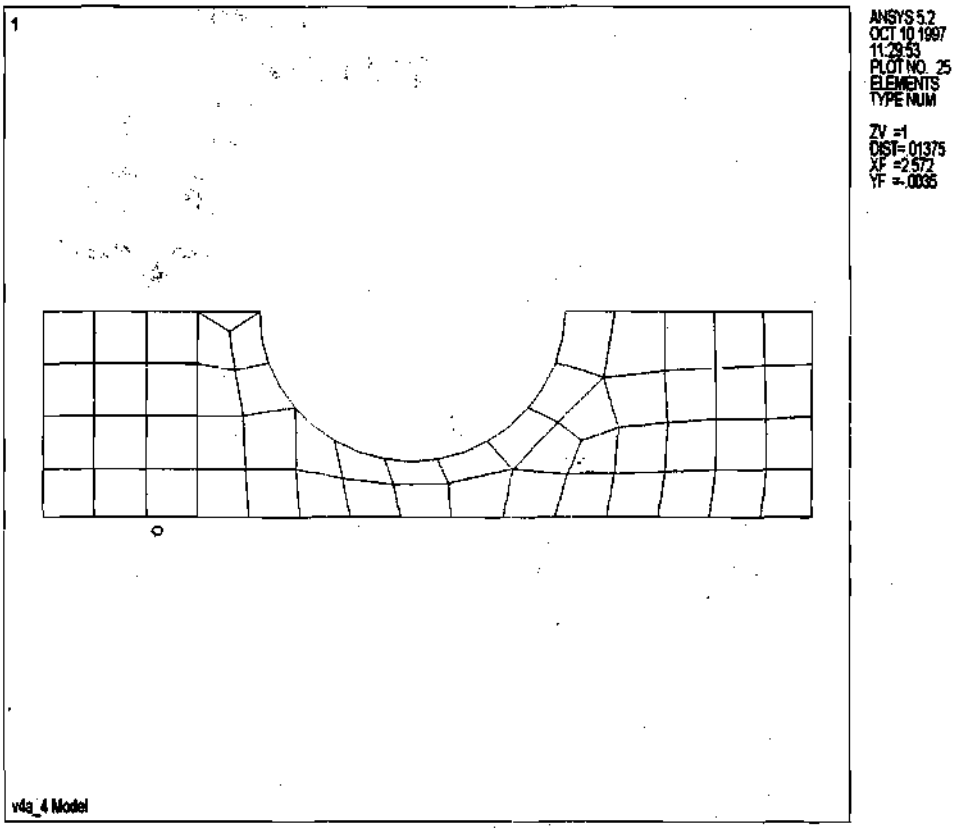

Figure 25 Finite Element Model of PFC
for V-4Cr-4Ti with q''_{peak} = 3.0 MW/m^2
and T_w^{exit}=281 ^{0}C (14 MPa water)

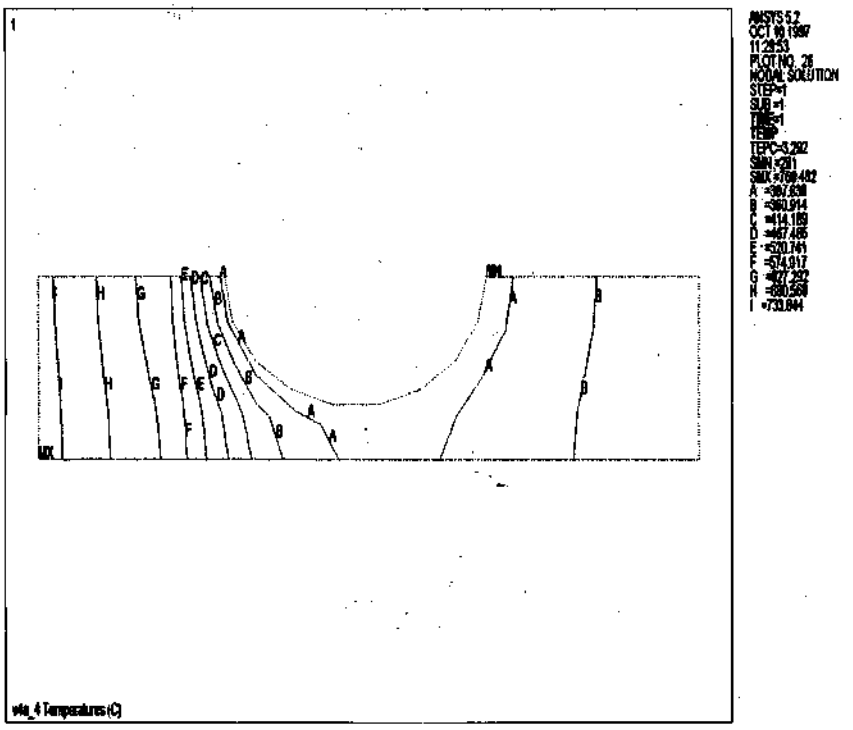

Figure 26 Temperature distribution in PFC for HT-9 with q''_{peak} = 3.0 MW/m^2 and T_w^{exit}=281 ^{0}C (14 MPa water)

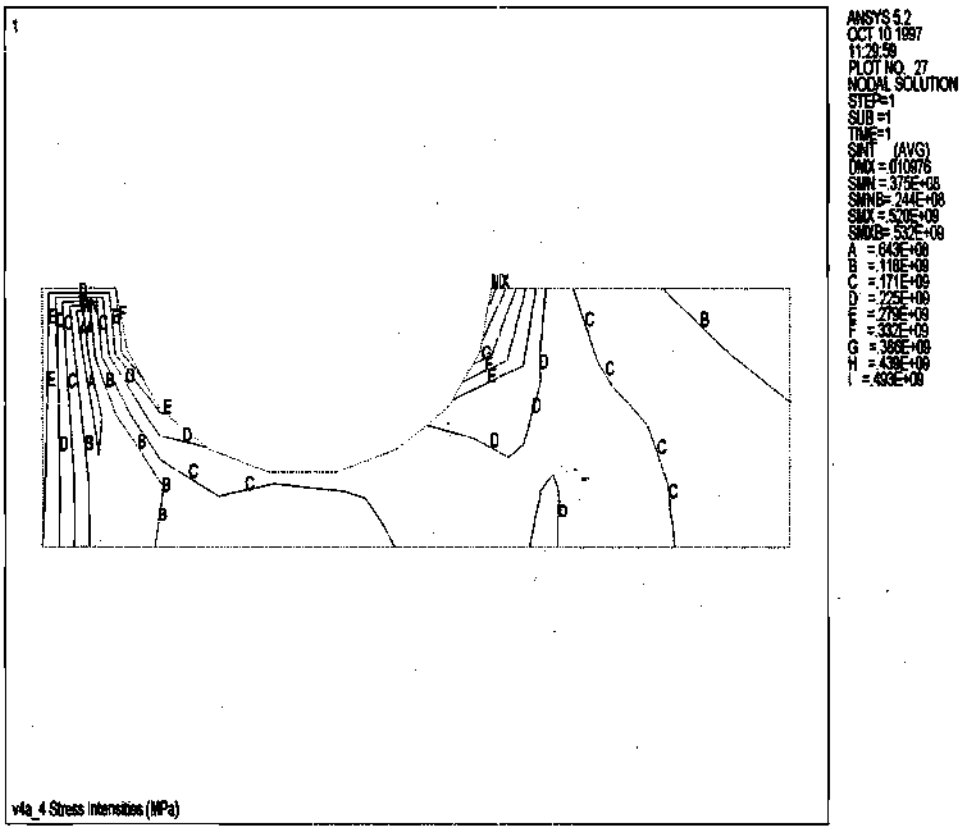

Figure 27 Thermal stress distribution in PFC for V-4Cr-4Ti with q''_{peak} = 3.0 MW/m^2 and T_w^{exit}=281 ^{0}C (14 MPa water)

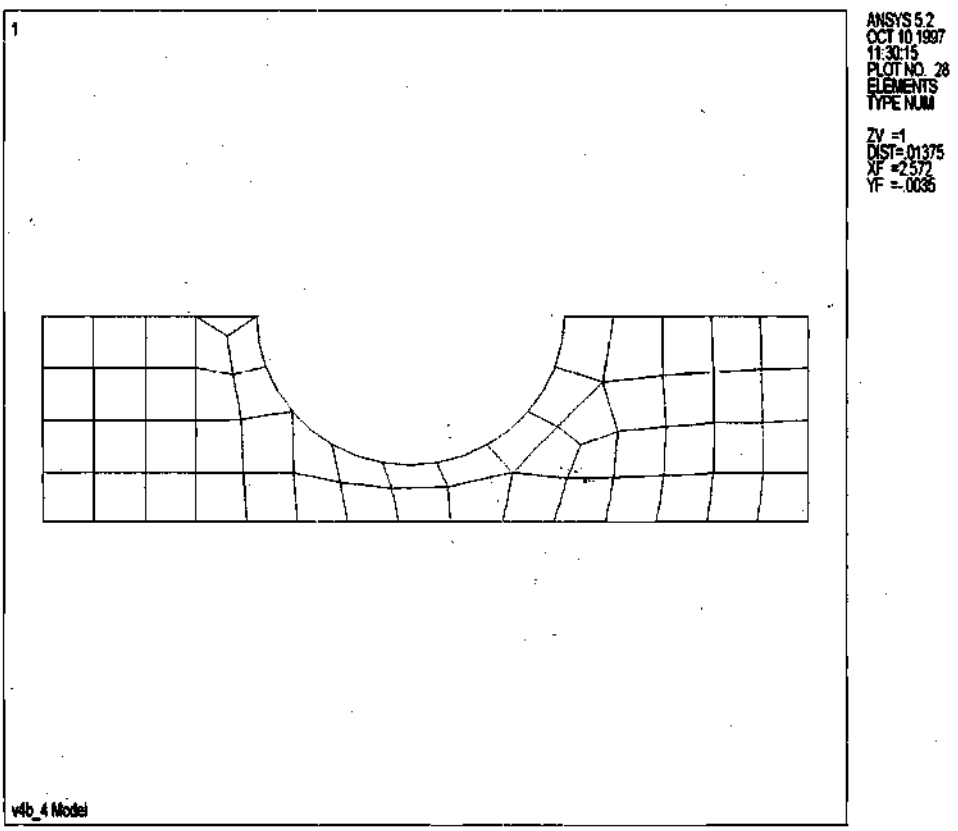

Figure 28 Finite Element Model of PFC
for V-4Cr-4Ti with q''_{peak} = 2.0 MW/m^2
and T_w^{exit}=277 ^{0}C (14 MPa water)

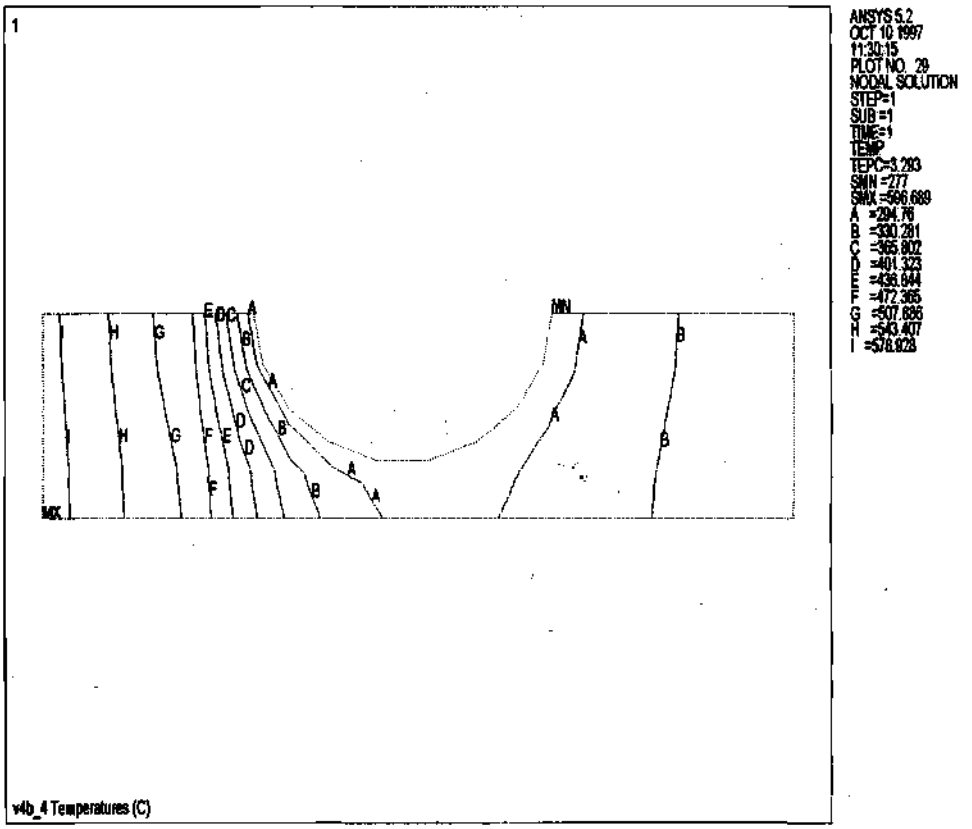

Figure 29 Temperature distribution in PFC for V-4Cr-4Ti with q''_{peak} = 2.0 MW/m^2 and T_w^{exit}=277 ^{0}C (14 MPa water)

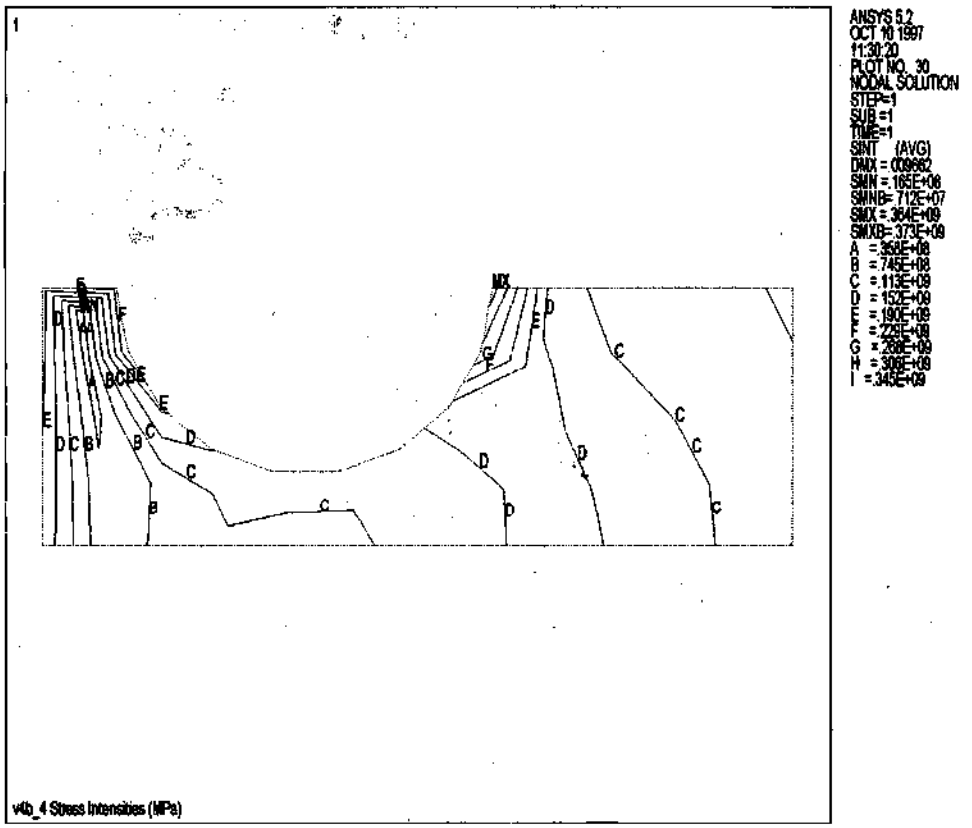

Figure 30 Thermal stress distribution in PFC for V-4Cr-4Ti with q''_{peak} = 2.0 MW/m^2 and T_w^{exit}=277 ^{0}C (14 MPa water)

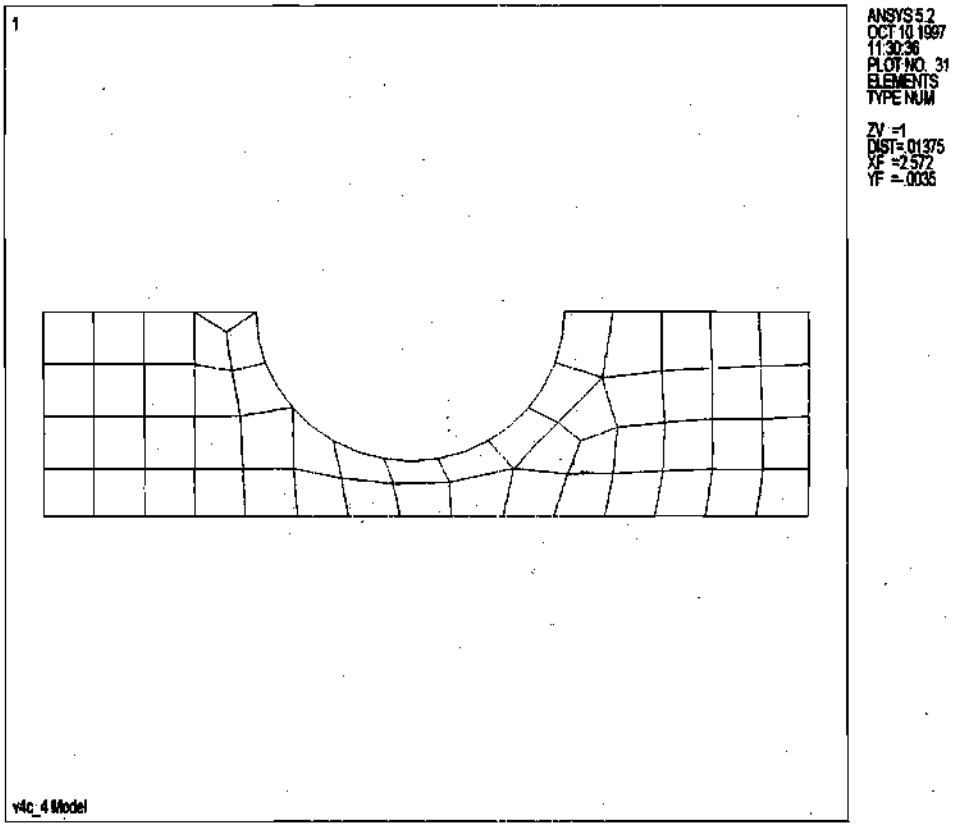

Figure 31 Finite Element Model of PFC
for V-4Cr-4Ti with q''_{peak} = 1.0 MW/m^2
and T_w^{exit}=270 ^{0}C (14 MPa water)

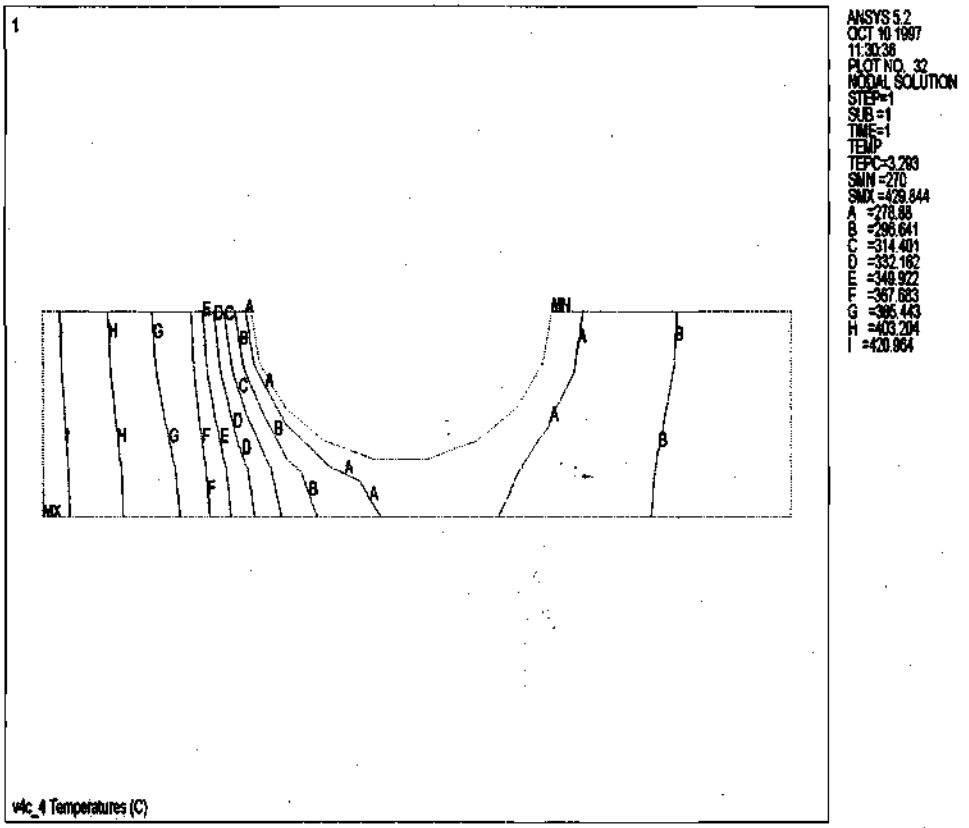

Figure 32 Temperature distribution in PFC for V-4Cr-4Ti with q''_{peak} = 1.0 MW/m^2 and T_w^{exit}=270 ^{0}C (14 MPa water)

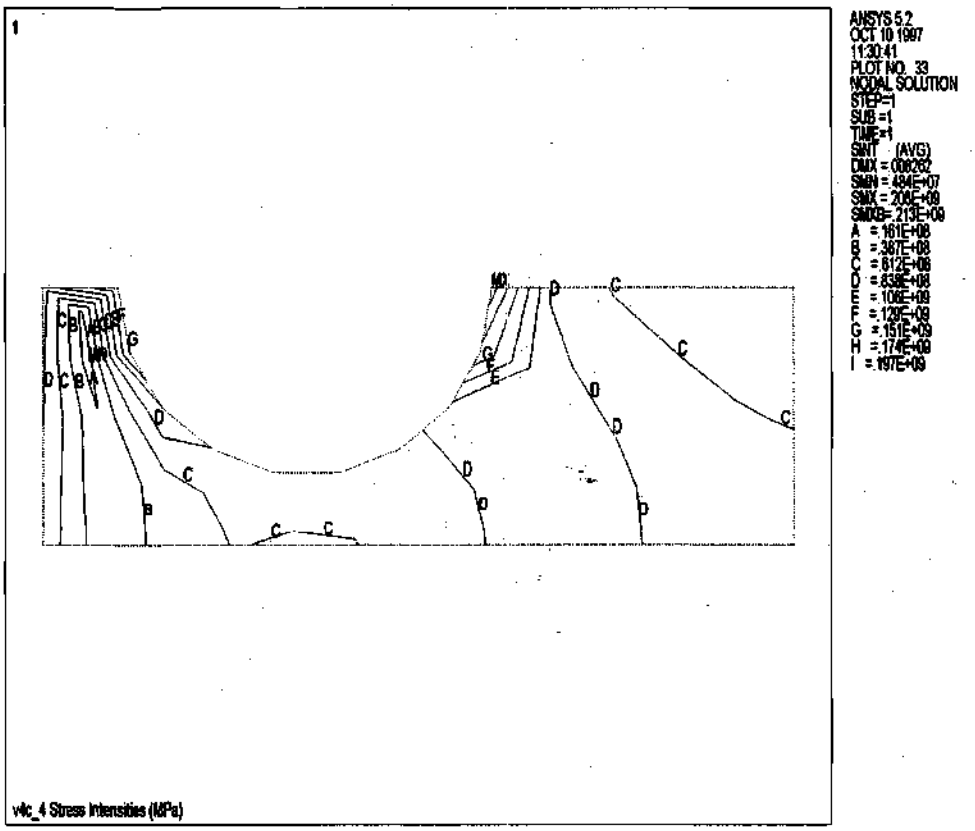

Figure 33 Thermal stress distribution in PFC for V-4Cr-4Ti with q''_{peak} = 1.0 MW/m^2 and T_w^{exit}=270 ^{0}C (14 MPa water)

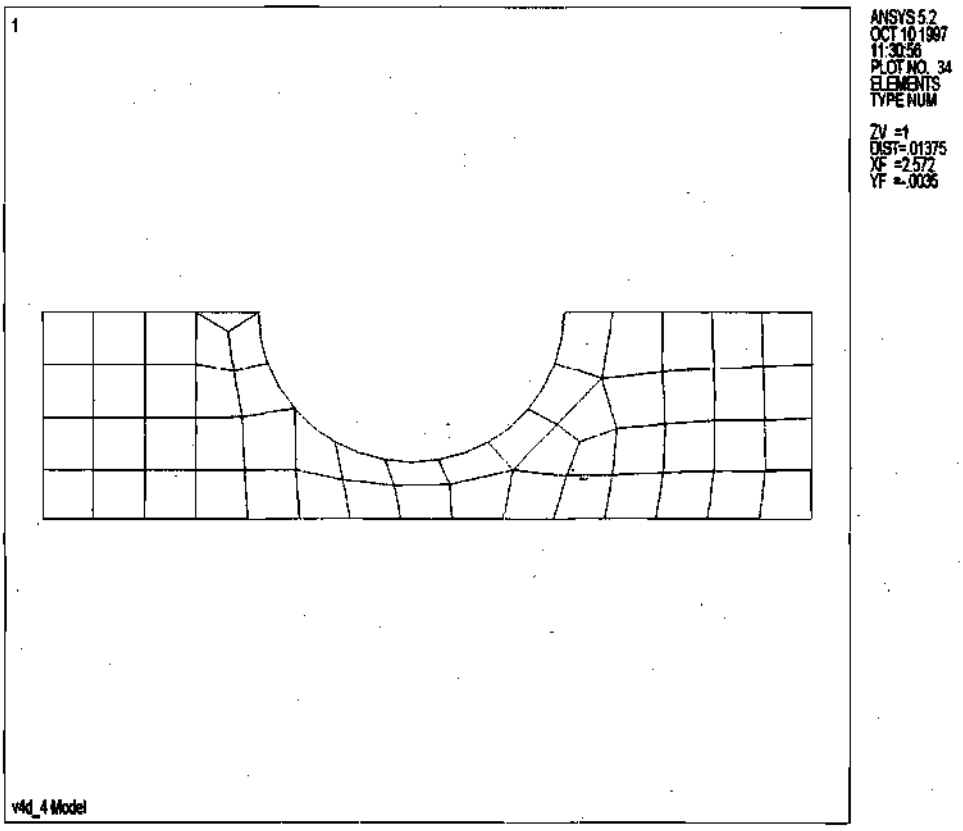

Figure 34 Finite Element Model of PFC
for V-4Cr-4Ti with $q''_{peak} = 0.5$ MW/m^2
and T_w^{exit}=265 ^{0}C (14 MPa water)

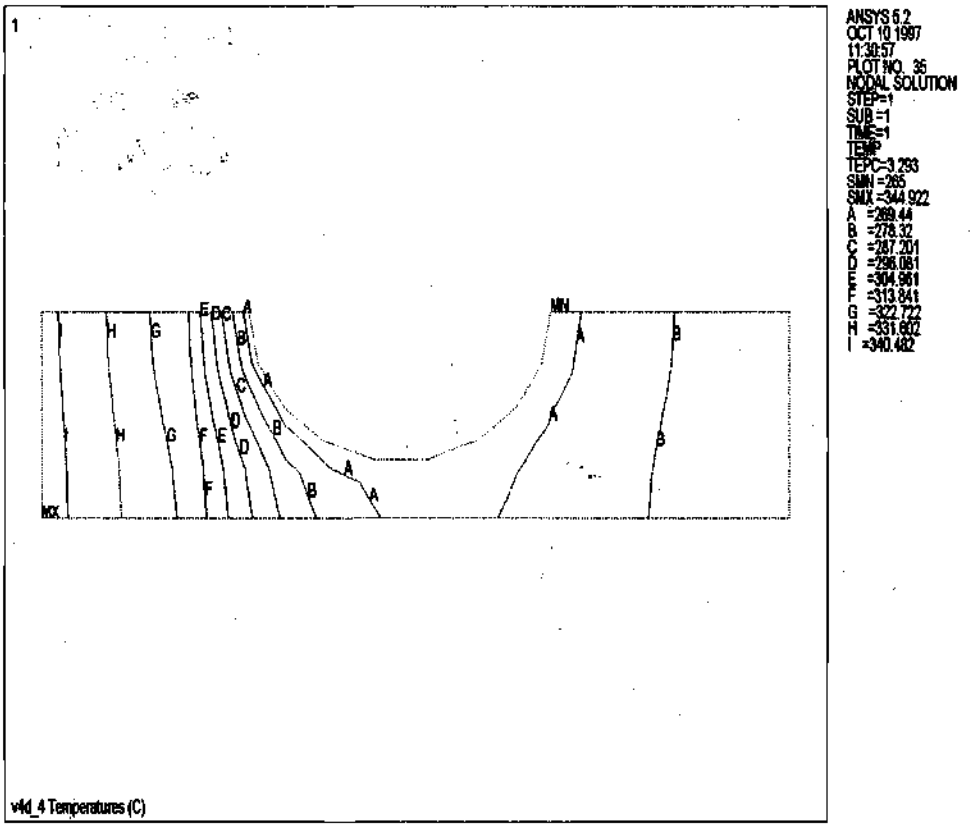

Figure 35 Temperature distribution in PFC for V-4Cr-4Ti with $q''_{peak} = 0.5$ MW/m^2 and T_w^{exit}=265 ^{0}C (14 MPa water)

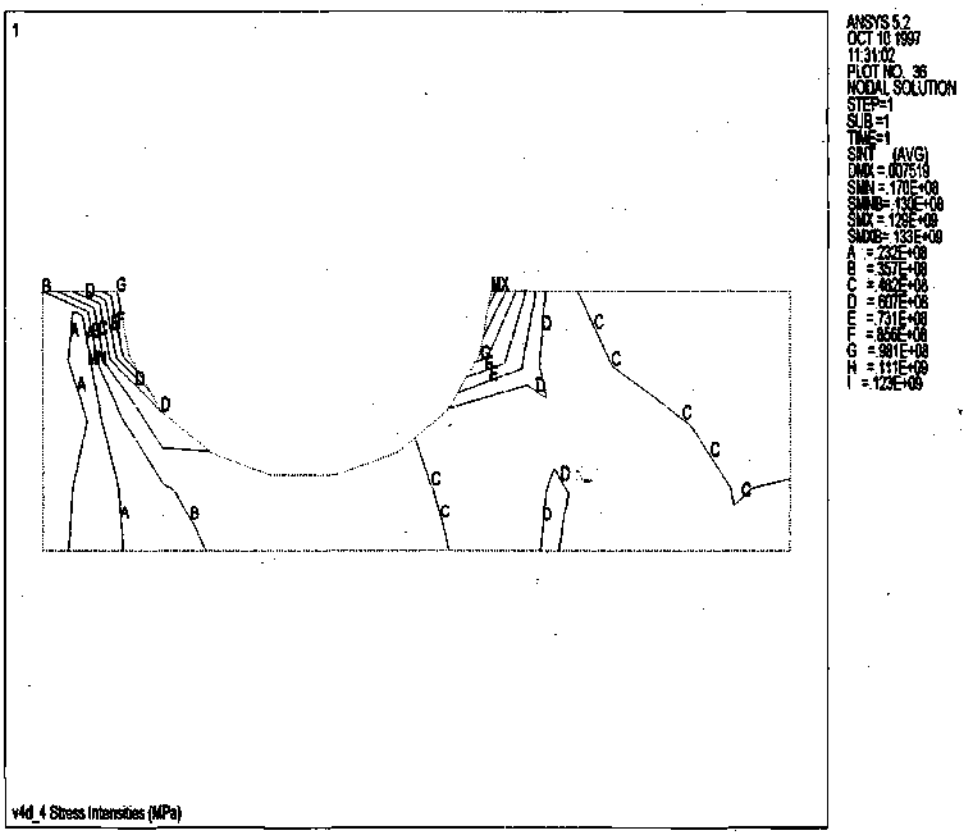

Figure 36 Thermal stress distribution in PFC for V-4Cr-4Ti with $q''_{peak} = 0.5$ MW/m^2 and T_w^{exit}=265 ^{0}C (14 MPa water)

Appendix D

ANSYS 5.2 Model, Temperature, and Thermal Stress Profiles for HT-9, and V-4Cr-4Ti for 15 MPa helium

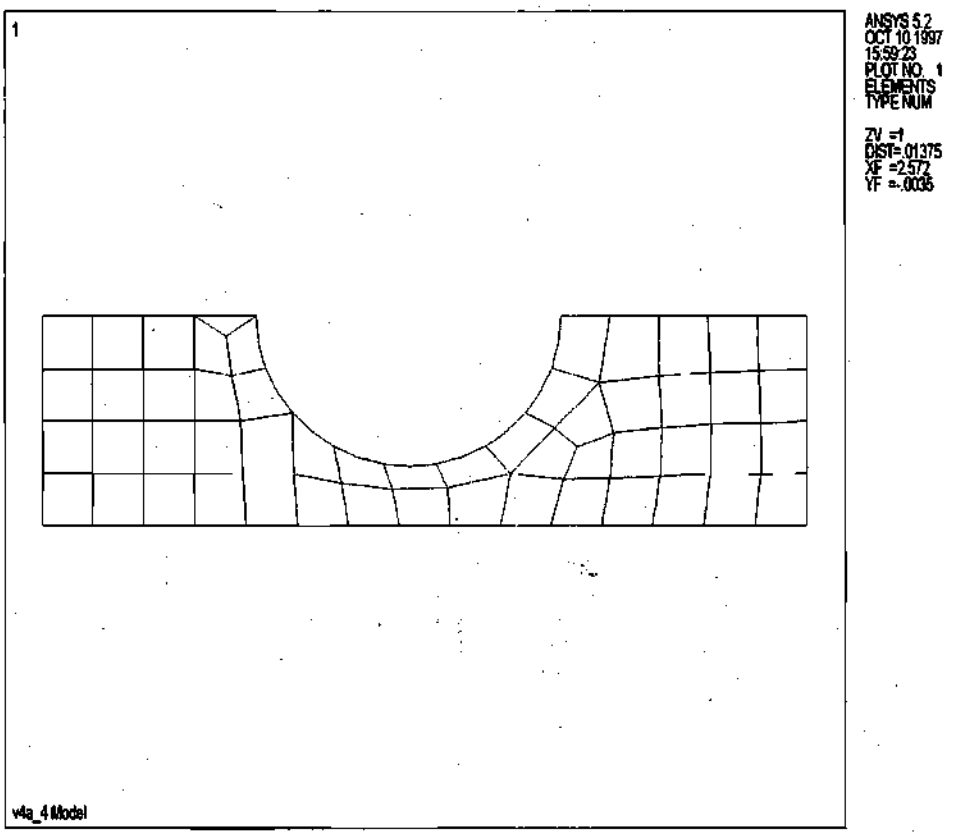

Figure 1 Finite Element Model of PFC V-4Cr-4Ti with

q''_{peak} = 3.0 MW/m^2 and T_w^{exit}=495 ^{0}C (15 MPa helium)

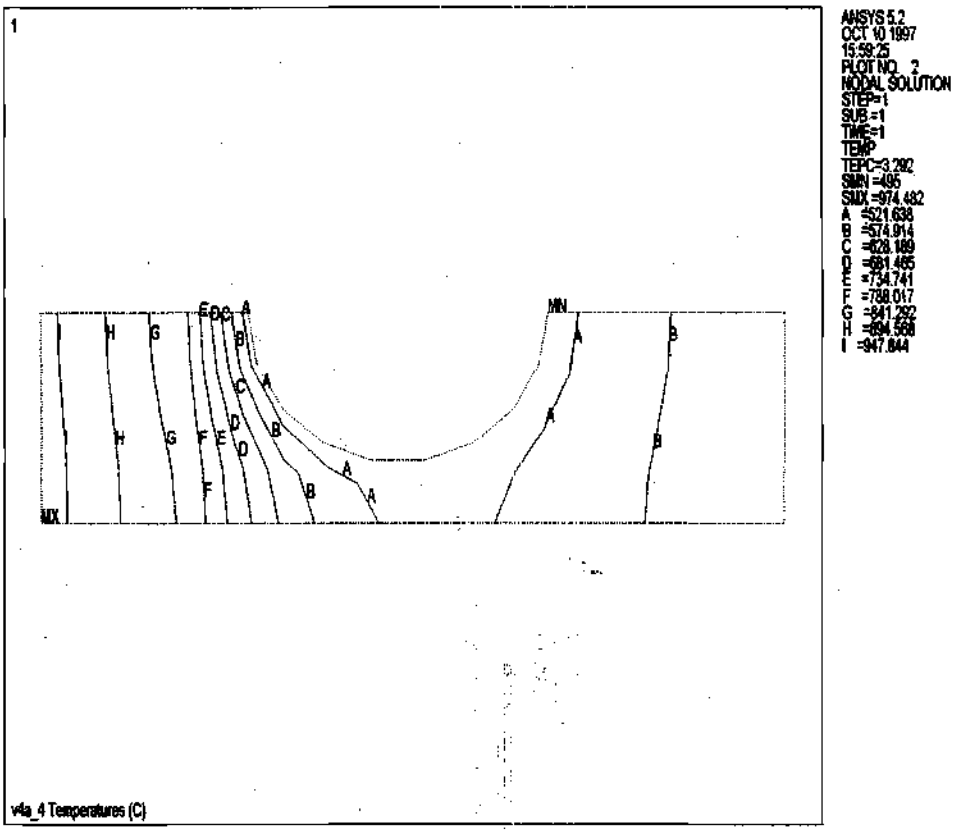

Figure 2 Temperature distribution in PFC V-4Cr-4Ti with q''_{peak} = 3.0 MW/m^2 and T_w^{exit}=495 ^{0}C (15 MPa helium)

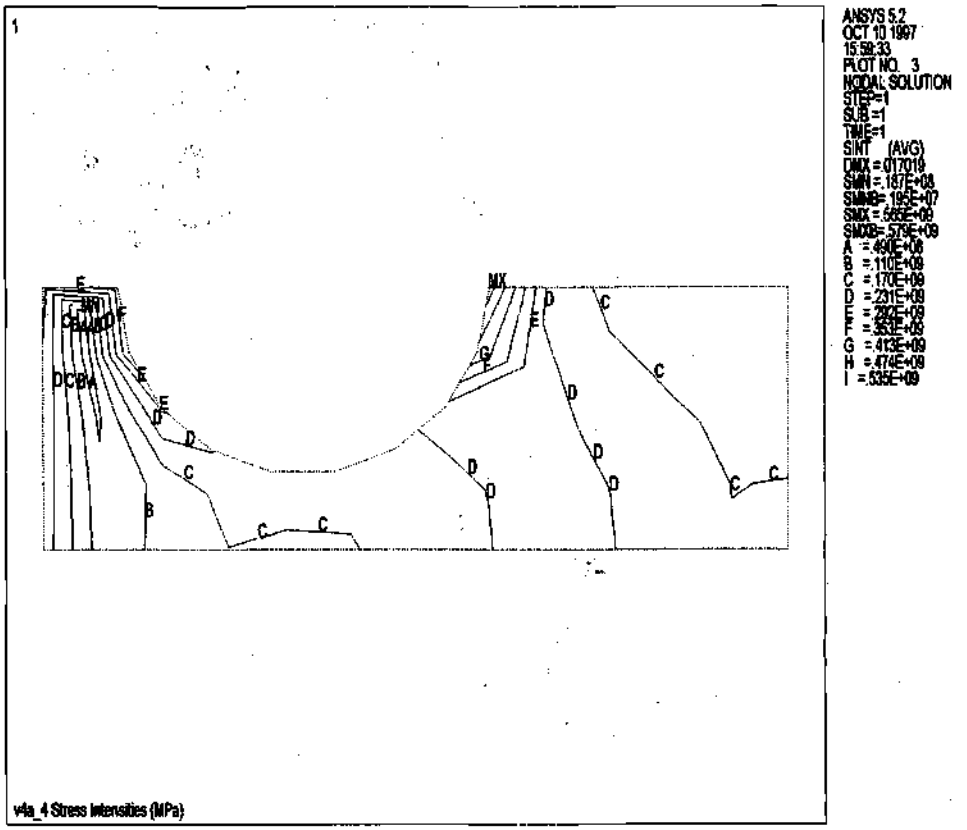

Figure 3 Thermal stress distribution in PFC V-4Cr-4Ti with

q''_{peak} = 3.0 MW/m^2 and T_w^{exit}=495 ^{0}C (15 MPa helium)

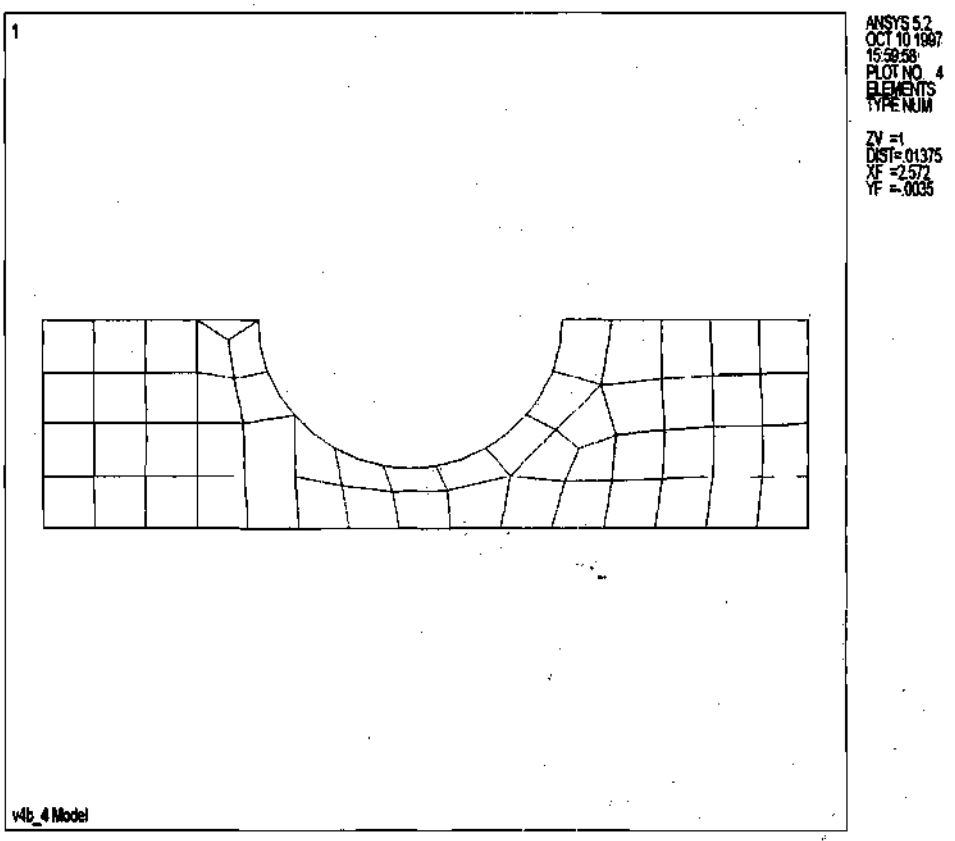

Figure 4 Finite Element Model of PFC V-4Cr-4Ti with q''_{peak} = 2.0 MW/m^2 and T_w^{exit}=495 ^{0}C (15 MPa helium)

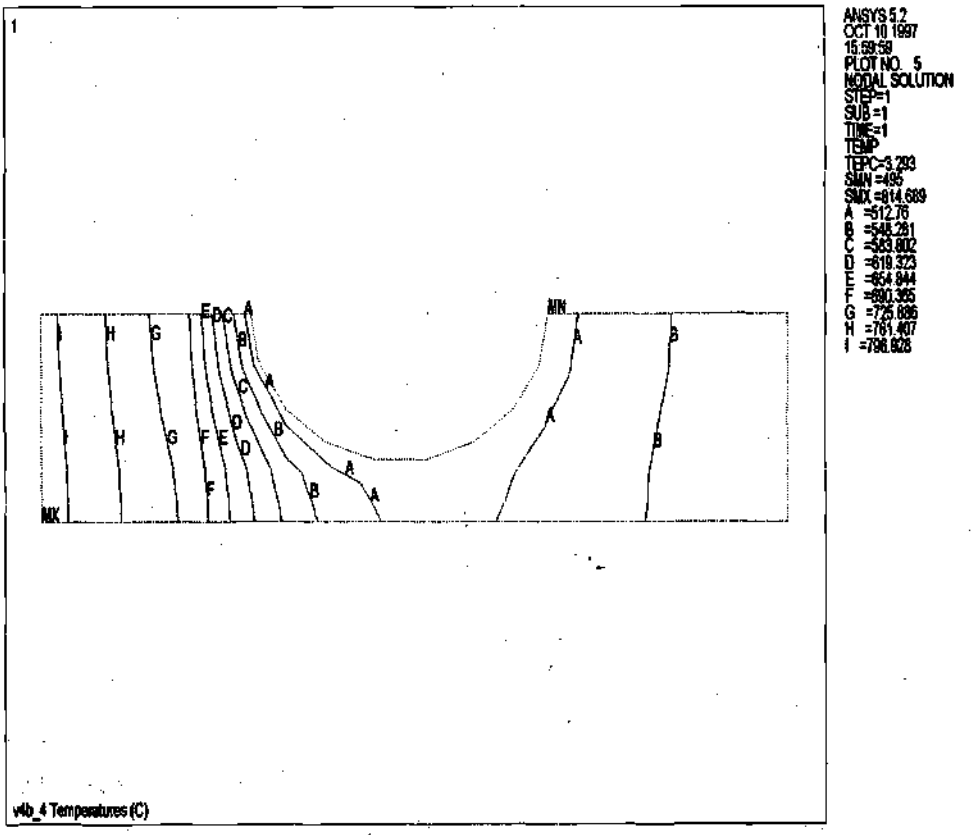

Figure 5 Temperature distribution in PFC V-4Cr-4Ti with q''_{peak} = 2.0 MW/m^2 and T_w^{exit}=495 ^{0}C (15 MPa helium)

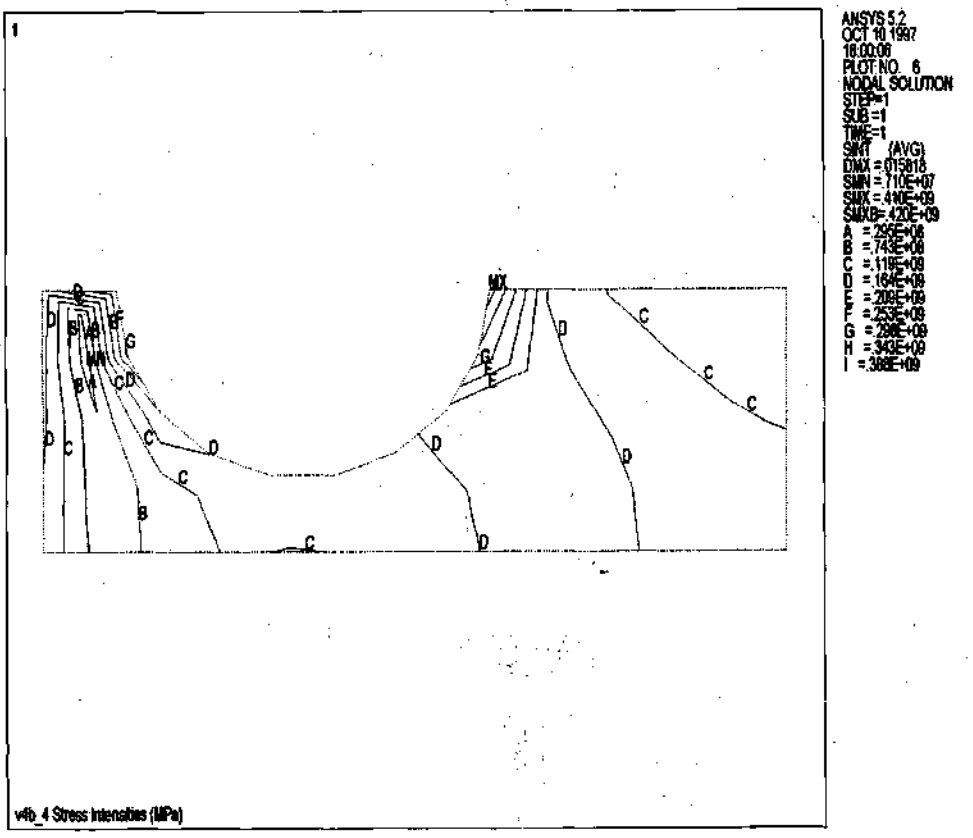

Figure 6 Thermal stress distribution in PFC V-4Cr-4Ti with q''_{peak} = 2.0 MW/m^2 and T_w^{exit}=495 ^{0}C (15 MPa helium)

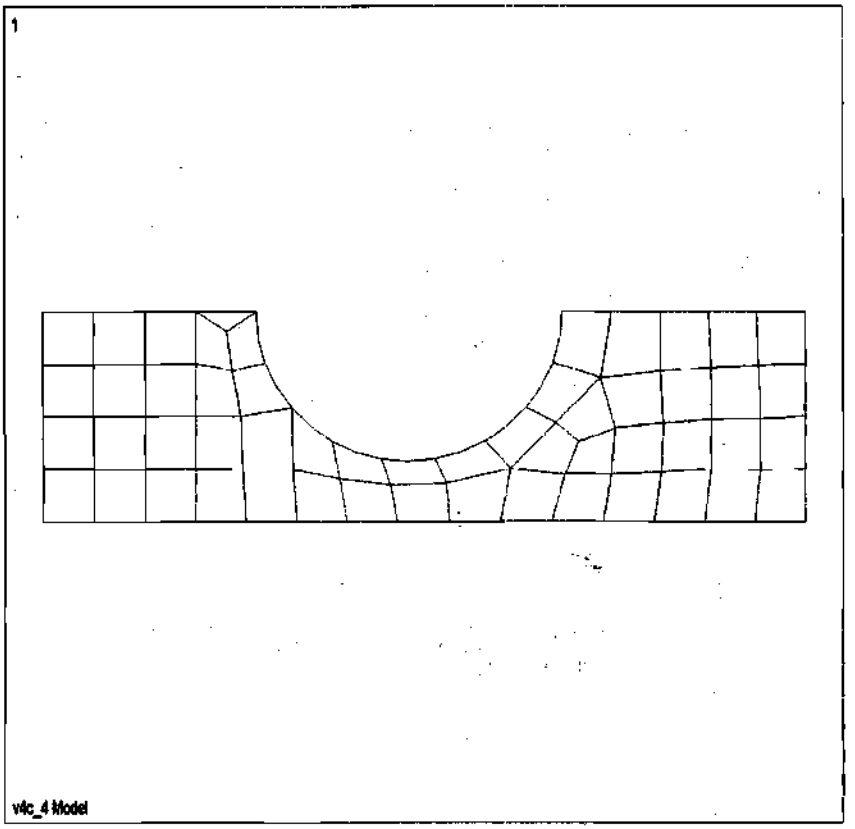

Figure 7 Finite Element Model of PFC V-4Cr-4Ti with

q''_{peak} = 1.0 MW/m^2 and T_w^{exit}=495 ^{0}C (15 MPa helium)

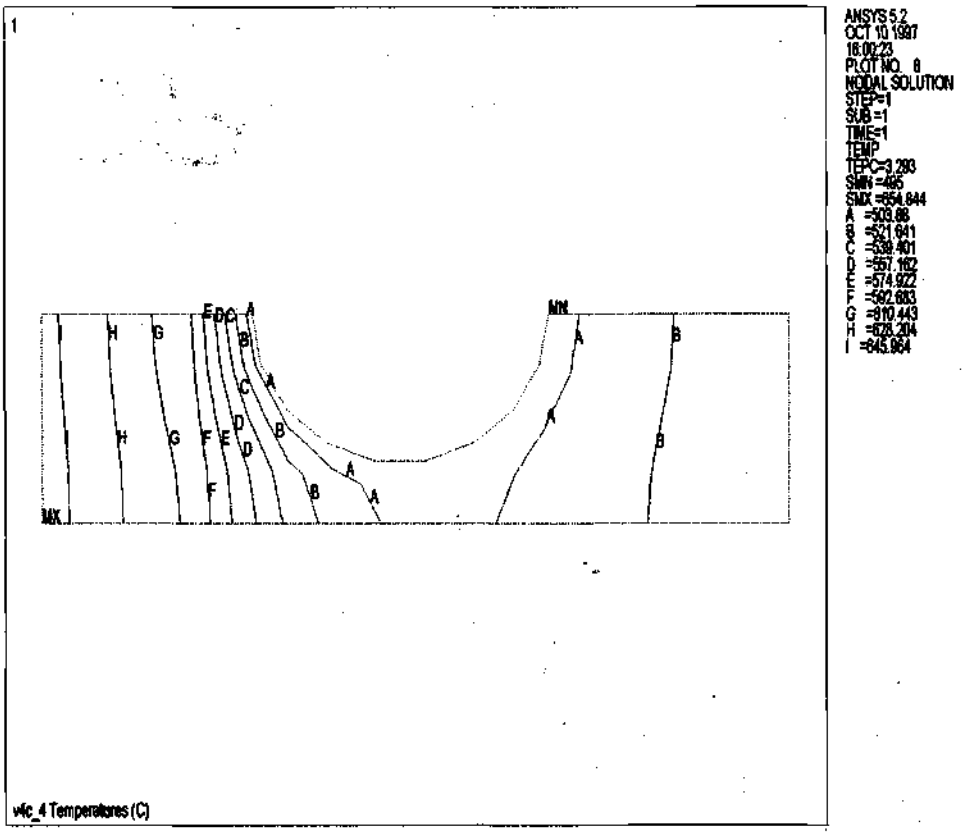

Figure 8 Temperature distribution in PFC V-4Cr-4Ti with

q''_{peak} = 1.0 MW/m^2 and T_w^{exit}=495 ^{0}C (15 MPa helium)

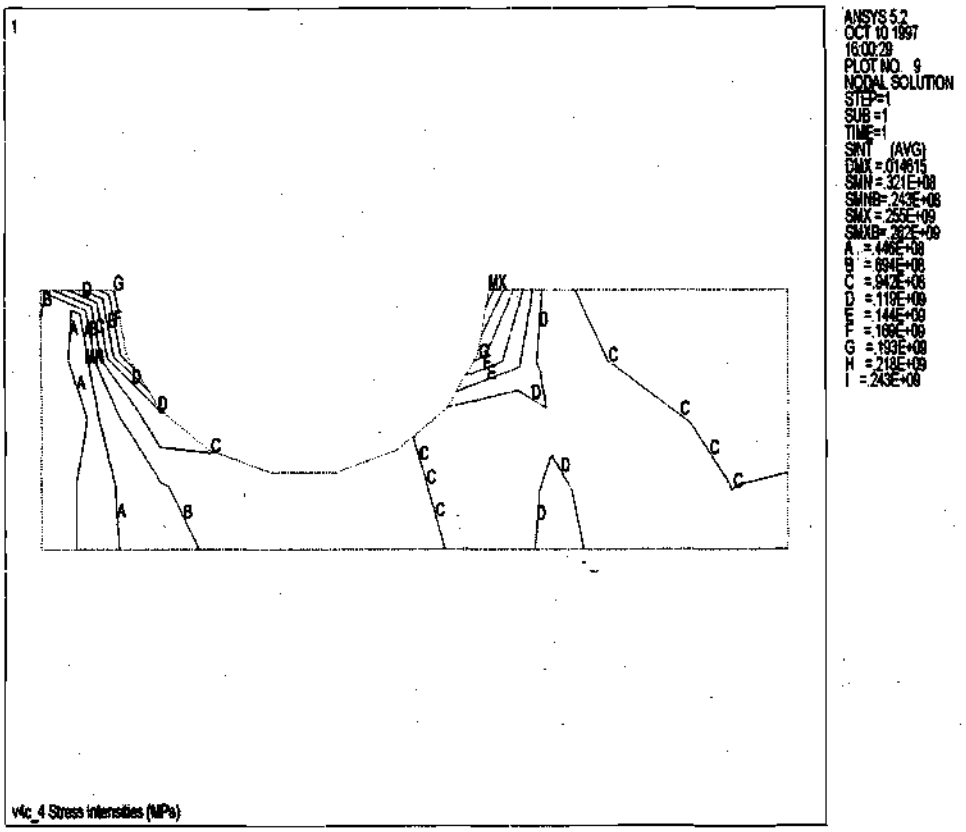

Figure 9 Thermal stress distribution in PFC V-4Cr-4Ti with

q''_{peak} = 1.0 MW/m^2 and T_w^{exit}=495 ^{0}C (15 MPa helium)

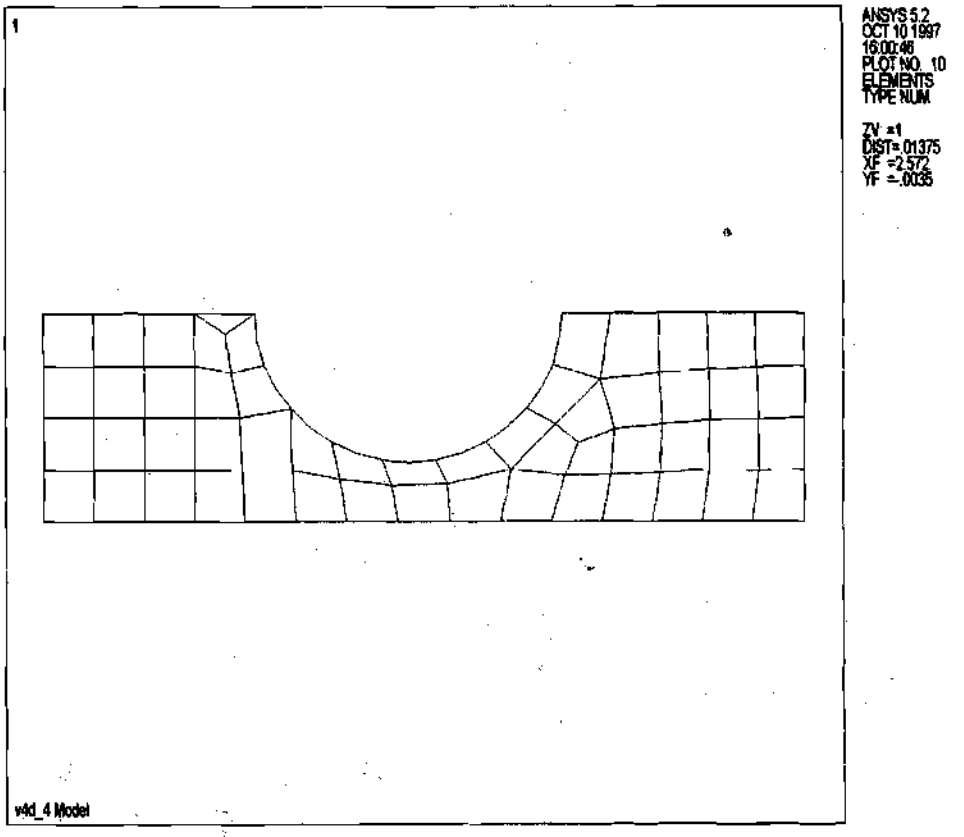

Figure 10 Finite Element Model of PFC V-4Cr-4Ti with q''_{peak} = 0.5 MW/m^2 and T_w^{exit}=495 ^{0}C (15 MPa helium)

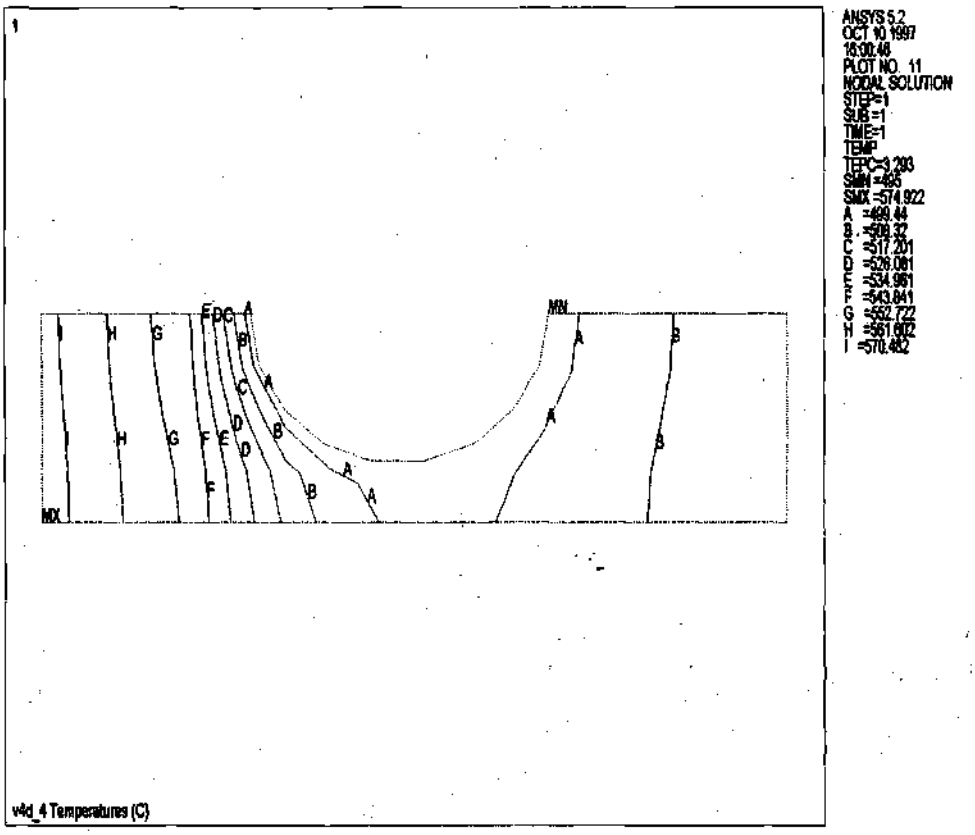

Figure 11 Temperature distribution in PFC V-4Cr-4Ti with

q''_{peak} = 0.5 MW/m^2 and T_w^{exit}=495 ^{0}C (15 MPa helium)

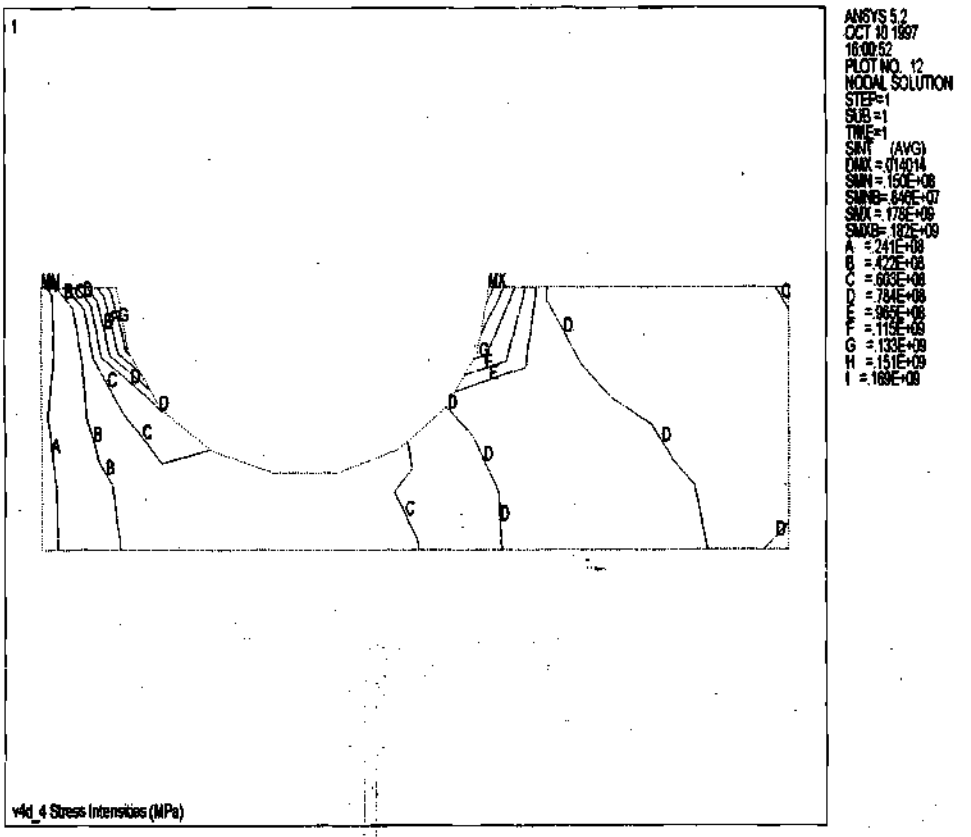

Figure 12 Thermal stress distribution in PFC V-4Cr-4Ti with q''_{peak} = 0.5 MW/m^2 and T_w^{exit}=495 ^{0}C (15 MPa helium)

APPENDIX E

INPUT AND OUTPUT ANSYS FILES FOR SS316 / H_2O (5 MPA)

Gen_inp.mac

```
/out,gen_inp,out
!  gen_inp.mac
!  Generates model, solve thermal and strutural
!  All parameters are in block
!
fini
*if,n_fac,le,0,then
 n_fac=1
*endif
parsav,all,m_sol,par
/nerr,0,1e6  !  turns off error messages
/cle,all
parres,,m_sol,par
/prep7
  immed  !  turns off the real time actions
/sho,m_sol,f33,1
et,1,77,,,1              !  defines thermal quad

/inp,%mname%,des          !  loads the parameters/material properties

!MODEL GEOMETRY        ! 10/02/97

!  parameters for the block with a hole

r1=2.56 !            PLASMA RADIUS        ! 10/02/97
t1=.005 !            SACRIFICIAL LAYER THICKNESS    ! 10/02/97
r2=.005 !            COOLANT TUBE DIAMETER ! 10/02/97
t2=.02  !           STRONGBACK THICKNESS    ! 10/02/97
t3=.002 !            COOLANT TUBE THICKNESS                ! 10/02/97
h1=t3+r2 !           POLOIDAL HEIGHT (HEIGHT IN Y DIRECTION)   !
10/02/97
r3=r1+t1+t3+r2  !       RADIAL DISTANCE AT CENTER OF COOLANT
TUBE ! 10/02/97


fini              ! 10/02/97
/prep7            ! 10/02/97

! model generation
```

```
wpave,r3                ! moves the wp to center of block
rectan,-t2/2,t2/2,-h1,0   ! ss316 block
adel,all,,,1
wpave,r1+t1+t2/2        ! moved wp to correct position
rectan,-t2/2,t2/2,-h1,0   ! ss316 block
wpave,r3                ! moved wp to circle center

PCIRC,r2,0,0180,360,      ! circle
wpave,r1                ! move wp to edge of BE block
rectan,0,t1,-h1,0         ! Be block
FLST,2,3,5,ORDE,2
FITEM,2,1
FITEM,2,-3
AOVLAP,P51X               ! overlap all areas
CM,_Y,AREA
ASEL, , , ,     4
CM,_Y1,AREA
CMSEL,S,_Y
CMSEL,S,_Y1
AATT,1,1,1,0,
CMSEL,S,_Y
CMDELE,_Y
CMDELE,_Y1
CM,_Y,AREA
ASEL, , , ,     5
CM,_Y1,AREA
CMSEL,S,_Y
CMSEL,S,_Y1
AATT,2,1,1,0,
CMSEL,S,_Y
CMDELE,_Y
CMDELE,_Y1
ASEL,S, , ,     2
adel,all,,,1
VSEL,ALL
ASEL,ALL
LSEL,ALL
KSEL,ALL
ESEL,ALL
NSEL,ALL
```

```
ASEL,S, , ,      5
VSEL,ALL
ASEL,ALL
LSEL,ALL
KSEL,ALL
ESEL,ALL
NSEL,ALL
KESIZE,ALL,t1/(n_fac*3), , , ,          !  sets element size
FLST,2,2,5,ORDE,2
FITEM,2,4
FITEM,2,-5
AMESH,P51X


FLST,2,97,2,ORDE,2
FITEM,2,1
FITEM,2,-97

VSEL,ALL
ASEL,ALL
LSEL,ALL
KSEL,ALL
ESEL,ALL
NSEL,ALL
bfe,all,hgen,1,qge_in     !  applies Hgen rate
nsel,,loc,x,r1
VSEL,ALL
ASEL,ALL
LSEL,ALL
KSEL,ALL
ESEL,ALL
NSEL,ALL
nsel,,loc,x,r1-.01,r1+.001
esel,all

sf,all,hflux,qfl_in    ! applies the heat flux at the inner radius
VSEL,ALL
ASEL,ALL
LSEL,ALL
KSEL,ALL
ESEL,ALL
```

```
NSEL,ALL
LSEL,S, , ,    5
NSLL,S,1
d,all,temp,t_sb     !  applies temperature to inner radius of hole
VSEL,ALL
ASEL,ALL
LSEL,ALL
KSEL,ALL
ESEL,ALL
NSEL,ALL
VSEL,ALL
ASEL,ALL
LSEL,ALL
KSEL,ALL
ESEL,ALL
NSEL,ALL
*get,num_n,node,,count
*get,num_e,elem,,count

fini
/sol
VSEL,ALL
ASEL,ALL
LSEL,ALL
KSEL,ALL
ESEL,ALL
NSEL,ALL
solve
fini
/post1
nsort,temp,,,,1
*get,max_t,sort,,max

/auto
/edge
/num,-1
/title,%mname% Model
eplo

/edge,,1
/num,2
```

```
/clab,,2
/title,%mname% Temperatures (C)
plns,temp
save,%mname%,db  ! saves the results to this filename
**************************
fini
/prep7
etch

/com,  add cp for other boundary      !  5/19/97
alls
nsel,,ext
*get,ymin,node,,mnloc,y          !  5/19/97
nsel,r,loc,y,ymin-.0001,ymin+.0001     !  5/19/97
cp,1,uy,all                    !  5/19/97
alls                         !  5/19/97



FINISH
/SOLU
NSEL,,LOC,y,0
d,all,uy,0    ! the one Y displacement along the plane of symmetry
NSEL,all
LDREAD,TEMP,1,,, ,file,rth,  !  reads the temperature from the thermal

tref,20   !  stress free temperature
LSEL,S, , ,      5
NSLL,S,1
sf,all,pres,p_in

VSEL,ALL
ASEL,ALL
LSEL,ALL
KSEL,ALL
ESEL,ALL
NSEL,ALL

!

fini
```

```
/sol
solve
fini
/post1
nsort,s,int,,,,1
*get,max_si,sort,,max
/title,%mname% Stress Intensities (MPa)
esel,,mat,,2   ! 9/18/97
nsle           ! 9/18/97
plns,s,int
save,%mname%,db ! saves the results to this filename
**************************
! /sho,xxx    !  closes out the block1.plt  file
! /sho,term   !  plots back to the terminal

/out
```

M_sol.mac

```
/out,m_sol,out
! m_sol.mac
!
n_fac=1    !  used to increase the mesh density
!          see gen_inp.mac


/com, Load the file names (*.inp) from "L_DIR" file
*set,_n_fil
*dim,_n_fil,,1
*vread,_n_fil(1),l_dir
(8x,f15.0)
*set,_nm_fil
*dim,_nm_fil,char,_n_fil(1)
*vread,_nm_fil(1),l_dir
(a8)

*stat,_nm_fil

/out

! results array
!   I= ith file name (i th case)
!  _ansum(i,j),
!    J   item
!    1   max temperature
!    2   max stress (SI)
!    3   heat generation
!    4   heat flux
!
!
*set,_ansum
*dim,_ansum,,_n_fil(1),4

parsav,m_sol,par

*do,_i11,1,_n_fil(1)
 /gopr
 *msg,info,_i11
```

```
cycle: %i
mname=_nm_fil(_i11)

gen_inp
/out,m_sol,out,,append

_ansum(_i11,1)=max_t
_ansum(_i11,2)=max_si
_ansum(_i11,3)=qge_in
_ansum(_i11,4)=qfl_in


*enddo

/out,m_sol,sum
*msg,info
_____SUMMARY OF RESULTS_____

*msg,info

*msg,info,_n_fil(1)
Number of Cases Evaluated:___ %i
*msg,info,num_n
Number of nodes:_____ %i
*msg,info,num_e
Number of elements:_____ %i
*msg,info,n_fac
Mesh Density factor:_____ %i
*msg,info
__Name_____Heat_____Heat_____Max_____Max_____
!aaaaaabbbbbbbbbbbbccccccccddddddddddeeeeeeeeeeeeeee
*msg,info
_____Generation____Flux___Temperature__Stress Int.__
*vwrit,_nm_fil(1),_ansum(1,3),_ansum(1,4),_ansum(1,1),_ansum(1,2)
(1x,a8,e11.4,3x,e9.4,2x,e10.4,e14.5)

*msg,info

*msg,info

_____
*msg,info
```

```
*msg,info
The plots are contained in M_SOL.F33, and the array&
data is stored in M_SOL.PAR
/out
/sho,xxx
/sho,term
*uili,m_sol,sum
```

l dir

```
sa_4     4.
sb_4
sc_4
sd_4
```

Sa_4.des

```
! THIS FILE PROVIDES DESIGN PARAMETER INPUT FOR BLOCK1.INP

!!!!!!!!!!!!!!!!!!!!!!!!!!!!!!!!!!!!!!!!!!!!!!!!!!!!!!!!!!!!!!!!!!!!!!!

!                    ITER

!!!!!!!!!!!!!!!!!!!!!!!!!!!!!!!!!!!!!!!!!!!!!!!!!!!!!!!!!!!!!!!!!!!!!!!

!STRUCTURAL MATERIAL:        SS316
!SACRIFICIAL LAYER MATERAL:  BERYLLIUM

!FILENAME:                   SA_4.des

!    Design Parameters


qge_in=83.33e6       !    heat generation rate (W/m^3)

qfl_in=3.0e6         !    surface heat flux (W/m^2)

t_sb=286             !    coolant tube surface temperature degree C


!    MATERIAL PROPERTIES

!    SACRIFICAL LAYER

mp,kxx,1,100.0       !    W/mK
mp,alpx,1,1.6e-5     !    1/K
mp,ex,1,48e9         !    Pa
mp,nuxy,1,.08        !    Poisson Ratio (dimensionless)

!    STRUCTURAL MATERIAL

mp,kxx,2,14.8        !    W/mK
mp,alpx,2,1.8e-5     !    1/K
mp,ex,2,166e9        !    Pa
mp,nuxy,2,.27        !    Poisson Ratio (dimensionless)
```

Sb_4.des

```
! THIS FILE PROVIDES DESIGN PARAMETER INPUT FOR BLOCK1.INP

!!!!!!!!!!!!!!!!!!!!!!!!!!!!!!!!!!!!!!!!!!!!!!!!!!!!!!!!!!!!!!!!!!!!!!!

!                    ITER

!!!!!!!!!!!!!!!!!!!!!!!!!!!!!!!!!!!!!!!!!!!!!!!!!!!!!!!!!!!!!!!!!!!!!!!

!STRUCTURAL MATERIAL:      SS316
!SACRIFICIAL LAYER MATERAL:   BERYLLIUM

!FILENAME:                 SB_4.des


!    Design Parameters


qge_in=55.6 e6       !    heat generation rate (W/m^3)

qfl_in=2.0e6         !    surface heat flux (W/m^2)

t_sb=367             !    coolant tube surface temperature degree C

fini
/prep7

!    MATERIAL PROPERTIES

!    SACRIFICAL LAYER

mp,kxx,1,100.0       !    W/mK
mp,alpx,1,1.6e-5     !    1/K
mp,ex,1,48e9         !    Pa
mp,nuxy,1,.08        !    Poisson Ratio (dimensionless)

!    STRUCTURAL MATERIAL

mp,kxx,2,14.8        !    W/mK
```

```
mp,alpx,2,1.8e-5    !    1/K
mp,ex,2,166e9       !    Pa
mp,nuxy,2,.27       !    Poisson Ratio (dimensionless)
```

Sc_4.des

```
! THIS FILE PROVIDES DESIGN PARAMETER INPUT FOR BLOCK1.INP

!!!!!!!!!!!!!!!!!!!!!!!!!!!!!!!!!!!!!!!!!!!!!!!!!!!!!!!!!!!!!!!!!!!!!!!

!                    ITER

!!!!!!!!!!!!!!!!!!!!!!!!!!!!!!!!!!!!!!!!!!!!!!!!!!!!!!!!!!!!!!!!!!!!!!!

!STRUCTURAL MATERIAL:      SS316
!SACRIFICIAL LAYER MATERAL:    BERYLLIUM

!FILENAME:                 SC_4.des

!     Design Parameters


qge_in=27.8e6        !     heat generation rate (W/m^3)

qfl_in=1.0e6         !     surface heat flux (W/m^2)

t_sb=276             !     coolant tube surface temperature degree C

fini
/prep7

!     MATERIAL PROPERTIES

!     SACRIFICAL LAYER

mp,kxx,1,100.0       !     W/mK
mp,alpx,1,1.6e-5     !     1/K
mp,ex,1,48e9         !     Pa
mp,nuxy,1,.08        !     Poisson Ratio (dimensionless)

!     STRUCTURAL MATERIAL

mp,kxx,2,14.8        !     W/mK
mp,alpx,2,1.8e-5     !     1/K
```

```
mp,ex,2,166e9        !    Pa
mp,nuxy,2,.27        !    Poisson Ratio (dimensionless)
```

Sd_4.des

```
! THIS FILE PROVIDES DESIGN PARAMETER INPUT FOR BLOCK1.INP

!!!!!!!!!!!!!!!!!!!!!!!!!!!!!!!!!!!!!!!!!!!!!!!!!!!!!!!!!!!!!!!!!!!!!!!

!                    ITER

!!!!!!!!!!!!!!!!!!!!!!!!!!!!!!!!!!!!!!!!!!!!!!!!!!!!!!!!!!!!!!!!!!!!!!!

!STRUCTURAL MATERIAL:        SS316
!SACRIFICIAL LAYER MATERAL:   BERYLLIUM

!FILENAME:                   SD_4.des
!    Design Parameters


qge_in=13.88e6       !    heat generation rate (W/m^3)

qfl_in=0.5e6         !    surface heat flux (W/m^2)

t_sb=271             !    coolant tube surface temperature degree C

fini
/prep7

!    MATERIAL PROPERTIES

!    SACRIFICAL LAYER

mp,kxx,1,100.0       !    W/mK
mp,alpx,1,1.6e-5     !    1/K
mp,ex,1,48e9         !    Pa
mp,nuxy,1,.08        !    Poisson Ratio (dimensionless)

!    STRUCTURAL MATERIAL

mp,kxx,2,14.8        !    W/mK
mp,alpx,2,1.8e-5     !    1/K
```

```
mp,ex,2,166e9       !   Pa
mp,nuxy,2,.27       !   Poisson Ratio (dimensionless)
```

m_sol.out

```
PARAMETER N_FAC   =     1.000000
 Load the file names (*.inp) from "L_DIR" file

 PARAMETER _N_FIL   DELETED.

 SET PARAMETER DIMENSIONS ON  _N_FIL  TYPE=ARRA
DIMENSIONS=     1   1  1


 VECTOR READ OPERATION  *VREAD
  _N_FIL  READ FROM FILE l_dir
 VECTOR LENGTH=     1
 FORMAT=(8x,f15.0)

 PARAMETER _NM_FIL  DELETED.

 SET PARAMETER DIMENSIONS ON  _NM_FIL  TYPE=CHAR
DIMENSIONS=     4   1  1


 VECTOR READ OPERATION  *VREAD
  _NM_FIL  READ FROM FILE l_dir
 VECTOR LENGTH=     4
 FORMAT=(a8)

 PARAMETER STATUS- _NM_FIL  (  3 PARAMETERS DEFINED)
          (INCLUDING    2 INTERNAL PARAMETERS)

    LOCATION        VALUE
    1    1    1 sa_4    (Char)
    2    1    1 sb_4    (Char)
    3    1    1 sc_4    (Char)
    4    1    1 sd_4    (Char)

 PARAMETER _ANSUM(_I11,1) =     1170.333

 PARAMETER _ANSUM(_I11,2) =     .1656783E+10
```

PARAMETER _ANSUM(_I11,3) = .8333000E+08

PARAMETER _ANSUM(_I11,4) = 3000000.

*ENDDO INDEX= _I11
Cycle: 2.

PARAMETER MNAME = sb_4

USE COMMAND MACRO GEN_INP

/OUTPUT FILE= gen_inp.out

PARAMETER _ANSUM(_I11,1) = 956.6251

PARAMETER _ANSUM(_I11,2) = .1091739E+10

PARAMETER _ANSUM(_I11,3) = .5560000E+08

PARAMETER _ANSUM(_I11,4) = 2000000.
Cycle: 3.

PARAMETER MNAME = sc_4

USE COMMAND MACRO GEN_INP

/OUTPUT FILE= gen_inp.out

PARAMETER _ANSUM(_I11,1) = 570.8125

PARAMETER _ANSUM(_I11,2) = .5394557E+09

PARAMETER _ANSUM(_I11,3) = .2780000E+08

PARAMETER _ANSUM(_I11,4) = 1000000.
Cycle: 4.

PARAMETER MNAME = sd_4

USE COMMAND MACRO GEN_INP

/OUTPUT FILE= gen_inp.out

PARAMETER _ANSUM(_I11,1) = 418.3762

PARAMETER _ANSUM(_I11,2) = .2668379E+09

PARAMETER _ANSUM(_I11,3) = .1388000E+08

PARAMETER _ANSUM(_I11,4) = 500000.0

/OUTPUT FILE= m_sol.sum

gen_inp.out

```
EXIT THE ANSYS POST1 DATABASE PROCESSOR

***** ROUTINE COMPLETED *****  CP =      116.720



*** NOTE ***                            CP=   116.720   TIME= 12:38:37
A total of 6 warnings and errors written to file.err.

*IF  n_fac                      ( =  1.00000    ) LE
   0                          ( =  .000000    ) THEN

*ENDIF

*** NOTE ***                            CP=   116.780   TIME= 12:38:37
Write parameters to file= m_sol.par.

*** NOTE ***                            CP=   116.830   TIME= 12:38:37
Parameters written.  Lines= 39.


NUMBER OF DISPLAYED ERRORS ALLOWED PER COMMAND=
0
NUMBER OF ERRORS ALLOWED PER COMMAND BEFORE ANSYS
ABORT= ******

CLEAR ANSYS DATABASE AND RESTART

*** NOTE ***                            CP=   117.820   TIME= 12:38:38
Restore ANSYS parameters from file= m_sol.par.

/INPUT FILE= m_sol.par  LINE=      0

      ***** ANSYS ANALYSIS DEFINITION (PREP7) *****

ENTER  /SHOW,DEVICE-NAME  TO ENABLE GRAPHIC DISPLAY
ENTER  FINISH         TO LEAVE PREP7
```

PRINTOUT KEY SET TO /GOPR (USE /NOPR TO SUPPRESS)

IMMEDIATE DISPLAY OFF

DISPLAYS PUT ON PLOT FILE m_sol.f33 - VECTOR MODE.

ELEMENT TYPE 1 IS PLANE77 AXI. 8-NODE THERMAL SOLID
KEYOPT(1-12)= 0 0 1 0 0 0 0 0 0 0 0 0

CURRENT NODAL DOF SET IS TEMP
AXISYMMETRIC MODEL

/INPUT FILE= sd_4.des LINE= 0

PARAMETER QGE_IN = .1388000E+08

PARAMETER QFL_IN = 500000.0

PARAMETER T_SB = 271.0000

***** ROUTINE COMPLETED ***** CP = 118.420

*** NOTE *** CP= 118.420 TIME= 12:38:38
A total of 6 warnings and errors written to file.err.

***** ANSYS ANALYSIS DEFINITION (PREP7) *****

ENTER /SHOW,DEVICE-NAME TO ENABLE GRAPHIC DISPLAY
ENTER FINISH TO LEAVE PREP7
PRINTOUT KEY SET TO /GOPR (USE /NOPR TO SUPPRESS)

MATERIAL 1 KXX = 100.0000

MATERIAL 1 ALPX = .1600000E-04

MATERIAL 1 EX = .4800000E+11

MATERIAL 1 NUXY = .8000000E-01

MATERIAL 2 KXX = 14.80000

MATERIAL 2 ALPX = .1800000E-04

MATERIAL 2 EX = .1660000E+12

MATERIAL 2 NUXY = .2700000

PARAMETER R1 = 2.560000

PARAMETER T1 = .5000000E-02

PARAMETER R2 = .5000000E-02

PARAMETER T2 = .2000000E-01

PARAMETER T3 = .2000000E-02

PARAMETER H1 = .7000000E-02

PARAMETER R3 = 2.572000

***** ROUTINE COMPLETED ***** CP = 119.030

*** NOTE *** CP= 119.030 TIME= 12:38:39
A total of 6 warnings and errors written to file.err.

***** ANSYS ANALYSIS DEFINITION (PREP7) *****

ENTER /SHOW,DEVICE-NAME TO ENABLE GRAPHIC DISPLAY
ENTER FINISH TO LEAVE PREP7
PRINTOUT KEY SET TO /GOPR (USE /NOPR TO SUPPRESS)

MOVE ORIGIN OF WORKING PLANE TO THE AVERAGE OF 1
LOCATIONS IN CSYS 0
2.57200 , .000000 , .000000

```
CREATE A PLANAR RECTANGULAR AREA WITH
X-DISTANCES FROM    -.1000000000E-01 TO     .1000000000E-01
Y-DISTANCES FROM    -.7000000000E-02 TO     .0000000000

   OUTPUT AREA =    1

DELETE  ALL  SELECTED AREAS.

   DELETED   1 AREAS,    4 LINES,    4 KEYPOINTS

MOVE ORIGIN OF WORKING PLANE TO THE AVERAGE OF     1
LOCATIONS IN CSYS     0
  2.57500    ,   .000000    ,   .000000

CREATE A PLANAR RECTANGULAR AREA WITH
X-DISTANCES FROM    -.1000000000E-01 TO     .1000000000E-01
Y-DISTANCES FROM    -.7000000000E-02 TO     .0000000000

   OUTPUT AREA =    1

MOVE ORIGIN OF WORKING PLANE TO THE AVERAGE OF     1
LOCATIONS IN CSYS     0
  2.57200    ,   .000000    ,   .000000

CREATE A CIRCULAR AREA WITH
INNER RADIUS        =     .0000000000
OUTER RADIUS        =     .5000000000E-02
STARTING THETA ANGLE =     180.0000000
ENDING  THETA ANGLE =     360.0000000

   OUTPUT AREA =    2

MOVE ORIGIN OF WORKING PLANE TO THE AVERAGE OF     1
LOCATIONS IN CSYS     0
  2.56000    ,   .000000    ,   .000000

CREATE A PLANAR RECTANGULAR AREA WITH
X-DISTANCES FROM    .0000000000    TO     .5000000000E-02
Y-DISTANCES FROM    -.7000000000E-02 TO     .0000000000

   OUTPUT AREA =    3
```

```
OVERLAP AREAS
   INPUT AREAS =    1   2   3
   INPUT AREAS WILL BE DELETED
   OUTPUT AREAS =    2   4   5

DEFINITION OF COMPONENT = _Y      ENTITY=AREA

SELECT      FOR ITEM=AREA COMPONENT=
 IN RANGE     4 TO      4 STEP      1

   1  AREAS (OF    3  DEFINED) SELECTED BY  ASEL  COMMAND.

DEFINITION OF COMPONENT = _Y1     ENTITY=AREA

SELECT     COMPONENT _Y

SELECT     COMPONENT _Y1

SET ATTRIBUTES FOR ALL SELECTED AREAS
   MAT =   1  REAL =      1  TYPE =    1  ESYS =   0
ATTRIBUTES SET FOR     1 AREAS (OUT OF     1 SELECTED)

SELECT     COMPONENT _Y

DELETE COMPONENT _Y

DELETE COMPONENT _Y1

DEFINITION OF COMPONENT = _Y      ENTITY=AREA

SELECT      FOR ITEM=AREA COMPONENT=
 IN RANGE     5 TO      5 STEP      1

   1  AREAS (OF    3  DEFINED) SELECTED BY  ASEL  COMMAND.

DEFINITION OF COMPONENT = _Y1     ENTITY=AREA

SELECT     COMPONENT _Y

SELECT     COMPONENT _Y1
```

```
SET ATTRIBUTES FOR ALL SELECTED AREAS
   MAT =   2  REAL =     1  TYPE =   1  ESYS =   0
ATTRIBUTES SET FOR     1 AREAS (OUT OF     1 SELECTED)

SELECT     COMPONENT _Y

DELETE COMPONENT _Y

DELETE COMPONENT _Y1

SELECT      FOR ITEM=AREA COMPONENT=
 IN RANGE     2 TO      2 STEP      1

   1  AREAS (OF    3  DEFINED) SELECTED BY  ASEL  COMMAND.

DELETE   ALL   SELECTED AREAS.

   DELETED    1 AREAS,    2 LINES,     1 KEYPOINTS

ALL SELECT   FOR ITEM=VOLU COMPONENT=
 IN RANGE     0 TO      0 STEP      1

    0  VOLUMES (OF     0  DEFINED) SELECTED BY  VSEL
COMMAND.

ALL SELECT   FOR ITEM=AREA COMPONENT=
 IN RANGE     1 TO      5 STEP      1

   2  AREAS (OF    2  DEFINED) SELECTED BY ASEL COMMAND.

ALL SELECT   FOR ITEM=LINE COMPONENT=
 IN RANGE     1 TO     15 STEP      1

   9  LINES (OF    9  DEFINED) SELECTED BY LSEL COMMAND.

ALL SELECT   FOR ITEM=KP   COMPONENT=
 IN RANGE     1 TO     11 STEP      1

    8 KEYPOINTS (OF     8 DEFINED) SELECTED BY  KSEL
COMMAND.
```

```
ALL SELECT   FOR ITEM=ELEM COMPONENT=
 IN RANGE     0 TO       0 STEP       1

   0 ELEMENTS (OF     0  DEFINED) SELECTED BY  ESEL
COMMAND.

ALL SELECT   FOR ITEM=NODE COMPONENT=
 IN RANGE     0 TO       0 STEP       1

   0 NODES (OF     0  DEFINED) SELECTED BY  NSEL  COMMAND.

SELECT       FOR ITEM=AREA COMPONENT=
 IN RANGE     5 TO       5 STEP       1

   1 AREAS (OF    2  DEFINED) SELECTED BY  ASEL  COMMAND.

ALL SELECT   FOR ITEM=VOLU COMPONENT=
 IN RANGE     0 TO       0 STEP       1

   0 VOLUMES (OF     0  DEFINED) SELECTED BY  VSEL
COMMAND.

ALL SELECT   FOR ITEM=AREA COMPONENT=
 IN RANGE     1 TO       5 STEP       1

   2 AREAS (OF    2  DEFINED) SELECTED BY ASEL COMMAND.

ALL SELECT   FOR ITEM=LINE COMPONENT=
 IN RANGE     1 TO      15 STEP       1

   9 LINES (OF    9  DEFINED) SELECTED BY LSEL COMMAND.

ALL SELECT   FOR ITEM=KP   COMPONENT=
 IN RANGE     1 TO      11 STEP       1

   8 KEYPOINTS (OF     8  DEFINED) SELECTED BY  KSEL
COMMAND.

ALL SELECT   FOR ITEM=ELEM COMPONENT=
 IN RANGE     0 TO       0 STEP       1
```

```
    0 ELEMENTS (OF     0  DEFINED) SELECTED BY  ESEL
COMMAND.

 ALL SELECT   FOR ITEM=NODE COMPONENT=
  IN RANGE      0 TO       0 STEP       1

    0  NODES (OF     0  DEFINED) SELECTED BY  NSEL  COMMAND.

 AT ALL SELECTED KEYPOINTS,
   SET DESIRED ELEMENT EDGE LENGTH TO  .16667E-02

 GENERATE NODES AND ELEMENTS  IN  ALL  PICKED   AREAS

 ** Meshing of area 4 in progress **
 ** Meshing of area 4 completed ** 12 elements.

 ** Meshing of area 5 in progress **

 ** Initial meshing of area 5 complete **
   ** AREA     5 MESHED WITH    40 QUADRILATERALS,      1
TRIANGLES **
 ** Meshing of area 5 completed ** 41 elements.

 NUMBER OF AREAS MESHED     =     2
 MAXIMUM NODE NUMBER        =   200
 MAXIMUM ELEMENT NUMBER     =    53

 ALL SELECT   FOR ITEM=VOLU COMPONENT=
  IN RANGE      0 TO       0 STEP       1

    0  VOLUMES (OF     0  DEFINED) SELECTED BY  VSEL
COMMAND.

 ALL SELECT   FOR ITEM=AREA COMPONENT=
  IN RANGE      1 TO       5 STEP       1

    2  AREAS (OF     2  DEFINED) SELECTED BY ASEL COMMAND.

 ALL SELECT   FOR ITEM=LINE COMPONENT=
  IN RANGE      1 TO      15 STEP       1
```

```
   9 LINES (OF    9 DEFINED) SELECTED BY LSEL COMMAND.

 ALL SELECT   FOR ITEM=KP   COMPONENT=
  IN RANGE      1 TO      11 STEP       1

    8 KEYPOINTS (OF     8 DEFINED) SELECTED BY  KSEL
COMMAND.

 ALL SELECT   FOR ITEM=ELEM COMPONENT=
  IN RANGE      1 TO      53 STEP       1

   53 ELEMENTS (OF    53 DEFINED) SELECTED BY  ESEL
COMMAND.

 ALL SELECT   FOR ITEM=NODE COMPONENT=
  IN RANGE      1 TO     200 STEP       1

  200 NODES (OF   200 DEFINED) SELECTED BY  NSEL  COMMAND.

 SPECIFIED BODY FORCE HGEN FOR ALL SELECTED ELEMENTS AT
STARTING LOCATION     1
   13880000.0     .000000000     .000000000     .000000000

 SELECT      FOR ITEM=LOC  COMPONENT=X    BETWEEN  2.5600
AND  2.5600
  KABS=  0.  TOLERANCE=  .128000E-01

   99 NODES (OF   200 DEFINED) SELECTED BY  NSEL  COMMAND.

 ALL SELECT   FOR ITEM=VOLU COMPONENT=
  IN RANGE      0 TO       0 STEP       1

    0 VOLUMES (OF     0 DEFINED) SELECTED BY  VSEL
COMMAND.

 ALL SELECT   FOR ITEM=AREA COMPONENT=
  IN RANGE      1 TO       5 STEP       1

    2 AREAS (OF    2 DEFINED) SELECTED BY ASEL COMMAND.
```

```
 ALL SELECT   FOR ITEM=LINE COMPONENT=
  IN RANGE      1 TO      15 STEP       1

    9  LINES (OF    9  DEFINED) SELECTED BY LSEL COMMAND.

 ALL SELECT   FOR ITEM=KP   COMPONENT=
  IN RANGE      1 TO      11 STEP       1

     8  KEYPOINTS (OF     8  DEFINED) SELECTED BY  KSEL
COMMAND.

 ALL SELECT   FOR ITEM=ELEM COMPONENT=
  IN RANGE      1 TO      53 STEP       1

    53  ELEMENTS (OF    53  DEFINED) SELECTED BY  ESEL
COMMAND.

 ALL SELECT   FOR ITEM=NODE COMPONENT=
  IN RANGE      1 TO     200 STEP       1

   200  NODES (OF   200  DEFINED) SELECTED BY  NSEL  COMMAND.

 SELECT      FOR ITEM=LOC  COMPONENT=X    BETWEEN  2.5500
AND  2.5610
  KABS=  0.  TOLERANCE=  .110000E-09

    14  NODES (OF   200  DEFINED) SELECTED BY  NSEL  COMMAND.

 ALL SELECT   FOR ITEM=ELEM COMPONENT=
  IN RANGE      1 TO      53 STEP       1

    53  ELEMENTS (OF    53  DEFINED) SELECTED BY  ESEL
COMMAND.

 GENERATE SURFACE LOAD HFLU ON SURFACE DEFINED BY ALL
SELECTED NODES
  VALUE=  500000.000

 NUMBER OF HFLU ELEMENT FACE LOADS STORED =      4

 ALL SELECT   FOR ITEM=VOLU COMPONENT=
```

```
 IN RANGE      0 TO       0 STEP       1

    0 VOLUMES (OF     0 DEFINED) SELECTED BY  VSEL
COMMAND.

 ALL SELECT   FOR ITEM=AREA COMPONENT=
 IN RANGE      1 TO       5 STEP       1

   2  AREAS (OF    2  DEFINED) SELECTED BY ASEL COMMAND.

 ALL SELECT   FOR ITEM=LINE COMPONENT=
 IN RANGE      1 TO      15 STEP       1

   9  LINES (OF    9  DEFINED) SELECTED BY LSEL COMMAND.

 ALL SELECT   FOR ITEM=KP   COMPONENT=
 IN RANGE      1 TO      11 STEP       1

    8 KEYPOINTS (OF     8  DEFINED) SELECTED BY  KSEL
COMMAND.

 ALL SELECT   FOR ITEM=ELEM COMPONENT=
 IN RANGE      1 TO      53 STEP       1

   53  ELEMENTS (OF    53  DEFINED) SELECTED BY  ESEL
COMMAND.

 ALL SELECT   FOR ITEM=NODE COMPONENT=
 IN RANGE      1 TO     200 STEP       1

  200  NODES (OF   200  DEFINED) SELECTED BY  NSEL  COMMAND.

 SELECT       FOR ITEM=LINE COMPONENT=
 IN RANGE      5 TO       5 STEP       1

   1  LINES (OF    9  DEFINED) SELECTED BY LSEL  COMMAND.

 SELECT      ALL NODES (INTERIOR TO LINE, AND AT KEYPOINTS)
     RELATED TO SELECTED LINE SET.

   19  NODES (OF   200  DEFINED) SELECTED FROM
```

1 SELECTED LINES BY NSLL COMMAND.

SPECIFIED CONSTRAINT TEMP FOR SELECTED NODES 1 TO 200 BY 1
REAL= 271.000000 IMAG= .000000000

ALL SELECT FOR ITEM=VOLU COMPONENT=
IN RANGE 0 TO 0 STEP 1

0 VOLUMES (OF 0 DEFINED) SELECTED BY VSEL COMMAND.

ALL SELECT FOR ITEM=AREA COMPONENT=
IN RANGE 1 TO 5 STEP 1

2 AREAS (OF 2 DEFINED) SELECTED BY ASEL COMMAND.

ALL SELECT FOR ITEM=LINE COMPONENT=
IN RANGE 1 TO 15 STEP 1

9 LINES (OF 9 DEFINED) SELECTED BY LSEL COMMAND.

ALL SELECT FOR ITEM=KP COMPONENT=
IN RANGE 1 TO 11 STEP 1

8 KEYPOINTS (OF 8 DEFINED) SELECTED BY KSEL COMMAND.

ALL SELECT FOR ITEM=ELEM COMPONENT=
IN RANGE 1 TO 53 STEP 1

53 ELEMENTS (OF 53 DEFINED) SELECTED BY ESEL COMMAND.

ALL SELECT FOR ITEM=NODE COMPONENT=
IN RANGE 1 TO 200 STEP 1

200 NODES (OF 200 DEFINED) SELECTED BY NSEL COMMAND.

ALL SELECT FOR ITEM=VOLU COMPONENT=
IN RANGE 0 TO 0 STEP 1

0 VOLUMES (OF 0 DEFINED) SELECTED BY VSEL COMMAND.

ALL SELECT FOR ITEM=AREA COMPONENT=
IN RANGE 1 TO 5 STEP 1

2 AREAS (OF 2 DEFINED) SELECTED BY ASEL COMMAND.

ALL SELECT FOR ITEM=LINE COMPONENT=
IN RANGE 1 TO 15 STEP 1

9 LINES (OF 9 DEFINED) SELECTED BY LSEL COMMAND.

ALL SELECT FOR ITEM=KP COMPONENT=
IN RANGE 1 TO 11 STEP 1

8 KEYPOINTS (OF 8 DEFINED) SELECTED BY KSEL COMMAND.

ALL SELECT FOR ITEM=ELEM COMPONENT=
IN RANGE 1 TO 53 STEP 1

53 ELEMENTS (OF 53 DEFINED) SELECTED BY ESEL COMMAND.

ALL SELECT FOR ITEM=NODE COMPONENT=
IN RANGE 1 TO 200 STEP 1

200 NODES (OF 200 DEFINED) SELECTED BY NSEL COMMAND.

*GET num_n FROM NODE ITEM=COUN VALUE= 200.000000

*GET num_e FROM ELEM ITEM=COUN VALUE= 53.0000000

***** ROUTINE COMPLETED ***** CP = 126.550

*** NOTE *** CP= 126.550 TIME= 12:38:47

A total of 6 warnings and errors written to file.err.

***** ANSYS SOLUTION ROUTINE *****

ALL SELECT FOR ITEM=VOLU COMPONENT=
IN RANGE 0 TO 0 STEP 1

0 VOLUMES (OF 0 DEFINED) SELECTED BY VSEL COMMAND.

ALL SELECT FOR ITEM=AREA COMPONENT=
IN RANGE 1 TO 5 STEP 1

2 AREAS (OF 2 DEFINED) SELECTED BY ASEL COMMAND.

ALL SELECT FOR ITEM=LINE COMPONENT=
IN RANGE 1 TO 15 STEP 1

9 LINES (OF 9 DEFINED) SELECTED BY LSEL COMMAND.

ALL SELECT FOR ITEM=KP COMPONENT=
IN RANGE 1 TO 11 STEP 1

8 KEYPOINTS (OF 8 DEFINED) SELECTED BY KSEL COMMAND.

ALL SELECT FOR ITEM=ELEM COMPONENT=
IN RANGE 1 TO 53 STEP 1

53 ELEMENTS (OF 53 DEFINED) SELECTED BY ESEL COMMAND.

ALL SELECT FOR ITEM=NODE COMPONENT=
IN RANGE 1 TO 200 STEP 1

200 NODES (OF 200 DEFINED) SELECTED BY NSEL COMMAND.

***** ANSYS SOLVE COMMAND *****

*** NOTE *** CP= 126.720 TIME= 12:38:47
There is no title defined for this analysis.

SOLUTION OPTIONS

PROBLEM DIMENSIONALITY. . . . . .AXISYMMETRIC
DEGREES OF FREEDOM. . . . . TEMP
ANALYSIS TYPE . . . . . .STATIC (STEADY-STATE)

*** NOTE *** CP= 126.940 TIME= 12:38:47
Axisymmetric elements present. Loads input with the F commands and the corresponding output quantities are on a full circle basis. This differs from pre-Rev 5.0 interpretation.

*** NOTE *** CP= 126.940 TIME= 12:38:47
Present time 0 is less than or equal to the previous time.
Time will default to 1.

LOAD STEP OPTIONS

LOAD STEP NUMBER. 1
TIME AT END OF THE LOAD STEP. 1.0000
NUMBER OF SUBSTEPS. 1
STEP CHANGE BOUNDARY CONDITIONS . . . . . NO
AXISYMMETRIC HARMONIC LOADING PARAMETERS
MODE 0
ISYM 1
PRINT OUTPUT CONTROLS . . . . . .NO PRINTOUT
DATABASE OUTPUT CONTROLS. . . . . .ALL DATA WRITTEN
FOR THE LAST SUBSTEP

Element Formation Element= 10 Cum. Iter.= 1 CP= 127.710
Time= 1.0000 Load Step= 1 Substep= 1 Equilibrium Iteration= 1.

Range of element maximum matrix coefficients in global coordinates
Maximum= 3825.75507 at element 3.
Minimum= 562.328104 at element 31.

*** ELEMENT MATRIX FORMULATION TIMES

TYPE	NUMBER	ENAME	TOTAL CP	AVE CP
1	53	PLANE77	.220	.004

```
Time at end of element matrix formulation CP= 127.93.

Estimated number of active DOF= 181.
Maximum wavefront= 19.

Time at end of matrix triangularization CP= 128.25.
Equation solver maximum pivot= 5879.01711 at node 40 TEMP.
Equation solver minimum pivot= 278.990485 at node 76 TEMP.

 *** ELEMENT RESULT CALCULATION TIMES
 TYPE  NUMBER   ENAME     TOTAL CP  AVE CP

   1     53  PLANE77       .330     .006

 *** NODAL LOAD CALCULATION TIMES
 TYPE  NUMBER   ENAME     TOTAL CP  AVE CP

   1     53  PLANE77       .110     .002
*** LOAD STEP   1   SUBSTEP    1 COMPLETED.   CUM ITER =     1
*** TIME =   1.00000       TIME INC =   1.00000     NEW TRIANG
MATRIX


 *** PROBLEM STATISTICS
 ACTUAL NO. OF ACTIVE DEGREES OF FREEDOM =    181
 R.M.S. WAVEFRONT SIZE =    12.5


*** ANSYS BINARY FILE STATISTICS
 BUFFER SIZE USED=  4096
      .047 MB WRITTEN ON ELEMENT MATRIX FILE: file.emat
      .047 MB WRITTEN ON ELEMENT SAVED DATA FILE: file.esav
      .031 MB WRITTEN ON TRIANGULARIZED MATRIX FILE: file.tri
      .078 MB WRITTEN ON RESULTS FILE: file.rth

FINISH SOLUTION PROCESSING


***** ROUTINE COMPLETED *****  CP =       129.630
```

*** NOTE *** CP= 129.630 TIME= 12:38:50
A total of 6 warnings and errors written to file.err.

***** ANSYS RESULTS INTERPRETATION (POST1) *****

ENTER /SHOW,DEVICE-NAME TO ENABLE GRAPHIC DISPLAY
ENTER FINISH TO LEAVE POST1

SORT ON ITEM=TEMP COMPONENT= ORDER= 0 KABS= 0
NMAX= 1

SORT COMPLETED FOR 1 VALUES.

*GET max_t FROM SORT ITEM=MAX VALUE= 418.376236

AUTOMATIC SCALING FOR WINDOW 1
 DISTANCE AND FOCUS POINT AUTOMATICALLY CALCULATED

EDGE KEY FOR WINDOW 1 IS 0 WITH TOLERANCE ANGLE OF 45.0
DEGREES.

NUMBER KEY SET TO -1 -1=NONE 0=BOTH 1=COLOR 2=NUMBER

TITLE=
sd_4 Model

PRODUCE ELEMENT PLOT IN DSYS = 0

CUMULATIVE DISPLAY NUMBER 10 WRITTEN TO FILE m_sol.f33
- VECTOR MODE.
DISPLAY TITLE=
sd_4 Model

*** NOTE *** CP= 129.900 TIME= 12:38:50
CUMULATIVE DISPLAY NUMBER 10 WRITTEN TO FILE m_sol.f33 -
VECTOR MODE.
 DISPLAY TITLE= sd_4 Model.

EDGE KEY FOR WINDOW 1 IS 1 WITH TOLERANCE ANGLE OF 45.0 DEGREES.

NUMBER KEY SET TO 2 -1=NONE 0=BOTH 1=COLOR 2=NUMBER

CONTOUR LABELING ON FOR WINDOW 1 WITH VECTOR LABEL SPACING OF 2

TITLE=
sd_4 Temperatures (C)

DISPLAY NODAL SOLUTION, ITEM=TEMP COMP=

CUMULATIVE DISPLAY NUMBER 11 WRITTEN TO FILE m_sol.f33 - VECTOR MODE.
DISPLAY TITLE=
sd_4 Temperatures (C)

*** NOTE *** CP= 130.510 TIME= 12:38:50
CUMULATIVE DISPLAY NUMBER 11 WRITTEN TO FILE m_sol.f33 - VECTOR MODE.
DISPLAY TITLE= sd_4 Temperatures (C).

ALL CURRENT ANSYS DATA WRITTEN TO FILE NAME= sd_4.db
FOR POSSIBLE RESUME FROM THIS POINT

EXIT THE ANSYS POST1 DATABASE PROCESSOR

***** ROUTINE COMPLETED ***** CP = 131.720

*** NOTE *** CP= 131.720 TIME= 12:38:52
A total of 7 warnings and errors written to file.err.

***** ANSYS ANALYSIS DEFINITION (PREP7) *****

ENTER /SHOW,DEVICE-NAME TO ENABLE GRAPHIC DISPLAY
ENTER FINISH TO LEAVE PREP7

PRINTOUT KEY SET TO /GOPR (USE /NOPR TO SUPPRESS)

CHANGE ALL ELEMENT TYPES TO THEIR COMPANION ELEMENT TYPE
FOR ELEMENT TYPE 1, PLANE77 IS CHANGED TO PLANE82

*** NOTE *** CP= 131.830 TIME= 12:38:52
Element KEYOPTs were not changed - please verify their settings.
add cp for other boundary ! 5/19/97

SELECT ALL ENTITIES OF TYPE= ALL AND BELOW

ALL SELECT FOR ITEM=VOLU COMPONENT=
IN RANGE 0 TO 0 STEP 1

0 VOLUMES (OF 0 DEFINED) SELECTED BY VSEL COMMAND.

ALL SELECT FOR ITEM=AREA COMPONENT=
IN RANGE 1 TO 5 STEP 1

2 AREAS (OF 2 DEFINED) SELECTED BY ASEL COMMAND.

ALL SELECT FOR ITEM=LINE COMPONENT=
IN RANGE 1 TO 15 STEP 1

9 LINES (OF 9 DEFINED) SELECTED BY LSEL COMMAND.

ALL SELECT FOR ITEM=KP COMPONENT=
IN RANGE 1 TO 11 STEP 1

8 KEYPOINTS (OF 8 DEFINED) SELECTED BY KSEL COMMAND.

ALL SELECT FOR ITEM=ELEM COMPONENT=
IN RANGE 1 TO 53 STEP 1

53 ELEMENTS (OF 53 DEFINED) SELECTED BY ESEL COMMAND.

ALL SELECT FOR ITEM=NODE COMPONENT=

```
 IN RANGE      1 TO     200 STEP      1

  200 NODES (OF   200 DEFINED) SELECTED BY  NSEL  COMMAND.

 SELECT     NODES ON EXTERIOR OF SELECTED ELEMENTS

   82 NODES (OF   200 DEFINED) SELECTED BY  NSEL  COMMAND.

 *GET ymin     FROM NODE ITEM=MNLO Y     VALUE= -.700000000E-
02

 RESELECT    FOR ITEM=LOC  COMPONENT=Y     BETWEEN -
.71000E-02 AND  -.69000E-02
  KABS=  0.  TOLERANCE=  .200000E-11

   31 NODES (OF   200 DEFINED) SELECTED BY  NSEL  COMMAND.

 COUPLED SET=    1  DIRECTION= UY    TOTAL NODES=    31
 MAXIMUM COUPLED SET NUMBER=    1

 SELECT ALL ENTITIES OF TYPE= ALL  AND BELOW

 ALL SELECT   FOR ITEM=VOLU COMPONENT=
  IN RANGE      0 TO       0 STEP       1

    0 VOLUMES (OF     0  DEFINED) SELECTED BY  VSEL
 COMMAND.

 ALL SELECT   FOR ITEM=AREA COMPONENT=
  IN RANGE      1 TO       5 STEP       1

   2  AREAS (OF    2  DEFINED) SELECTED BY ASEL COMMAND.

 ALL SELECT   FOR ITEM=LINE COMPONENT=
  IN RANGE      1 TO      15 STEP       1

   9  LINES (OF    9  DEFINED) SELECTED BY LSEL COMMAND.

 ALL SELECT   FOR ITEM=KP   COMPONENT=
  IN RANGE      1 TO      11 STEP       1
```

```
    8 KEYPOINTS (OF     8 DEFINED) SELECTED BY KSEL
COMMAND.

 ALL SELECT   FOR ITEM=ELEM COMPONENT=
  IN RANGE      1 TO      53 STEP       1

    53 ELEMENTS (OF    53 DEFINED) SELECTED BY ESEL
COMMAND.

 ALL SELECT   FOR ITEM=NODE COMPONENT=
  IN RANGE      1 TO     200 STEP       1

   200 NODES (OF   200 DEFINED) SELECTED BY NSEL COMMAND.


***** ROUTINE COMPLETED *****  CP =      132.430



*** NOTE ***                            CP=   132.430   TIME= 12:38:52
A total of 7 warnings and errors written to file.err.

***** ANSYS SOLUTION ROUTINE *****

 SELECT      FOR ITEM=LOC  COMPONENT=Y    BETWEEN  .00000
AND  .00000
  KABS=  0.  TOLERANCE=  .100000E-05

    20 NODES (OF   200 DEFINED) SELECTED BY NSEL COMMAND.

 SPECIFIED CONSTRAINT UY   FOR SELECTED NODES       1 TO
200 BY      1
 REAL=  .000000000     IMAG=  .000000000

 ALL SELECT   FOR ITEM=NODE COMPONENT=
  IN RANGE      1 TO     200 STEP       1

   200 NODES (OF   200 DEFINED) SELECTED BY NSEL COMMAND.

 READ SOLUTION RESULTS DATA ( TEMP ) FROM LOAD STEP=     1
SUBSTEP=     0
```

```
TIME=  .000000      ON FILE= file.rth
READ "REAL" PART OF OF THE SOLUTION.

   200 NODAL TEMPERATURES WERE STORED ON SELECTED
NODES.
 READ FROM LOAD STEP=     1  SUBSTEP=     1  TIME=  1.00000

 REFERENCE TEMPERATURE=  20.000  (TUNIF=  20.000)

 SELECT      FOR ITEM=LINE COMPONENT=
  IN RANGE      5 TO       5 STEP       1

    1  LINES (OF    9  DEFINED) SELECTED BY LSEL  COMMAND.

 SELECT     ALL NODES (INTERIOR TO LINE, AND AT KEYPOINTS)
      RELATED TO SELECTED LINE SET.

    19  NODES (OF   200  DEFINED) SELECTED FROM
     1 SELECTED LINES BY NSLL COMMAND.

 GENERATE SURFACE LOAD PRES ON SURFACE DEFINED BY ALL
SELECTED NODES
 VALUES= 7.888609052E-31  .000000000

 NUMBER OF PRES ELEMENT FACE LOADS STORED =     9

 ALL SELECT   FOR ITEM=VOLU COMPONENT=
  IN RANGE      0 TO       0 STEP       1

    0  VOLUMES (OF     0  DEFINED) SELECTED BY  VSEL
COMMAND.

 ALL SELECT   FOR ITEM=AREA COMPONENT=
  IN RANGE      1 TO       5 STEP       1

    2  AREAS (OF    2  DEFINED) SELECTED BY ASEL COMMAND.

 ALL SELECT   FOR ITEM=LINE COMPONENT=
  IN RANGE      1 TO      15 STEP       1

    9  LINES (OF    9  DEFINED) SELECTED BY LSEL COMMAND.
```

```
ALL SELECT   FOR ITEM=KP   COMPONENT=
 IN RANGE      1 TO      11 STEP       1

    8 KEYPOINTS (OF     8 DEFINED) SELECTED BY  KSEL
COMMAND.

ALL SELECT   FOR ITEM=ELEM COMPONENT=
 IN RANGE      1 TO      53 STEP       1

   53 ELEMENTS (OF    53 DEFINED) SELECTED BY  ESEL
COMMAND.

ALL SELECT   FOR ITEM=NODE COMPONENT=
 IN RANGE      1 TO     200 STEP       1

  200 NODES (OF   200 DEFINED) SELECTED BY  NSEL  COMMAND.

FINISH SOLUTION PROCESSING


***** ROUTINE COMPLETED *****  CP =       133.200


*** NOTE ***                            CP=   133.200   TIME= 12:38:53
A total of 7 warnings and errors written to file.err.

*****  ANSYS SOLUTION ROUTINE  *****

*****  ANSYS SOLVE   COMMAND  *****

                S O L U T I O N   O P T I O N S

 PROBLEM DIMENSIONALITY. . . . . .AXISYMMETRIC
 DEGREES OF FREEDOM. . . . . UX  UY
 ANALYSIS TYPE . . . . . .STATIC (STEADY-STATE)

*** NOTE ***                            CP=   133.250   TIME= 12:38:53
Axisymmetric elements present.  Loads input with the F commands and the
 corresponding output quantities are on a full circle basis.  This
```

differs from pre-Rev 5.0 interpretation.

*** NOTE *** CP= 133.250 TIME= 12:38:53
Present time 0 is less than or equal to the previous time.
Time will default to 1.

LOAD STEP OPTIONS

LOAD STEP NUMBER. 1
TIME AT END OF THE LOAD STEP. 1.0000
NUMBER OF SUBSTEPS. 1
STEP CHANGE BOUNDARY CONDITIONS . . . . . NO
AXISYMMETRIC HARMONIC LOADING PARAMETERS
MODE 0
ISYM 1
PRINT OUTPUT CONTROLS . . . . . .NO PRINTOUT
DATABASE OUTPUT CONTROLS. . . . . .ALL DATA WRITTEN
FOR THE LAST SUBSTEP

Range of element maximum matrix coefficients in global coordinates
Maximum= 1.384329789E+13 at element 17.
Minimum= 1.613370346E+12 at element 10.

*** ELEMENT MATRIX FORMULATION TIMES
TYPE NUMBER ENAME TOTAL CP AVE CP

1 53 PLANE82 .220 .004
Time at end of element matrix formulation CP= 133.64.

Estimated number of active DOF= 350.
Maximum wavefront= 35.

Time at end of matrix triangularization CP= 133.8.
Equation solver maximum pivot= 1.4887499E+13 at node 140 UY.
Equation solver minimum pivot= 44925522.2 at node 22 UX.

*** ELEMENT RESULT CALCULATION TIMES
TYPE NUMBER ENAME TOTAL CP AVE CP

```
  1     53  PLANE82       .220     .004

 *** NODAL LOAD CALCULATION TIMES
 TYPE  NUMBER   ENAME     TOTAL CP  AVE CP

  1     53  PLANE82       .050     .001
*** LOAD STEP    1  SUBSTEP    1  COMPLETED.   CUM ITER =     1
*** TIME =  1.00000       TIME INC =  1.00000     NEW TRIANG
MATRIX


 *** PROBLEM STATISTICS
 ACTUAL NO. OF ACTIVE DEGREES OF FREEDOM =    350
 R.M.S. WAVEFRONT SIZE =    22.6


*** ANSYS BINARY FILE STATISTICS
 BUFFER SIZE USED=  4096
      .141 MB WRITTEN ON ELEMENT MATRIX FILE: file.emat
      .047 MB WRITTEN ON ELEMENT SAVED DATA FILE: file.esav
      .078 MB WRITTEN ON TRIANGULARIZED MATRIX FILE: file.tri
      .125 MB WRITTEN ON RESULTS FILE: file.rst

FINISH SOLUTION PROCESSING


***** ROUTINE COMPLETED *****  CP =       134.960



*** NOTE ***                            CP=    134.960   TIME= 12:38:55
A total of 7 warnings and errors written to file.err.

      ***** ANSYS RESULTS INTERPRETATION (POST1) *****

ENTER  /SHOW,DEVICE-NAME  TO ENABLE GRAPHIC DISPLAY
ENTER  FINISH          TO LEAVE POST1

 SORT ON ITEM=S    COMPONENT=INT   ORDER= 0  KABS= 0
NMAX=   200
```

SORT COMPLETED FOR 74 VALUES.

*GET max_si FROM SORT ITEM=MAX VALUE= 266837907.

TITLE=
sd_4 Stress Intensities (MPa)

SELECT FOR ITEM=MAT COMPONENT=
IN RANGE 2 TO 2 STEP 1

41 ELEMENTS (OF 53 DEFINED) SELECTED BY ESEL COMMAND.

SELECT ALL NODES HAVING ANY ELEMENT IN ELEMENT SET.

158 NODES (OF 200 DEFINED) SELECTED FROM
41 SELECTED ELEMENTS BY NSLE COMMAND.

DISPLAY NODAL SOLUTION, ITEM=S COMP=INT

CUMULATIVE DISPLAY NUMBER 12 WRITTEN TO FILE m_sol.f33 - VECTOR MODE.
DISPLAY TITLE=
sd_4 Stress Intensities (MPa)

*** NOTE *** CP= 135.670 TIME= 12:38:56
CUMULATIVE DISPLAY NUMBER 12 WRITTEN TO FILE m_sol.f33 - VECTOR MODE.
DISPLAY TITLE= sd_4 Stress Intensities (MPa).

*** NOTE *** CP= 136.110 TIME= 12:38:56
NEW BACKUP FILE NAME= sd_4.dbb.

ALL CURRENT ANSYS DATA WRITTEN TO FILE NAME= sd_4.db
FOR POSSIBLE RESUME FROM THIS POINT

m_sol.par

```
/NOPR
*SET,H1     , .7000000000000E-02
*SET,MAX_SI , 539455682.3932
*SET,MAX_T  , 570.8125498950
*SET,MNAME  ,'sd_4   '
*SET,NUM_E  , 53.00000000000
*SET,NUM_N  , 200.0000000000
*SET,N_FAC  , 1.000000000000
*SET,QFL_IN , 1000000.000000
*SET,QGE_IN , 27800000.00000
*SET,R1     , 2.560000000000
*SET,R2     , .5000000000000E-02
*SET,R3     , 2.572000000000
*SET,T1     , .5000000000000E-02
*SET,T2     , .2000000000000E-01
*SET,T3     , .2000000000000E-02
*SET,T_SB   , 276.0000000000
*SET,YMIN   , -.7000000000000E-02
*DIM,_ANSUM ,ARRAY,     4,     4,     1
*SET,_ANSUM (    1,  1, 1), 1170.332511672
*SET,_ANSUM (    2,  1, 1), 956.6250997900
*SET,_ANSUM (    3,  1, 1), 570.8125498950
*SET,_ANSUM (    1,  2, 1), 1656783363.182
*SET,_ANSUM (    2,  2, 1), 1091739325.520
*SET,_ANSUM (    3,  2, 1), 539455682.3932
*SET,_ANSUM (    1,  3, 1), 83330000.00000
*SET,_ANSUM (    2,  3, 1), 55600000.00000
*SET,_ANSUM (    3,  3, 1), 27800000.00000
*SET,_ANSUM (    1,  4, 1), 3000000.000000
*SET,_ANSUM (    2,  4, 1), 2000000.000000
*SET,_ANSUM (    3,  4, 1), 1000000.000000
*SET,_I11   , 4.000000000000
*DIM,_NM_FIL ,CHAR,     4,     1,     1
*SET,_NM_FIL (    1,  1, 1),'sa_4   '
*SET,_NM_FIL (    2,  1, 1),'sb_4   '
*SET,_NM_FIL (    3,  1, 1),'sc_4   '
*SET,_NM_FIL (    4,  1, 1),'sd_4   '
*DIM,_N_FIL ,ARRAY,     1,     1,     1
*SET,_N_FIL (    1,  1, 1), 4.000000000000
```

/GO

Sa_4.inp

```
!  SA_4.inp
/inp,SA_4,des        ! loads the parameters/material properties
```

Sb_4.inp

```
!  SB_4.inp
/inp,SB_4,des        ! loads the parameters/material properties
```

Sc_4.inp

```
!  SC_4.inp
/inp,SC_4,des        ! loads the parameters/material properties
```

Sd_4.inp

```
!  SD_4.inp
/inp,SD_4,des        ! loads the parameters/material properties
```